DISSERTATION THESIS

Study of evolution of insect pheromone biosynthetic fatty acyl desaturases

Aleš Buček, MSc

SCIENTIFIC SUPERVISOR: Iva Pichová, PhD

Department of Biochemistry
Faculty of Science
Charles University in Prague

Institute of Organic Chemistry and Biochemistry
of the Czech Academy of Sciences

Prague 2016

Acknowledgement

Firstly, I'd like to thank my scientific supervisor, Iva Pichová, for providing me excellent conditions for conducting my PhD research. I also would like to acknowledge Aleš Svatoš and Irena Valterová for co-supervising several of the research projects in which I have participated during my PhD. I thank all the past and present members of the research team of Iva Pichová but also others from IOCB, namely next-door-colleagues from Jan Konvalinka group, for their help without hesitation and also for inspiring me by their attitudes and personalities. I learnt a lot also from students whom I was supervising at some point during my stay at IOCB – Sarah Edwards, Petra Wenzelová and Michal Tupec – thank you for your curiosity.

Going back to the beginning of my research stay at IOCB, I'd like to thank to Petra Matoušková, Olga Hrušková and Elena Dolejší for guiding me through my first scientific experiments and daily lab work. I also would like to thank Darina Prchalová for being a great emphatic collaborator and a sister-in-arms.

Still on the scientific side of my acknowledgement, my sincere thanks go to Vláďa Vrkoslav for his help with GC/MS analyses; to Sagar Pandit and Heiko Vogel for their help with RNA interference experiments and analyses of RNA-seq data, respectively; to Hana Sychrová for introducing me into yeast microbiology; to Jan Šobotník for spreading his contagious enthusiasm for just anything connected to insects.

I also thank the people above who helped me to see research as fun, excitement and a privilege despite the plentiful obstacles on the way.

Moving out of the lab with my acknowledgment, I'd like to thank all my friends whom I met in Prague during my studies at the Charles University, and particularly at the university dormitory, for showing me that eating ketchup pasta, drinking stream water and camping in the open air in the mountains across the world as well as in the woods just outside of Prague is enough to have a great day, as long as there is somebody to share it with. Thank you also for constantly reminding me that life is not only about research or PhD degree.

Lastly and importantly, I thank my mother for her unconditional support during my whole university studies.

Declaration of authorship

I declare that I elaborated this PhD thesis independently under the supervision of my supervisor Ing. Iva Pichová, CSc., I cited all used literature sources, and this thesis or its parts were not used to obtain any other academic degree than PhD degree from the Faculty of Sciences of Charles University in Prague.

Prague, 19th July 2016 .....

Abstract

Insects account for more than one million of described species with an ecological and economic impact disproportional to their minute body size. Among the factors which have contributed to their evolutionary success, insect secondary metabolites such as defensive compounds and chemical signals are regarded to play a major role. This thesis aims at uncovering the molecular mechanisms underlying evolution of ubiquitous insect secondary metabolites – sex pheromones (SPs), i.e. chemical signals mediating mate finding and mating between individuals of the same species. The thesis focuses on a class of oxidoreductase enzymes, membrane fatty acid desaturases (mFADs), which introduce double bonds into hydrocarbon chains of fatty acyls and thus produce precursors of unsaturated fatty acid-derived SPs. mFADs are involved in SP biosynthesis in e.g. moths (Lepidoptera), flies (Diptera), cockroaches and termites (Blattodea), wasps and bees (Hymenoptera) - some of the most species-rich insect orders. Since SPs are principal to species reproductive isolation, uncovering the molecular basis of insect SP biosynthesis holds promises to contribute to answering fundamental questions concerning the insect ecology and evolution. The insect mFADs with diverse enzymatic specificities also represent a naturally available resource for study of enzyme function evolution.

This thesis explores mFADs in Hymenoptera (bumblebees - *Bombus*) and Lepidoptera (tobacco hornworm moth - *Manduca sexta*) as well as in non-insect organism (yeast – *Candida parapsilosis*). We demonstrate that the ability to produce a wide range of unsaturated fatty acids is inherent to mFADs across kingdoms (Publications I and III). We show that pheromone-biosynthetic mFADs can synthesize novel unsaturated SP precursors as a result of a single amino acid substitution, a mechanism which might have a high potential in generating novel SP components in moths and represents thus a possible molecular mechanism of SP evolution (Publication I). Our finding that the amino acid residue which controls *M. sexta* mFAD specificities resides in the kink of the mFAD substrate binding channel provides novel insights into mechanism of mFAD substrate specificity determination (Publication I). By study of mFADs from three bumblebee species we show that post-transcriptional regulation of mFAD activity represents an alternative possible regulatory mechanism of pheromone composition in hymenopterans (Publication II). Together, these findings expand our knowledge on determinants of mFADs enzymatic specificities and contribute to our understanding of the role which mFADs play in SP biosynthesis and evolution of SP communication in moths and bees.

Abstrakt

Hmyz čitající více než jeden milion popsaných druhů představuje skupinu organismů s ekologickým a ekonomickým významem disproporčně větším než je jejich často zanedbatelná tělesná velikost. Mezi faktory, které zásadní měrou přispěly k evoluční úspěšnosti hmyzu, je počítána schopnost produkovat řadu sekundárních metabolitů, jako jsou obranné látky a chemické signály. Tato disertační práce se věnuje studiu molekulárních mechanismů evoluce jedné široce zastoupené skupiny hmyzích chemických signálů – pohlavních feromonů – tedy látek, které zprostředkovávají vyhledávání pohlavních partnerů a páření jedinců téhož druhu. Téma práce je zaměřeno na membránové desaturasy mastných kyselin (dále jen desaturasy), oxidoreduktasy, které zavádí dvojné vazby do uhlovodíkových řetězců mastných kyselin a tak produkují nenasycené prekurzory pohlavních feromonů odvozených od mastných kyselin. Desaturasy jsou zapojeny v biosyntéze pohlavních feromonů například u můr (Lepidoptera), dvoukřídlých (Diptera), blanokřídlých (Hymenoptera), švábů a termitů (Blattodea) – tedy jedněch z druhově nejbohatších hmyzích řádů. Jelikož pohlavní feromony slouží jako reprodukční bariéry u mnohých blízce příbuzných druhů či subpopulací, odhalení molekulárních základů biosyntézy feromonů může pomoci zodpovědět klíčové otázky týkající se ekologie a evoluce hmyzu. Hmyzí desaturasy s různorodými enzymovými specifitami také představují přirozeně dostupný zdroj pro studium evoluce enzymů.

Disertační práce se věnuje desaturasam blanokřídlých (čmeláci - *Bombus*), můr (lišaj tabákový - *Manduca sexta*) a pro srovnání také jednobuněčných organismů (patogenní kvasinka *Candida parapsilosis*). Výsledky práce ukazují, že schopnost produkovat široké spektrum nenasycených mastných kyselin je sdílena desaturasami napříč biologickými říšemi (Publikace I a III). Desaturasy zapojené v biosyntéze feromonů mohou získat schopnost produkovat nové nenasycené mastné kyseliny důsledkem substitutce jediného aminokyselinového zbytku – mechanismus, který má značný potenciál v evoluci feromonového složení můr (Publikace I). Zjištění, že tato aminokyselina se v desaturase lišaje tabákového nachází v ohybu tunelu, který váže substrát, poskytuje nový vhled do mechanismů určujících desaturasovou specifitu (Publikace I). Studium desaturas u třech druhů čmeláků odhaluje post-transkripční regulaci aktivity desaturas jako možný alternativní mechanismus určující druhově specifické feromonové složení u blanokřídlých (Publikace II). Tato disertační práce tak na genetické úrovni poodhaluje roli desaturas v evoluci feromonové komunikace u můr a blanokřídlých.

List of abbreviations

FAD	Fatty acyl desaturase
mFAD	Membrane fatty acyl desaturase
sFAD	Soluble fatty acyl desaturase
ER	Endoplasmic reticulum
FA	Fatty acid
UFA	Unsaturated fatty acid
1UFA	Monounsaturated fatty acid
2UFA	Diunsaturated fatty acid
3UFA	Triunsaturated fatty acid
PUFA	Polyunsaturated fatty acid
FAR	Fatty acyl reductase
SP	Sex pheromone
GC/MS	Gas chromatography/Mass spectrometry
LG	Labial gland
MP	Marking pheromone
FAS	Fatty acid synthase
RNAi	RNA interference
dsRNA	Double-stranded RNA
RNA-seq	RNA sequencing

Table of contents

1 Introduction

1.1 Insect pheromone research – a historical perspective

The 19th century observations and experiments with male great peacock moths (*Saturnia pyri*) attracted by, at that time, elusive female-produced air-born signal are among the first scientific description of species-specific communication in insects[1]. Despite the conspicuous behavior, the identification of chemical compounds underlying the observed behavior was hampered by their nanogram and sub-nanogram quantities present in a single insect specimen. It took another almost 90 years and over 500,000 abdomens of female silk moth (*Bombyx mori*) to identify bombykol, a volatile unsaturated fatty acid-derived alcohol produced by the *B. mori* females to attract conspecific males[2]. Bombykol represented the first chemically identified pheromone, i.e. a compound or a mixture of compounds which is secreted by an individual to trigger a response, such as a behavioral or physiological change, in an individual of the same species[3].

The possibility that economically important insect pests might be controlled using laboratory-synthesized pheromones[4] provided an impulse to study and identify pheromones from other insect pest species such as female sex pheromone (SP) from the cabbage looper moth[5], aggregation pheromone produced by the male bark beetles[6], or a female housefly SP[7]. The increased sensitivity of analytical tools, particularly gas chromatography coupled with mass spectrometry detectors[8] and development of gas chromatography coupled with electroantennographic detector which uses insect antennae as a pheromone-specific detector[9] led to rapid increase in number of insect species for which their pheromones were chemically identified, reaching 200 moth species in 1985[10], more than 500 moth species in 2004[11], and now reaching probably well over 1,000 insect species[12].

The amassed knowledge on pheromones structure and composition indicated that moth female SPs are generally mixtures of saturated or unsaturated fatty acid (FA) derived alcohols, aldehydes, esters, hydrocarbons, or epoxides[13] and that similar FA derivatives are components of pheromones also in flies (Diptera), cockroaches (Blattodea), wasps and bees (Hymenoptera)[12].

Initial pheromone biosynthetic studies on FA-derived pheromones in moths, which remained the model organisms for insect pheromone research, addressed the questions i) whether pheromones were biosynthesized through minor modifications of precursors taken up via insects diet or whether they are biosynthesized *de novo* and ii) how is the particular chain length and double bond position determined. *In vivo* experiments employing isotopically

labeled candidate pheromone precursors confirmed the labeled precursors are incorporated into pheromones implying that majority of female moth SPs are produced in the moth SP glands *de novo* (from acetate) via FA biosynthetic pathway[14]. It was established that a particular combination of pheromone biosynthetic steps, i.e. fatty acyl chain shortening, double bond introduction, reduction and esterification of carbonyl group, each with its inherent specificity, is responsible for the species-specific pheromone blend[15,16] and broadening the research to more species indicated that this SP biosynthetic scheme is generally conserved in moths[17,18]. Analogous experiments uncovered biosynthetic origin of pheromones also in other insect orders, e.g. *de novo* biosynthesis of FA- derived cuticular hydrocarbons in some fly species or contribution of both *de novo* biosynthesis and dietary acquisition of pheromone precursors to the biosynthesis of isoprenoid bark beetle pheromones[19]. Membrane fatty acyl desaturases (mFADs), i.e. enzymes introducing double bonds into fatty acyl hydrocarbon chains at a variety of specific position and in either *Z* or *E* stereo configuration via action of fatty acid desaturase enzyme were recognized as key players in generation of the female moth SP diversity[20].

Subsequent advances in molecular biology enabled shift of research focus from identification of biochemical pathways to study of molecular biology and genetics of pheromone biosynthesis and thus gain further insight into the genetic basis of pheromone production and perception and inference on evolutionary processes which shapes the pheromone communication[21]. Studies on moth SP-biosynthetic desaturases indicated that they biochemically closely related to the animal fatty acid desaturases involved in primary metabolism of fatty acids[22,23]. The knowledge on mFAD gene sequences from rat liver[24] and yeast[25] enabled first isolation of functional characterization of insect pheromone-producing mFAD gene from the cabbage looper moth[26], soon followed by description of mFAD genes involved in biosynthesis of cuticular pheromones in *Drosophila melanogaster*[27] which was boosted by sequencing of the *D. melanogaster* genome[28]. The mFADs substrates and products were determined by its heterologous expression in yeast *Saccharomyces cerevisiae*, benefiting from previous work which showed that a rat mFAD is active when heterologously expressed in *S. cerevisiae*[25]. Characterization of insect mFADs via determination of their unsaturated products directly in the yeast heterologous expression system overcame inherent difficulties connected to the in vitro work with membrane enzymes[26] and started a prolific research field centered around insect pheromone biosynthetic mFADs. Employing yeast expression system, 45 years after the first pheromone discovery, a multifunctional mFAD from *B. mori* involved in biosynthesis of the pheromone, bombykol, was described[29]. mFADs retained position of the most studied pheromone-biosynthetic enzymes with over 50 insect mFADs functionally

characterized until these days[30] and were implied in evolution of pheromone communication and in origin of new lepidopteran and dipteran species[31].

Currently, powerful novel techniques such as next-generation sequencing methods[32] are revolutionizing biological sciences. With respect to the insect research, cost-effective genome and transcriptome sequencing deepen our insight into biology of model insect species but importantly also provides an unprecedented access to the biology and evolution of non-model insect species[33,34], including the molecular basis of insect SP communication and its evolution[35–40].

1.2 Unsaturated fatty acid (UFA) biosynthesis

Unsaturated fatty acids (UFAs) play an essential role in maintenance of the proper cell membrane structure and function in virtually all organism[41,42]. In mammals, polyunsaturated FAs serve as precursors of biologically active eicosanoids, i.e. prostaglandins and leukotrienes, which are involved in regulation of key biological processes such as inflammation or pain[43]. In insects, UFA-derivatives represent one of the most widespread pheromone structural type[44].

Majority of organisms can produce UFAs *de novo* from basic building blocks such as acetyl-CoA via either of two fundamentally distinct pathways; in some bacteria, such as *Escherichia coli*[45] or *Streptococcus* sp.[46], monounsaturated fatty acids are produced anaerobically by skipping one double bond reduction step during FA biosynthesis which results in retention of a double bond in the growing FA chain[47]. In contrast, UFAs in all eukaryotes and many prokaryotes are biosynthesized from saturated FAs by oxygen-dependent di-iron oxidoreductases, fatty acyl desaturases (FADs)[48].

FADs are remarkable enzymes which can break a strong C-H bond (dissociation energy ≈ 400 kJ/mol) in an unactivated fatty acyl chain at a precise position along its hydrocarbon backbone in a process involving reactive oxo-intermediate formed by activation of molecular oxygen by di-iron center[49]. Two evolutionary unrelated classes of apparently convergent FADs exist[50]: soluble FADs (sFADs), which are expressed exclusively in the stroma of plant plastids and desaturate fatty acyls bound to acyl carrier protein (ACP), and membrane-bound FADs (mFADs), which are ubiquitous in eukaryotes and some prokaryotes and desaturate fatty acyls in form of fatty acyl-CoA or lipid-linked fatty acyls. The two FAD classes share di-iron active center which is in each FAD class, however, coordinated by distinctly organized histidine-rich motifs[48,51].

1.2.1 Membrane fatty acyl desaturases (mFADs)

mFADs belong to a superfamily of oxygen-dependent membrane di-iron-containing enzymes which share common features such as a conserved tripartite histidine-rich motif coordinating two iron atoms in active center. The superfamily further includes enzymes involved in oxygenation and desaturation of lipidic and hydrophobic compounds such as bacterial membrane alkane hydroxylases/epoxidases [52] and xylene hydroxylases[53], membrane sphingolipid hydroxylases[54], membrane fatty acyl desaturase/conjugases[55], membrane fatty acyl acetylenases and epoxidases[56] and membrane fatty acyl hydroxylases[48,49,51,57,58].

mFADs are present in cell membranes of some bacteria[59,60], thylakoid and cytoplasmic membranes of cyanobacteria[61], thylakoid and cytoplasmic membranes of plants, and ubiquitously in the eukaryotic endoplasmic reticulum membranes[48]. The ER mFADs, which we will focus on throughout this thesis, use an electron pair supplied by NADH via an electron transport system consisting of NADH: cyctochrome b5 reductase and cytochrome b5[49]. Slight modification of this electron-supply chain is seen in some mFADs which are fused with an N- or C-terminal cytochrome b5 domain which functionally replaces cytochrome b5[62,63].

1.2.1.1 mFAD structure

The recently published crystal structures of two closely related mammalian mFADs with bound fatty-acyl CoA substrate provided first direct structural insights into mFADs[64,65] (Figure 1). In agreement with previous topology predictions[25] and topology-mapping experiments[66], the crystal structure shows 4 transmembrane α-helices and a large extramembrane portion of the enzyme including active center localized to the cytosolic side of the ER membrane (Figure 1). The di-iron active center is coordinated by an ordered water molecule and nine conserved histidine residues. Eight of the coordinating histidines are organized in a tripartite histidine-rich motif which was previously shown to be essential for mFAD activity[53] (Figure 1D). As an exception, a distinct class of mFADs was described to have a histidine residue in the third histidine-rich motif replaced by catalytically essential glutamine[67]. Notably, the iron atoms of the mFAD active center are replaced in crystal structures of both mammalian mFADs by zinc atoms, presumably as an artifact of protein heterologous expression[64,65].

The organization of the mFAD active center contrasts with the carboxylate-bridged di-iron active center of sFADs which is coordinated by conserved histidine and aspartic or glutamic acid residues[49,68,69]. The crystalized mouse mFADs is a monomer according to the small interacting surfaces in crystal lattice and size-exclusion chromatography[65] although previous experiments indicated that yeast mFAD is a homodimer *in vivo*[70].

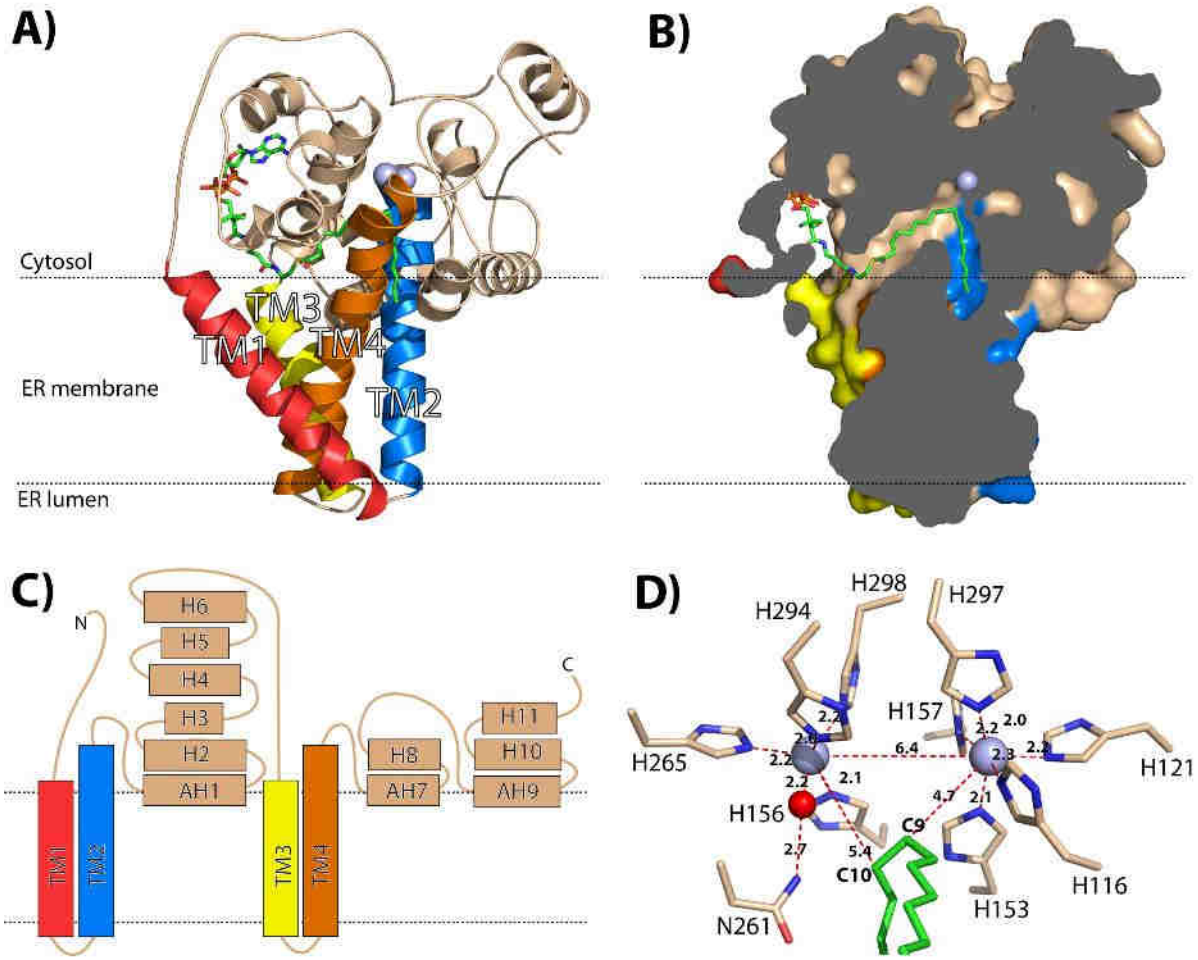

Figure 1. Crystal structure of mouse Z9-mFAD. (A-C) mFAD is predicted to be anchored in the endoplasmic reticulum (ER) membrane (displayed as dashed lines) by four transmembrane helices (TM1-TM4). **(B)** The cross-section of mFAD protein surface shows the long, narrow, and bend substrate binding tunnel occupied by 16:0-CoA substrate (shown as a stick model with green hydrocarbon chain). The zinc atoms of di-metal active center are shown as light-blue spheres (only one atom visible here). **(C)** Membrane topology of mFAD shows transmembrane helices TM1 - TM4, amphipathic helices AH1 – AH3 presumably residing at the interface of the mFAD cytosolic domain and the ER membrane, and cytosolic helices H2 – H11. **(D)** Detailed view of the mFAD active center displays interatomic distances (in Å) between the nine histidine residues and a water molecule (shown as a red sphere hydrogen bonded by asparagine residue) coordinating two zinc atoms, and C9 and C10 atoms of 16:0-CoA hydrocarbon moiety (truncated chain shown in green) which are the site of catalytic hydrogen removal. The structure models were rendered in PyMOL Viewer software[71] using mouse Z9-mFAD crystal structure (Protein Data Bank code 4YMK)[65]. The topology model was adapted from[65].

1.2.1.2 mFAD enzymatic specificity

Since the number, position and stereochemistry of double bond(s) critically influence the biophysical properties of UFAs and, with respect to FA-derived pheromones, also underlies their behavioral activity, the investigation of mechanisms, which underlie particular desaturase specificity, represents an active research field. The research conducted on mFADs mainly aims

at identifying desaturase specificity determinants which would enable engineering of mFADs for production of economically or industrially relevant UFAs such as polyunsaturated UFAs serving as nutritional supplements or starting material in chemical industry[72]. Another major goal is uncovering structural details of mFADs which might enable rational design of specific inhibitors targeting mFADs involved in human metabolic diseases such as diabetes or obesity[73] or mFADs essential for human pathogenic microorganisms such as pathogenic yeasts[74–76] and trypanosomatids[77,78]. Finally, the third source of mFAD research motivation is uncovering the molecular basis of pheromone evolution by studying pheromone biosynthetic mFADs[40].

Enzymatic specificities of FADs can be classified using a range of criteria. Stereospecificity describes the preferential production of one stereoisomer (*E* or *Z*). Regiospecificity refers to the FAD preference towards the particular position of introduced double bond along the fatty acyl hydrocarbon chain and also indicates which part of the substrate molecule presumably serves as a reference point for positioning of the double bond. Substrate specificity denotes the FAD preference towards a particular chain length, towards presence of pre-existing double bond(s) at particular position(s) or of particular stereochemical configuration, and towards particular head group of fatty acyl substrate, i.e. acyl-CoA or acyl-lipid substrates[79]. Moreover, hydroxylated (and less commonly also acetylenated - i.e. bearing a triple bond) products can accompany the desaturated products as a result of mechanistic similarity between the reaction mechanisms[80,81], introducing chemospecificity as an additional specificity mode. Some mFADs also exhibit fatty acyl conjugase activity, i.e. capability to produce a system of conjugated double bonds by a reaction mechanism involving shift of the position of preexisting double bond[82,83]. Together, the amassed knowledge on FADs indicates that, although numerous FADs are highly specific and produce only a limited set of unsaturated products, FADs often follow more than one specificity mode, such as mFADs involved in sequential biosynthesis of UFAs with multiple double bonds[84,85].

Throughout this work we will adhere to the established nomenclature for UFAs and FADs, i.e. ΔX to indicate that the double bond of unspecified stereoisomerism is positioned between X and X+1 atom of fatty acyl chain; *E*/*Z*X to indicate the position of *E*- or *Z*-double bond; and X:Y to indicate a fatty acyl chain with X carbon atoms containing Y double bonds[86]. As an example, *E*10,*Z*12-16:2 represents diunsaturated 16 carbon atom-long FA with double bonds of *E* and *Z*-stereochemistry at positions Δ10 and Δ12, respectively. The "ΔX" notation provides an apparent FAD regiospecificity with respect to the carboxyl group, however, it was shown that particularly for mFADs introducing successive double bonds, the preexisting double bond or methyl-end carbon atom might also act as a reference for positioning the successive

double bonds, so additional information might be necessary to comprehensively describe the mFAD specificity[84,85].

mFADs producing Z9-16:1 and Z9-18:1 monounsaturated FAs are the most wide-spread eukaryotic mFADs, followed by mFADs with *Z*5, *Z*6, *Z*12 and *Z*15-regiospecificity which introduce subsequent double bonds into UFAs. mFADs however evolved an excessively wide range of specificities[48]. With respect to the preferred substrate head group, majority of mFADs in animals and insects desaturate acyl-CoA with possible exception of some animal mFADs which presumably desaturate acyl-lipids and are involved in biosynthesis of polyunsaturated fatty acids[87,88]. The experimental evidence on the identity of mFAD substrate head group is, however, scarce and its prediction relies mainly on mFAD protein sequence comparison[79].

1.2.1.3 mFAD enzymatic specificity determinants

The lack of structural data for mFADs until recently[64,65] was compensated by efforts to identify the specificity determinants by either random mutagenesis or rational mutagenesis of mFADs guided by topology predictions and sequence comparisons of mFADs with distinct specificities. For the characterization of mFADs and their mutants, functional expression in yeast *Saccharomyces cerevisiae* was developed to overcome the necessity of isolation and purification of mFADs[25]. In this assay, a desaturase-deficient yeast strain heterologously expresses mFAD of interest which forms an active desaturase complex with the yeast cytochrome b5 and NADH: cyctochrome b5 reductase and produces UFAs which complement the yeast UFA auxotrophy. UFA products can be subsequently extracted from yeast biomass and analyzed using e.g. gas chromatography with mass spectrometric detection (GC/MS). The system can be employed also for characterization of mFADs which produce UFAs not complementing the yeast UFA auxotrophy[89] by *i)* using yeast strain which is not desaturase-deficient (in this case, the rather simple UFA profile of yeast resulting from presence of a single yeast Z9-mFAD facilitates the identification of novel UFA products[90]) or *ii)* by supplementing the desaturase-deficient yeast strain with *Z*9-UFAs into the cultivation medium[91]. Alternatively, baculovirus-insect cells expression system were used for functional characterization of heterologously expressed mFADs[29]. and plant expression systems were used for study of plant acyl-lipid mFADs[58].

Mutageneses of acyl-lipid and acyl-CoA mFADs from diverse organisms indicate that the determinants of the substrate chain length preference can be localized to the second transmembrane helix (TM2)[65,92,93]. The comparison of the mutated mFADs sequences to the sequences of crystalized mammalian mFADs indicates that amino acid residues from TM2 form

the end of the substrate binding channel which presumably interacts with the methyl end of the mFAD substrate acyl moiety[64,65]. Mutagenesis studies which probed the effect of individual residues suggests that the volume of a limited number of amino acid residues presumably capping the end of the substrate binding tunnel plays a pivotal role in the substrate chain length preference[65,92]. Also sequence comparison of closely related mFADs which differ in the substrate chain length preference supports the role of the residues localized in the TM2 region[27,65]. In insect acyl-CoA mFAD, a single amino acid mutation in TM1 was sufficient for shifting both its regio- and substrate specificity[94]. A recent study on rat Δ6-acyl-lipid mFAD indicated that its Δ6-specificity can be *i)* transformed into Δ5/Δ6-specificity by mutating a single aa which is localized in the rat mFAD structural homology model to the end of the substrate binding tunnel or *ii)* changed to Δ5-specificity by several amino acid mutations, some of them localized to the opening of substrate binding tunnel, a presumed site of fatty-acyl head group binding[95].

The acyl-lipid mFAD regiospecificity was shown to be controlled by regions or individual amino acid residues which are located in the mFAD primary structure adjacent to the conserved histidine motifs[84,96,97], in the third predicted transmembrane helix[98], or in the region between the first and second conserved histidine-rich motif[99].

The analysis of effect of targeted mutagenesis on plant acyl-lipid mFAD stereospecificity highlighted four amino acid residues, each of them capable of substantially shifting the E/Z ratio of desaturated products[100]. Mutagenesis of a plant acyl-lipid mFAD exhibiting conjugase activity indicated that two amino acid residues adjacent to the first histidine-rich conserved region cooperatively influence the ratio of produced conjugated *E*/*Z* isomers *Z*9,*E*11,*Z*13-18:3 and *Z*9,*E*11,*E*13-18:3[101].

The shift in of chemispecificity, i.e. shift from desaturation to hydroxylation[58,80] reaction, requires in acyllipid mFADs as little as single amino acid residue substitution localized to the proximity of the conserved mFAD histidines. The mFAD catalytic plasticity, i.e. the ability to change the chemispecificity as a result of limited number of amino acid substitutions, is proposed to substantially contribute to the plant lipid diversity[58]. Another example of mFAD catalytic plasticity is the shift of enzymatic activity in a plant acetylenase towards desaturase activity following one to four amino acid mutations. However, these mutations are localized to mFAD structural features distinct from those which influence hydroxylation/desaturation ratio[100].

Yet another mechanism of control of mFAD regiospecificity, which was identified in plant acyllipid mFAD, is represented by the identity of the lipidic substrate head group which can influence the regiospecificity of the desaturation reaction[102].

The crystal structures provided a direct experimental evidence for a kinked narrow hydrophobic substrate binding tunnel which extends approximately 24 Å into the enzyme interior and binds fatty acyl tail of fatty acyl-CoA substrate (Figure 1). The binding of fatty acyl-CoA is further mediated by interaction of polar CoA substrate moiety with residues at the enzyme surface in the vicinity of substrate binding pocket[64,65]. The carbon atoms C9 and C10 of the fatty acyl substrate moiety are positioned in the binding tunnel in proximity of di-iron active center, resulting in the Z9-regioselective and stereoselective desaturation (Figure 1D). The kink in the binding tunnel, however, acts also as barrier which hinders the binding and release of fatty acyl substrate and product, respectively. One plausible mechanism of the substrate insertion and product egress from the narrow kinked binding tunnel is the breakage of hydrogen bond between the kink-forming amino acid residues[65].

To summarize, substantial research efforts led to identification of sequence determinants of mFADs specificity in diverse organisms. However, the absence of experimental structure or a reliable mFAD homology model until recently precluded formulation of a definite hypothesis on mechanism of specificity determination. Instead, these studies mainly correlated specificity determinants with predicted mFAD structural features such as transmembrane helices or conserved histidine-rich motifs. Importantly the mutagenesis experiments concordantly indicated that all specificity modes of mFADs can be substantially influenced by a small number of amino acid residue substitutions.

1.2.2 Soluble fatty acyl desaturases (sFADs)

The much easier purification of sFADs facilitated the determination of the sFADs crystal structures[68,69]. The sFAD crystal structures showed that each monomer of the sFAD homodimer has a bent hydrophobic cavity extending into the enzyme interior (resembling the substrate tunnel in mFADs) (Figure 2).

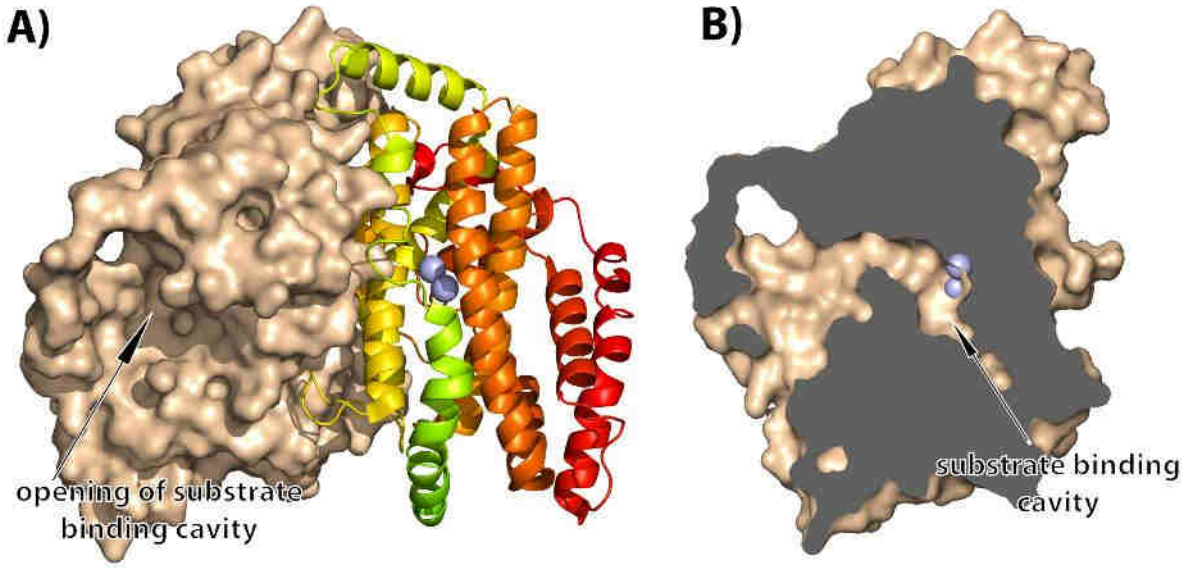

Figure 2. The crystal structure of Z4-sFAD from English ivy (*Hedera helix*). (A) The sFAD homodimer model rendered to show the enzyme surface (left monomer) and secondary structure features (right monomer). Two active center iron atoms (light-blue spheres) are visible in the right monomer. **(B)** The cross section of sFAD monomer showing an unoccupied substrate binding cavity and two iron atoms of the active center localized in the vicinity of the kink in the substrate binding cavity. The structure models were rendered in PyMOL Viewer software[71] using Z4-sFAD crystal structure (Protein Data Bank code 2UW1)[68].

The fatty acyl-ACP substrate is presumably inserted into the substrate binding cavity with the methyl end first leaving the ACP substrate moiety interacting with the surface-exposed amino acid residues[68,69,103]. The presence of active center consisting of di-iron center coordinated by histidine residues, and glutamate carboxylate groups which form carboxylate-bridged di-iron active center places sFADs into class I di-iron protein family, together with enzymes which catalyze diverse oxygen-dependent reactions, such as hydroxylation (soluble methane monooxygenase[104] and toluene/o-xylene monooxygenase [105]), aryl amine oxidation (p-aminobenzoate N-oxygenase[106]), synthesis of deoxyribonucleotides (ribonucleotide reductase R2)[107], and epoxidation (benzoyl-CoA epoxidase)[108] (reviewed by [49,109,110]). sFADs provided hypothetical models for the architecture of substrate binding region in mFADs although the early experiments indicated that the substrate binding channel of mFADs is able to accommodate substrates with bulky side chains in contrast to sFADs, indicating that the substrate binding site might have fundamentally different architecture in mFADs and sFADs[111].

1.2.2.1 sFAD enzymatic specificity determinants

Given the extensive similarities of substrate binding site and di-iron active center architecture of mFADs and sFADs, we will briefly summarize also studies of specificity

determinants in sFADs as these provide insights into desaturase specificity determinants presumably transferable also to mFADs. In sFADs, the length of substrate binding channel from the enzyme surface to the di-iron active center was proposed, based on the sFAD crystal structure, as a plausible determinant of position of introduced double bond with respect to the carboxy terminus of the fatty acyl-ACP substrate; the length of substrate binding channel from the active center to the end was proposed to influence the preferred fatty acyl chain length. The geometry of fatty acyl substrate is presumably constrained by the bend in the substrate binding channel which explains the *Z*-stereospecifity of the crystalized sFADs[68,69]. The substrate chain length selectivity for 18 carbon atom long acyls over shorter fatty acyls was correlated with the higher hydrophobic binding energy of longer fatty acyls[112].

Discrimination of fatty acyl substrate chain length was demonstrated to be controlled by the volume of amino acid residues at the bottom of the substrate binding cavity. In site-directed mutagenesis experiments, sFAD mutants with bulkier and smaller residues in this region exhibited increased preference towards shorter and longer fatty acyl chains, respectively[113]. The critical role of residue volume at the bottom of sFAD substrate binding channel was confirmed also in additional mutagenesis experiments[114,115]

The regiospecificity of sFADs was demonstrated to be controlled by regions localized distantly to the active center, i.e. by charged residues at the opening of substrate binding cavity that interact with the negatively charged residues of ACP substrate moiety. In this structure-aided study, substitution of negatively charged residues for positively charged residues switched Δ9 and Δ4 regiospecificity presumably by influencing the depth of insertion of fatty acyl into the substrate binding tunnel[103]. Combination of amino acid substitutions at the end of substrate binding channel and in the ACP-binding site at the opening of the substrate binding channel triggered even more profound changes in the reaction outcome of Z9-sFAD, resulting in introduction of hydroxyl group and double bond isomerization in the sFAD products. The novel enzymatic activities of this sFAD mutant were rationalized by modified positioning of the substrate with respect to the active center, which results in shift of the site of the initial hydrogen removal and subsequent hydroxyl rebound[116].

1.3 Pheromones

Exchange of information between an organism and its environment is one of the characteristics of life. Chemical compounds probably represent the evolutionary first communication medium used by aquatic and terrestrial organisms.

Pheromones, a large class of chemical signals which mediate communication between organisms of the same species[3], presumably evolved from metabolites leaking from the organism and this evolutionary transition occurred independently many times as is indicated by the diversity of *i)* specialized cells, glands and organs used for production and detection of chemical signals, *ii)* chemical compounds serving as pheromones, *iii)* physiological and behavioral responses which pheromones trigger in organisms, and *iv)* by the wide phylogenetic distribution of pheromone communication in eukaryotic organisms. Pheromones serve as one of communication channels in extant terrestrial and aquatic organisms including insects, mammals, reptiles, amphibians, birds, and marine invertebrates[117].

The pheromone diversity is reflected by the numerous criteria according which they can be categorized. According to the character of their biological effect, pheromones can be classified as releaser and primer pheromones. Releaser pheromones trigger rapid and temporary changes in behavior whereas primer pheromones cause long-lasting changes of behavior and physiology. Hundreds of releaser pheromones from thousands of organisms are known but much less primer pheromones are described, mainly because of the difficulties connected with assaying of their mainly physiological effects on organisms. Pheromones can be further classified according to the biosynthetic origin of the compound or according to the particular biological function they serve[117]. In this thesis we will focus on FA-derived releaser pheromones which are used by insects to find a partner of the same species for mating – i.e. sex pheromones.

1.3.1 Insect pheromones

Pheromones are involved in intraspecific communication in diverse prokaryotic and eukaryotic organisms, presumably also humans[118], but particularly in insects they serve a variety of functions and influence almost all aspects of the insects lives including attraction of mating partners; communication of imminent danger; providing navigation cues for orientation and foraging; marking the fertility and dominance status, sex or relatedness; and organizing social insect communities[117].

The pheromone communication system generally involves pheromone producer which biosynthesizes and secretes the pheromone on its surface or into its environment, and a conspecific pheromone receiver which detects the signal, neurally processes it and responds via a change in its behavior or physiology[119].

Based on their chemical structure, pheromones can be classified as acyclic hydrocarbon chains (branched or unbranched, with various functional modifications, with or without

heteroatoms), lactones, aromatics, and heterocycles. According to their biosynthetic origin, insect pheromones can be classified as FAs and their derivatives, polyketides, terpenoids, derivatives of amino acids and peptides, derivatives of diet-acquired alkaloids, and compounds of mixed biosynthetic origin[44].

A comprehensive review of the almost ubiquitous insect pheromones is beyond the scope of this thesis. Below we rather provide examples of those insect pheromones which were studied with respect to their biosynthesis with a focus on FA-derived insect sex pheromones (SPs) (Figure 3). We define SPs here as either male or female-produced compounds and their mixtures which attract mating partner of the same species, encourages it for mating or triggers other behavioral response related to reproduction. SPs are possibly the most studied pheromone class thanks to the extensive research of moth female FA-derived SPs and of cuticular hydrocarbon SPs present across insect orders.

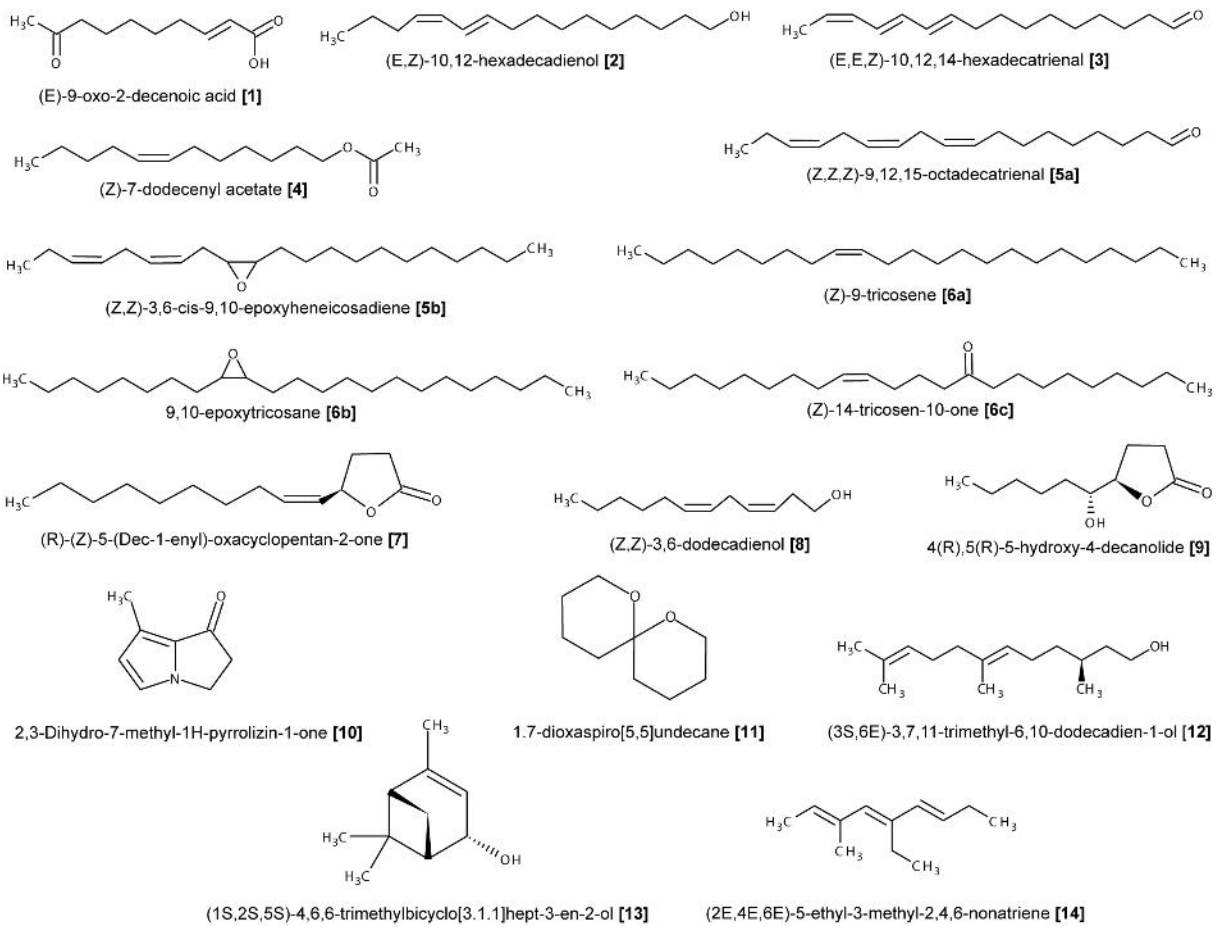

Figure 3. Examples of FA-derived [1-9] and non-FA-derived [10-13] insect pheromones and pheromone components. [1] Honeybee (*Apis mellifera*) queen sex pheromone and major component of honeybee retinue pheromone; [2] bombykol, female silkmoth (*Bombyx mori*) sex pheromone; [3] an essential component of the tobacco hornworm moth (*Manduca sexta*) female SP; [4] SP of the cabbage looper moth (*Trichoplusia ni*); [5a-b] female SP components of the saltmarsh caterpillar moth (*Estigmene acrea*); [6a-c] major and minor components of the common housefly (*Musca domestica*) female cuticular hydrocarbon SP; [7] japonilure, female SP of some Scarabaeidae beetles; [8] trail pheromone and SP of a termite *Ancistrotermes pakistanicus* (Termitidae, Macrotermitinae); [9] major male SP component in *Nasonia* parasitic wasps; [10] danaidone, major male SP component of many danaid butterfly species; [11] spiroacetal compound used as female SP in the olive fly *Bactrocera oleae*; [12] (S)-2,3-dihydrofarnesol, major component of the buff-tailed bumblebee (*Bombus terrestris*) male marking pheromone; [13] cis-verbenol, a major aggregation pheromone component in many bark beetles; [14] the principal component of the nitidulid beetle *Carpophilus freemani* aggregation pheromone;. Structures redrawn according to[44,120,121].

1.3.1.1 Non-FA-derived insect pheromones

Terpenoids (also called isoprenoids), i.e. derivatives of compounds consisting of one or more isoprene units, are among the most widespread and diverse groups of insect secondary metabolites. In many bark beetle species (Coleoptera: Scolytinae), economically important

pests of conifer trees, terpenoids are used as major components of aggregation pheromones attracting both sexes to a host tree to overwhelm the host tree defense[122]. Terpenoids are also components of bumblebee male marking pheromones used to attract virgin bumblebee queens (compound [12] in Figure 3)[123] (see chapter 2.3.1.2 - FA-derived insect pheromones for further details on bumblebee pheromones).

Another vastly diverse group of insect pheromones are (putative) polyketides. These compounds have often unclear biosynthetic origin but based on their structure they are proposed to be produced by polyketide synthases (PKS) which catalyze condensation of carboxyl units, analogously to fatty acid synthases (FASs). In contrast to FASs, PKSs can produce much more complex chemical structures than FASs[124]. Polyketides serve a variety of biological roles in diverse insects, such as male-produced aggregation pheromones or female-produced SPs in various anobiid beetles (Coleoptera: Anobiidae) (compound [14] in Figure 3); alarm and trail pheromones in ants; or SPs in some flies (compound [11] in Figure 3)[125].

Some insects also modify complex chemicals from their diet to produce pheromones such as some lepidopteran males including danaid butterflies (Lepidoptera: Danaidae) and tiger moths (Lepidoptera: Arctiinae) which transform plant pyrrolizidine alkaloids to volatile SPs (compound [10] in Figure 3)[126] or bark beetles which produce some of their aggregation pheromone components by modification of diet-acquired compounds (i.e. of host tree derived α-pinene or heptane) (compound [13] in Figure 3)[122].

1.3.1.2 FA-derived insect pheromones

FA-derived pheromones are the most common pheromone structural theme in insects involved in diverse biological contexts[44], represented by thousands of described compounds and their mixtures. Depending on the chain length, unsaturation and presence of oxygenated groups, FA-derived pheromones function either as volatile compounds for communication at long-range, or, less volatile compounds function as contact or short-range pheromones**.** The contact pheromones are mainly represented by cuticular FA-derived hydrocarbons and function as nestmate- and reproductive status clues in complex interactions between social insects. In non-social insects they serve mainly as species- or gender-recognition signals[127,128]. In contrast, volatile FA-derived pheromones, such as female moth SPs, generally function as long-range attractants.

Moths and butterflies (Lepidoptera)

Finding of a conspecific mating partner is in majority of noctuid lepidopterans – moths mediated by female-produced SPs. Two major types of female moth SPs are recognized – i) saturated or unsaturated C10-C18 straight-chain FA- derived aldehydes, alcohols and acetates (compounds [2-4] in Figure 3), and ii) C17-C23 UFA-derived hydrocarbons and their epoxides (compounds [5a-b] in Figure 3)[13]. The former female moth SP class accounts for cca 75% of identified female moth pheromones[11] and represents thus probably the most studied type of insect pheromones, being described from hundreds of moth species[12] where they act as long-range SPs.

Butterflies, i.e. lepidopterans with day activity, use visual signals rather than pheromones as the principal mating cues[129], but FA-derived SPs were found to be used in some butterfly species as components of male short-range SPs[130].

Ants, wasps and bees (Hymenoptera)

In social hymenoptera, i.e. ants, and social wasps and bees, a spectrum of FA-derived pheromones - particularly hydrocarbons but also free FAs and FA-derivatives with oxygenated functional groups, FA-derived alcohols and esters function in coordinating the complex interactions among the members of the insect society[131]. I will briefly review their spectrum and functions in the honeybee (*Apis mellifera*).

In the honeybee, pheromones constitute the most complex described pheromone communication system in insects[132,133]. Many of the honeybee pheromones include FA derivatives. These are i) the queen retinue pheromone, a blend of short-chain hydroxy-FAs, FA-derived alcohols, methyl esters and free FAs, and non-FA-derived compounds. The components of queen retinue pheromone act in synergy or as individual components as both primer and releaser pheromone regulating many aspects of the bee colony organization and function also as a long-range SP attracting honeybee males for mating (compound [1] in Figure 3)[134,135]; ii) fatty acyl ethyl esters produced by foraging bee workers to inhibit the transition of bee workers from nurses to foragers[136]; iii) brood pheromone consisting of mixture of fatty acyl ethyl esters and non-FA-derived compounds produced by bee larva which triggers a range of behavioral and physiological responses in bee workers[137–139]; iv) cuticular hydrocarbons contributing to recognition of honeybee nestmates[140]; and v) certain cuticular hydrocarbons produced by foraging bees performing waggle dance serving as an additional signal to recruit foragers to a food resource[141].

In majority of bumblebee species, primitively eusocial bees, FA derivatives in form of both saturated and unsaturated alcohols, ethyl esters and aldehydes are components of complex

labial gland secretion, termed marking pheromones, which are deposited by males on prominent objects to attract and arrest conspecific virgin females and thus mediate mating[123]. Despite the absence of behavioral assay for the individual compounds of labial gland extract, the FA derivatives are presumed to be biologically active components of the marking pheromone since i) isolated virgin bumblebee queen antennae respond in electroantennogram recordings to the FA-derived components[142,143] and ii) FA-derivatives represent the major components in the labial gland secretion of some bumblebee species such as the while-tailed bumblebee *Bombus lucorum*[144,145] and the red-tailed bumblebee *B. lapidarius*[146].

In parasitic wasps of the genus *Nasonia*, males use FA-derived lactones as SPs (compound [9] in Figure 3)[147,148].

Flies (Diptera)

Research on the house fly *Musca domestica* and *Drosophila* flies followed by research on other economically important dipteran species indicates that many fly species use saturated or unsaturated very long chain FA- derived cuticular hydrocarbons (more than 20 carbon atoms) and corresponding epoxides and ketones as contact pheromones mediating a broad range of behavioral effects connected to mating such as species and sex recognition (compounds [6a-c] in Figure 3). The courtship signals in flies are, however, complex, and in numerous fly species visual and acoustic stimuli accompany or replace the pheromone stimuli[149].

Cockroaches and termites (Blattodea)

Cuticular contact pheromones in form of saturated long chain methyl-branched ketones are used by females of the German cockroach *Blattella germanica* to mediate sex and species recognition and induce courtship[44,150].

In termites (Blattodea: Isoptera), eusocial insect group taxonomically positioned within cockroaches, cuticular hydrocarbons play a range of roles in colony organization similar to those in social Hymenoptera and they also serve as trail marking pheromones involved in navigation of nestmates (compound [8] in Figure 3)[131].

Beetles (Coleoptera)

Beetles are with over 350,000 described species and up to several millions of presumably undescribed species the largest animal group. Their diversity is reflected by the diversity of their pheromone chemical structures[151]. Beetles frequently employ also FA-derived

pheromones such as hydroxy-FA-derived lactones functioning as female SPs in many scarab beetles (Coleoptera: Scarabaeidae)[152] (compound [7] in Figure 3) or cuticular hydrocarbons in longhorn beetles (Coleoptera: Cerambycidae) serving as female contact SP[153].

1.4 Biosynthesis of insect FA-derived sex pheromones (SPs)

FA-biosynthetic and FA-modifying enzymes, which in insect biosynthesize ubiquitous FA-derived constituents of cellular membrane lipids, storage lipids, and protective cuticular waxes and hydrocarbons[154], presumably served as a genetic pool from which pheromone biosynthetic enzymes evolved via divergence of the original functions[155].

Pheromones are produced in a variety of glandular cell types classified based on the route which pheromones follows to cross the cuticular barrier, such as glandular cells localized under the cuticle versus cells which are connected with the insect exterior via a duct. Glandular cells, which localize to a discrete area, form pheromone glands, which can either include a reservoir to store the pheromone for later release (such as bumblebee male labial glands) or releases the pheromone immediately upon biosynthesis (e.g. female moth SP glands)[156].

The research of FA-derived SP biosynthesis in a limited number of model insect species, i.e. cuticular hydrocarbons in cockroaches, flies and bees[127], and female SPs in moths[157] indicates that the species-specific pheromone structure or pheromone blend composition is a result of combination of several conserved biosynthetic steps acting in a particular order[157] (Figure 4). Each of these steps exhibit distinct binding or catalytic selectivity and contribute to the unique pheromone compound structure or pheromone blend composition. Notably, selectivity in each biosynthetic step can differently contribute to the final pheromone composition - some of the steps are highly selective whereas others accept and transform broad spectrum of pheromone precursors[158,159].

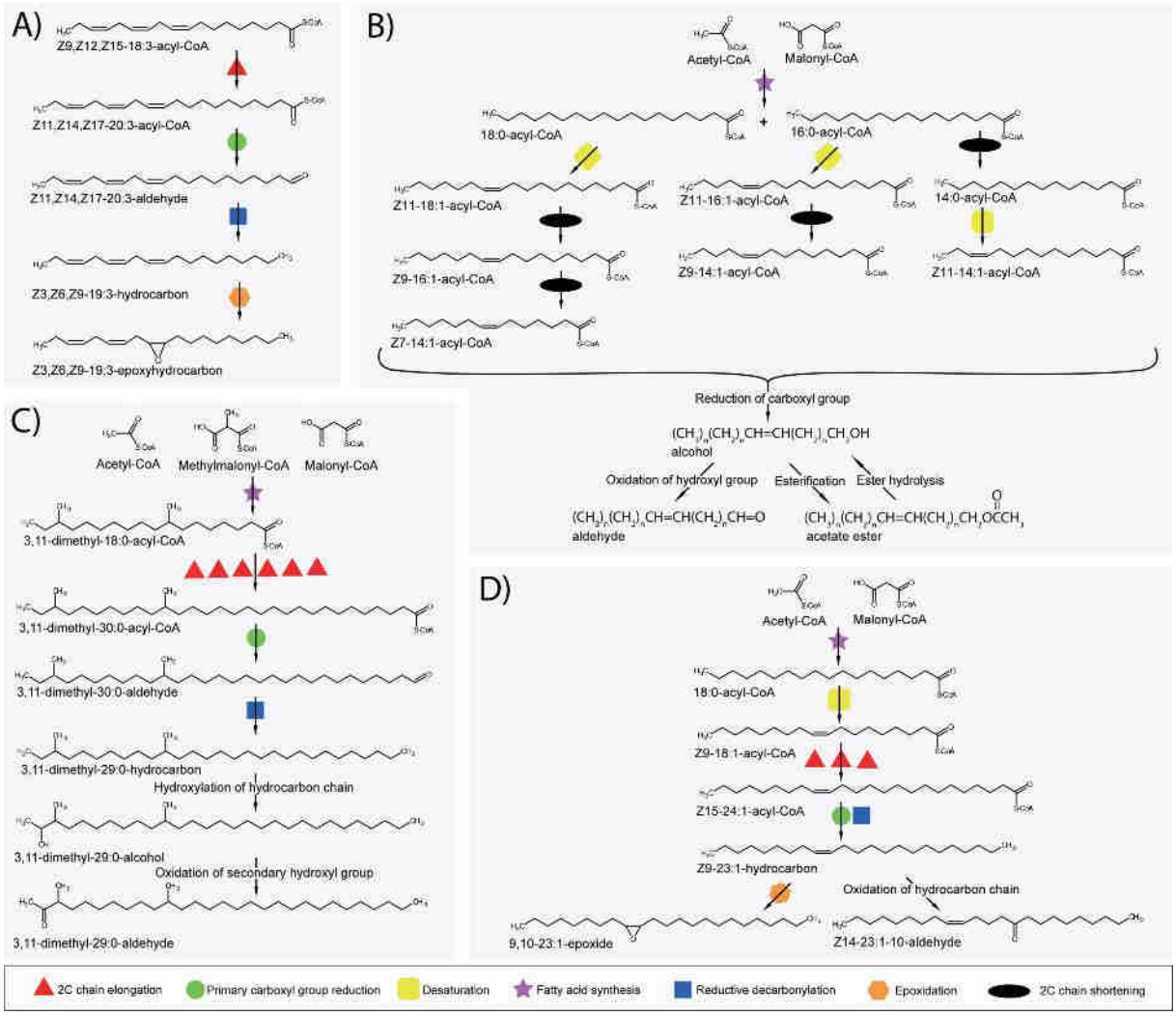

Figure 4. Representative examples of FA-derived pheromone biosynthetic pathways in moths (Lepidoptera; A and B), cockroaches (Blattodea; C), and flies (Diptera; D). (**A**) Biosynthesis of salt marsh caterpillar moth (*Estigmene acrea*) female SP from diet-acquired PUFA. (**B**) A general biosynthetic scheme of moth female SPs illustrating how alternative orders of FA chain shortening and desaturation steps combined with modification of the primary oxygenated functional group generate diverse SP structures. For clarity, only one desaturation step (with *Z*11 regiospecificity) is shown. (**C**) Biosynthesis of the female German cockroach (*Blattela germanica*) SP. (**D**) Biosynthesis of the female housefly (*Musca domestica*) SP. The pheromone biosynthetic schemes were adapted from[157].

The first pheromone biosynthetic step is *de novo* biosynthesis of FA. The length of synthesized FA chain is influenced by either the specificity of fatty acid synthases (FASs), by activity of FA elongases (which are of particular importance in the biosynthesis of the C20+ long cuticular hydrocarbons[127]), by β-oxidation resulting in FA chain shortening, or by combination of these mechanisms. Notably, a distinct class of membrane-bound FASs, rather

than the ubiquitous soluble cytosolic FASs, is involved in biosynthesis of methyl-branched hydrocarbons[160–162]. The composition of pool of FAs available for pheromone biosynthesis can be further influenced by extracellular uptake of long FAs[163], synthesis of FA-storing triacylglycerols[164,165], and selective release of FAs from their storage (or transport) form[166]. As a deviation from the *de novo* FA biosynthetic scheme, some moths biosynthesize FA-derived SPs from diet-acquired polyunsaturated FAs[167] which are either in form of pheromone precursor or as a final pheromone compounds transported to the pheromone gland[168].

Subsequent SP biosynthetic steps generally involve modifications of the fatty acyl hydrocarbon chain, i.e. introduction of double or triple bond(s), or introduction of oxygenated groups such as hydroxyl or epoxide groups. After this step, additional round(s) of β-oxidation can shorten the hydrocarbon chain of fatty acyl pheromone precursors. The order of chain shortening and hydrocarbon modification steps is of particular importance as it defines the position of the modifications along the fatty acyl hydrocarbon chain in the final pheromone compound[157].

Next, the primary carboxyl group of fatty acyls can be esterified to e.g. ethyl esters, reduced to alcohol (which can be further esterified to e.g. acetate) or to aldehyde. Aldehydes can be reductively decarbonylated to hydrocarbons. The FA-modifying enzymes generally accept as substrate fatty acyl-CoA rather than free, non-activated FAs[157].

Some of the pheromone biosynthetic proteins were studied both *in vivo* and, using isolated genes and proteins, also *in vitro*, i.e. mFADs (see further below), fatty acyl reductases involved in production of fatty alcohols[158,169–176], acyltransferase involved in synthesis of FA-storing triacylglycerols[165,177], lipases involved in hydrolytic release of FA pheromone precursors from storage triacylglycerols[166,178,179], lipid storage droplet protein involved in activation of triacylglycerols for hydrolysis[180], long chain acyl-CoA binding protein presumably involved in protecting fatty acyl-CoA against hydrolysis and establishment of a cellular fatty acyl-CoA pool[181], fatty acid transport proteins mediating extracellular uptake of FAs[163], and cytochrome P450 enzyme involved in reductive decarbonylation of FAs to hydrocarbons[182].

For majority of the pheromone biosynthetic steps, however, the genes and enzymes remain to be identified and characterized, i.e. enzymes catalyzing FA elongation [183,184] and FA chain shortening[15,134,185,186], epoxide group formation[187,188], acetate ester formation [159,189], oxidation of fatty alcohols to aldehydes[190–193]; lipophorins transporting hydrocarbon pheromone precursors[168]; and enzymes involved in FA biosynthesis - acetyl-CoA carboxylase[194] and fatty acid synthase (FAS)[195].

Among the pheromone biosynthetic enzymes, the most attention received mFADs. The research focus on pheromone biosynthetic mFADs is in part result of the sequence conservation of mFAD sequences which facilitated isolation of desaturase genes from a broad range of species and their subsequent study. But despite this research bias, diverse enzymatic specificities of mFADs are now recognized as key contributors to the diversity of female moth SPs and important players in biosynthesis of cuticular hydrocarbon profiles in many insect families (see also chapter 2.5.1.2.1 – Evolution of insect mFADs).

1.5 Evolution of insect FA-derived SPs

The diversity of FA-derived SPs has been documented on thousands of insect species[12], but the molecular mechanisms as well as the ecological selective forces underlying this diversity remain not well understood.

Presumably a key ecological driving force for SP divergence is the role of species-specific SP composition as a pre-mating reproductive barrier which prevents hybridization between closely related sympatric species, i.e. species co-occurring in the same geographic area[196,197]. Notably, the divergence of cuticular hydrocarbon SPs was demonstrated in two related *Drosophila* species which were experimentally kept in sympatry, representing thus a rare experimental evidence of the evolutionary selection towards SP diversification[198]. The change in pheromone composition can also be an adaptation to prevent eavesdropping on pheromone communication by parasites and predators[199] as was proposed for the distinct terpenoid pheromone composition in two bark beetle (Coleoptera: Scolytidae) populations in response to the pressure exerted by predatory clerid beetles (Coleoptera: Cleridae)[200]. Similar mechanism might presumably shape also composition of FA-derived SPs[197]. Also the physiochemical properties of the pheromone compounds can be under differential selective pressure exerted by the environment as was proposed and then also experimentally demonstrate for *Drosophila* cuticular hydrocarbon SPs which besides serving as a chemical signal also protect the insects from desiccation[201,202 203].

A major conundrums of SP composition evolution is the genetic mechanism which maintains the high attractiveness and species-specificity of the signal[204] but at the same time enables rapid evolution of SP composition[197]. A physical linkage between genes controlling signal production and signal reception would facilitate a rapid and evolution of the signal, as is the case of acoustic sexual communication in crickets[205]. A linkage between female pheromone production and male pheromone response was experimentally rejected in moths[206–208] although some evidence supports a common genetic basis of signal production and response in

Drosophila[209,210]. As an alternative explanation for coordinated evolution of the signal and response, research on SPs in moths helped establish asymmetric tracking as a major hypothetical mechanism of SP diversification[211]. The hypothesis assumes that the asymmetry in parental investments (larger investment of female and smaller investment of male moths) results in lower selection pressure exerted on the female-produced signal than on the male response. This evolutionary model would enable much higher variance in female moth pheromone composition than have been previously assumed[212]. An abrupt "saltational" change in female SP composition would result in a distinct SP that attracts males with more broadly or differentially tuned SP preference – so called "rare males"[211–214]. Strong argument for non-gradual change in SP composition is that small gradual changes might not establish an efficient reproductive barrier to prevent hybridization of related sympatric species. Assortative mating (the preferential mating of females producing a novel SP with males attracted by this SP) could then restrict gene flow between subpopulations with distinct SP which can ultimately lead to fixation of a novel SP composition and possibly speciation. The model of asymmetric tracking, however, does not explain how new female SP can become fixed if only few rare males respond to it[31]. Also challenging is to demonstrate the direct role of SP diversification in speciation by study of SP differences in isolated species, as the observed differences in SP communication might have accumulated only after the speciation event[31].

The asymmetric tracking is considered as a potential speciation mechanism in moths[215] and flies[203]. Saltational shift in pheromone composition was shown to be characteristic also for the non-FA-derived aggregation pheromones of bark beetles (Coleoptera: Scolytinae)[216]. The reproductive barrier imposed by SP communication system can be further strengthened and fine-tuned by behavioral antagonists, i.e. pheromone components which acts as deterrent for non-conspecifics[217].

In contrast to SPs, other pheromones such as trail pheromones used for navigation or alarm pheromones used to signal danger in ants and termites are not required to be highly species specific and divergence of these types of pheromones in different species may mainly represent adaptations to different habitats[218].

1.5.1 Molecular basis of insect FA-derived SP evolution

1.5.1.1 Signal receiver

In this thesis we focus on production of pheromone signal. The understanding of mechanisms driving diversity of the signal receivers' preference is, however, equally important for understanding of the SP evolution[31,197].

The pheromones are detected by olfactory sensory neurons (localized to the olfactory sensillas in antennae or in some insect groups such as Diptera also to maxillary palps) in a process involving odorant binding proteins and pheromone receptors[219]. Besides the pheromone receptor genes which are obvious and relatively easily testable candidates for SP preference divergence, male pheromone preference might diversify also via changes in other components of the neurophysiological pathway[31].

Multiple lines of evidence support the plasticity of moth male response to female SPs. Male moths *Adoxophyes honmai* were found to exhibit broadened pheromone preference in field and laboratory conditions by exposition to large quantities of synthetic pheromones[220]. In male *Trichoplusia ni* moths, their pheromone preference broadened after 49 generations of laboratory rearing with females producing abnormal pheromone blend[221]. In the population of European corn borer moth males (*Ostrinia nubilalis*), rare males exist which are attracted by the SP of the related Asian corn borer moth (*O. furnacalis*)[213]. Finally, *in vitro* characterization of odorant receptors of male *Ostrinia* moth indicated that a single aa substitution can alter the pheromone specificity of the receptor[222].

1.5.1.2 Signal producer

Experimental evidence from research on fruit flies[27,203,223], recent pioneering work on male wasp SPs[147] but particularly the amassed knowledge on moth SP communication (see further below) indicate that the divergence of enzymatic specificities or regulation of SP biosynthetic enzymes, including FA chain-shortening enzymes, FARs, and FADs, can underlie SP signal divergence and potentially speciation. Changes in FA chain-shortening was associated with changes in SP composition in several moth species[186,224,225], however the respective genes remain to be identified and functionally characterized. In contrast, FAR[171,174] and FAD genes responsible for the shift of SP composition were previously isolated and the respective enzymes functionally characterized.

1.5.1.2.1 Evolution of insect mFADs

The mFAD gene family in insects presumably expanded before the divergence of the lepidopteran and dipteran lineages between 330 and 350 million years ago[226] and particularly in flies and moths underwent extensive diversification under the birth-and-death evolutionary model, that is, mFADs underwent numerous gene duplications and some of the gene duplicates stayed active whereas some were inactivated or deleted from the genome[227,228]. Subsequent divergence of the mFADs gave rise to a functionally diverse mFAD multigene family which substantially contributes to the diversity of pheromone structures and pheromones blends used

by extant moth species[155,229,230]. Similarly, the mFAD gene family expanded also in ants (Hymenoptera: Formicidae), presumably in connection with their role in chemical communication[231].

Research of moth female SP biosynthetic genes led to characterization of more than 50 lepidopteran mFADs clustering into multiple well-supported clades including two evolutionary distinct classes of mFADs exhibiting *Z*9-desaturase specificity and multitude of functionally diverse classes, the largest of them encompassing *Z*11-mFADs[229] (Figure 5).

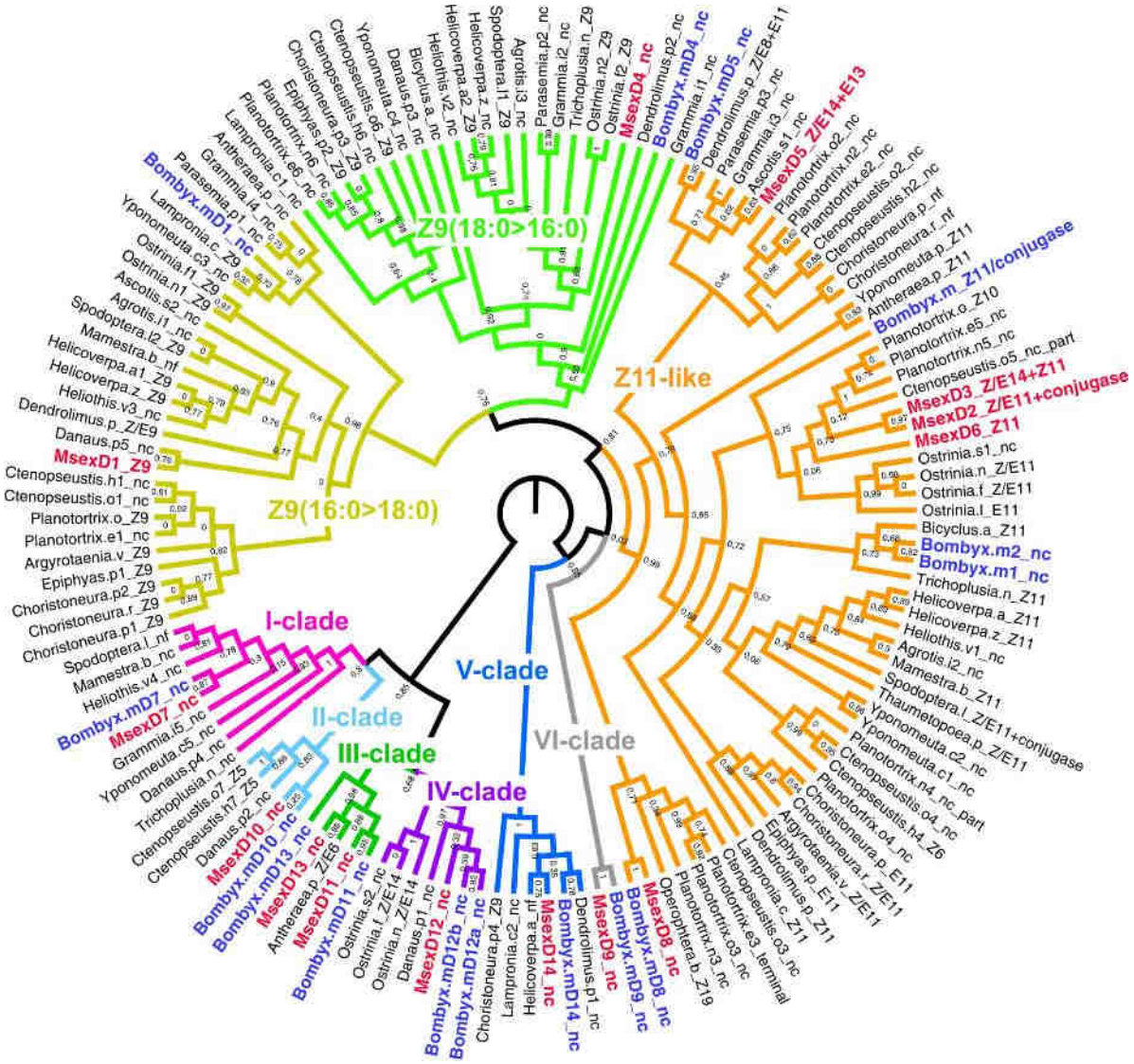

Figure 5. Lepidopteran mFAD gene family tree. Phylogenetic tree showing the relationships between lepidopteran FADs. *M. sexta* desaturases are highlighted in red. *B. mori* desaturases are highlighted in blue. Eight highly supported clades are colored and named. FADs are named by the genus and a single letter abbreviation of the source species name followed by designation of the mFAD specificity, when available, or by "nc" for mFADs that have not been functionally characterized or "nf" for mFADs that were functionally assayed but no desaturase activity was detected. Numbers along branches indicate branch support calculated by approximate likelihood ratio test (aLRT, minimum of SH- like and Chi2-based values). For GenBank sequence accession numbers and full species names, see SI Appendix,Table S2 in[232]. Figure adapted from[232].

In other insect species which use FA-derived pheromones, FADs have received considerably less attention. To date, very few non-lepidopteran FADs involved in pheromone production have been identified; such FADs have been reported in *Drosophila* (Diptera)[27,233] and the housefly *Musca domestica* (Diptera)[234]. We have identified Z9-FADs from bumblebee

species involved in biosynthesis of male marking pheromones[30,235] representing the only functionally characterized hymenopteran pheromone biosynthetic mFADs.

Besides pheromone-biosynthetic mFADs, Z9-mFADs involved in primary FA metabolism have been cloned and functionally characterized from the red flour beetle *Tribolium castaneum* (Coleoptera)[236] and the house cricket Acheta domesticus (Orthoptera)[237]. Two *Z*12-mFADs involved in biosynthesis of physiologically important polyunsaturated FAs were identified in the red flour beetle and the house cricket; these mFADs were proposed to evolve independently from the ancestral *Z*9-mFADs[238].

In *Drosophila* fly and several moth species, multiple genetic mechanism underlying mFAD activity diversification were established or proposed to play a role in the pheromone evolution, including activation of a nonfunctional FAD gene[213,239]; mFAD neofunctionalization, i.e. mFAD gene duplication followed by its functional divergence[240]; inactivation of mFAD gene[241], or differential regulation of FAD gene expression[27,242–245].

Together, the reviewed literature indicates that in Lepidoptera and Diptera, SP communication is, despite the presumed restrictions imposed on the pheromone signal producer and receiver, evolutionary surprisingly plastic. The genetic changes of pheromone-producing mFADs are recognized as one of the major yet not fully understood molecular mechanisms of the FA-derived pheromone evolution. In other insect orders, the molecular mechanisms of FA-derived pheromone evolution are understood to even a lesser extent.

2 Research aims

- To explore the molecular basis of the moth sex pheromone evolution *via* identification and characterization of the tobacco hornworm (*Manduca sexta*) fatty acid desaturases involved in biosynthesis of unusual triunsaturated sex pheromone components (Publication I).

- To elucidate the contribution of differential enzymatic selectivities and expression patterns of fatty acid desaturases to the species-specific composition of FA-derived male marking pheromones in three European bumblebee species (*Bombus terrestris*, *B. lucorum*, and *B. lapidarius*) (Publication II).

- To identify fatty acid desaturases involved in biosynthesis of polyunsaturated fatty acids in the opportunistic pathogenic yeast *Candida parapsilosis* and based on a comprehensive analysis of the fatty acid desaturase products revise the current classification of yeast desaturases (Publication III).

3 Publications

Publications included in the dissertation thesis

I. Buček A, Matoušková P, Vogel H, Šebesta P, Jahn U, Weißflog J, Svatoš A, Pichová I (**2015**) *Evolution of moth sex pheromone composition by a single amino acid substitution in a fatty acid desaturase.* Proc Natl Acad Sci **112**(41): 12586–12591.

II. Buček A, Vogel H, Matoušková P, Prchalová D, Záček P, Vrkoslav V, Šebesta P, Svatoš A, Jahn U, Valterová I, Pichová I (**2013**) *The role of desaturases in the biosynthesis of marking pheromones in bumblebee males.* Insect Biochem Mol Biol **43**(8): 724–31.

III. Buček A, Matoušková P, Sychrová H, Pichová I, Hrušková-Heidingsfeldová O (**2014**) *Δ12-fatty acid desaturase from* Candida parapsilosis *is a multifunctional desaturase producing a range of polyunsaturated and hydroxylated fatty acids.* PLoS One **9**(3):e93322.

Publications not included in the dissertation thesis

I. Prchalová D, Buček A, Brabcová J, Žáček P, Kindl J, Valterová I, Pichová I (**2016**) *Regulation of isoprenoid pheromone biosynthesis in bumblebee males.* ChemBioChem **17**(3), 260–267.

II. Bourguignon T, Šobotník J, Brabcová J, Sillam-Dussès D, Buček A, Krasulová J, Vytisková B, Demianová Z, Mareš M, Roisin Y, Vogel H (**2016**) *Molecular mechanism of the two-component suicidal weapon of* Neocapritermes taracua *old workers*. Mol Biol Evol **33**(3), 809–819

III. Buček A, Brabcová J, Vogel H, Prchalová D, Kindl J, Valterová I, Pichová I (**2016**) *Exploring complex pheromone biosynthetic processes in the bumblebee male labial gland by RNA sequencing*. Insect Mol Biol. **25**(3), 295-314

3.1 *Publication I:* Evolution of moth sex pheromone composition by a single amino acid substitution in a fatty acid desaturase

Background

Tobacco hornworm moth (*Manduca sexta*) females attract males by releasing a sex pheromone (SP) containing in addition to mono- and diunsaturated aldehydes, which are typical structural themes in SPs of Bombycoidea moths[12], also uncommon conjugated triunsaturated aldehydes. The production of triunsaturated SP components represents an easily traceable rare phenotype, thus making *M. sexta* a convenient yet unexploited model organism for unraveling the mechanisms of chemical communication evolution via novel SP component recruitment. In our previous attempts to decipher the desaturation pathway leading to triunsaturated SP precursors E10,E12,E14-16:3 and E10,E12,Z14-16:3 (3UFAs), we identified the *Msex*D2 desaturase, which exhibits Z/E11-desaturase and conjugase (1,4-dehydrogenase) activity and participates in stepwise production of monounsaturated SP precursors Z11-16:1 and E11-16:1 (1UFAs) and diunsaturated SP precursors E10,E12-16:2 and E10,Z12-16:2 (2UFA)[246]. The terminal desaturation step resulting in the third conjugated double bond and the respective enzyme remained, however, elusive[246,247].

Summary

In the search for FAD genes involved in pheromone biosynthesis, we performed RNA sequencing of *M. sexta* female PGs, the site of pheromone biosynthesis[247], as well as nonpheromone-producing tissues (female fat body, female labial palps, and larval midgut). We identified 14 desaturase transcripts, of which 4 were abundant and enriched in the PG: MsexD2, a previously characterized Z11-desaturase/conjugase involved in sequential biosynthesis of 1UFA and 2UFA pheromone precursors[246], and three FAD gene products, MsexD3, MsexD5 and MsexD6. We expressed the candidate pheromone-biosynthetic FADs in *Saccharomyces cerevisiae* and using GC/MS analysis of transesterified lipidic yeast extracts we determined the content of novel UFAs produced by the heterologously expressed FADs. MsexD3 and MsexD5 biosynthesized 3UFAs via E/Z14 desaturation from diunsaturated fatty acids (along with additional minor FA products) whereas MsexD6 produced Z11-18:1, a tentative precursor of minor *M. sexta* SP component. The substrates and products of *M. sexta* SP-biosynthetic FADs determined in yeast expression system were confirmed application of metabolic probes *in vivo* in the form of FAs and FAMEs to female *M. sexta* PGs, particularly demonstrating the biosynthesis of 3UFAs from E10,E12-16:2 *in vivo*. Sequentially highly similar yet functionally

diverse MsexD3 and MsexD2 were used in site-directed mutagenesis experiments to uncover their specificity determinants. Initial set of mutagenesis experiments highlighted the predicted fourth transmembrane helix as critical for desaturase specificity and subsequent mutagenesis of nonconserved aa residues in the transmembrane helix demonstrated that swapping of a single amino acid residue Ala224/Ile224 introduced E/Z14-desaturase specificity to mutated MsexD2 (and reciprocally, abolished E/Z14-desaturase specificity in mutated MsexD3). In protein structure models of MsexD2 and MsexD3, which we generated employing recently available structures of mammalian Z9-FADs[64,65] as a template in homology structure modeling, we showed that the residue Ala224/Ile224 contributes to formation of a kink in the substrate binding channel, which was hypothesized to be involved in the positioning of the fatty acyl substrate with respect to the di-iron active center[65]. These results demonstrated that a change as small as a single amino acid substitution in a pheromone-biosynthetic FAD might result in the acquisition of novel desaturase specificity potentially leading to recruitment of novel SP components (Figure 6). Reconstruction of FAD gene phylogeny indicated that MsexD3 was recruited for biosynthesis of 3UFA SP components in *M. sexta* lineage via gene duplication and neofunctionalization, whereas MsexD5 representing an alternative 3UFA-producing FAD has been acquired via activation of a presumably inactive ancestral MsexD5.

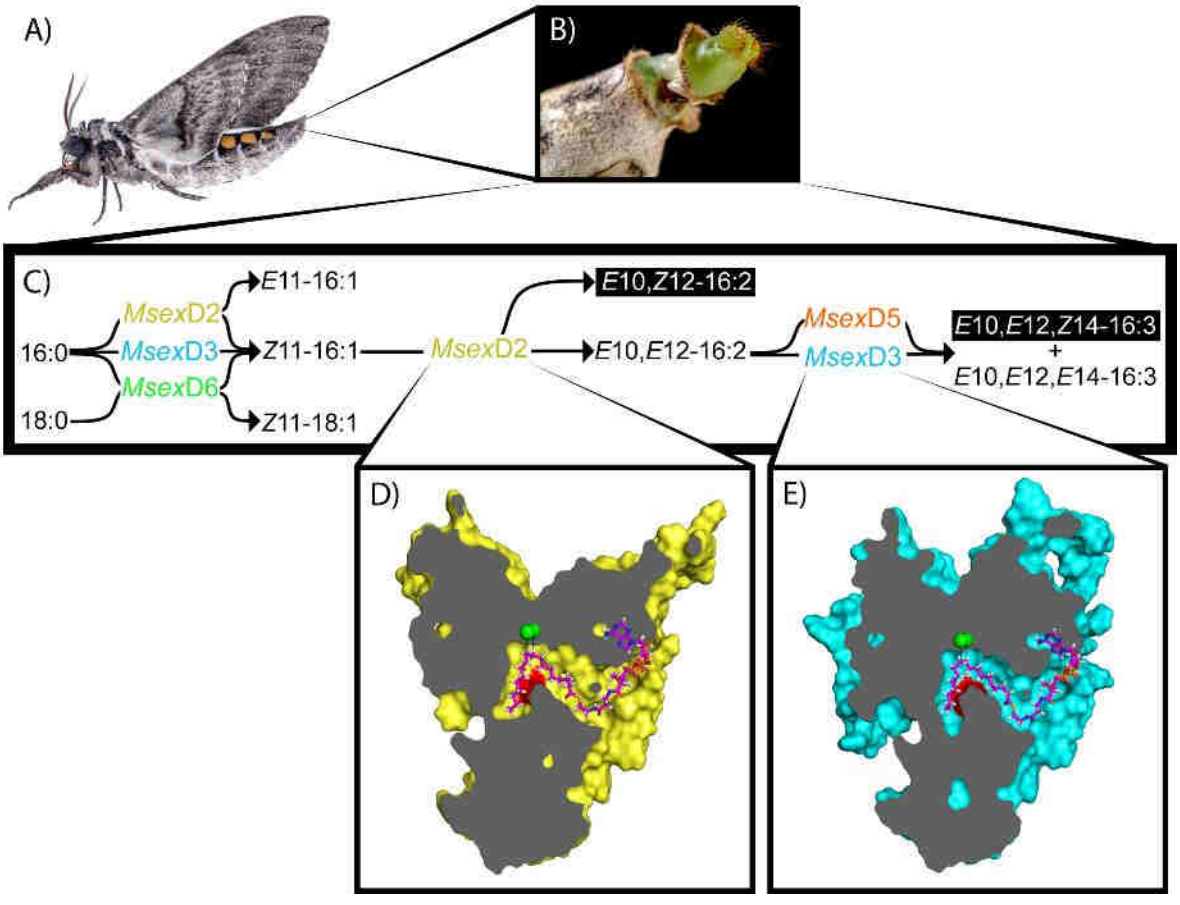

Figure 6: Reconstructed biosynthetic pathway of *Manduca sexta* UFA precursors of SP. *M. sexta* females **(A)** biosynthesize sex pheromones in the pheromone gland localized in the evertible abdominal tip **(B)**. We have identified pheromone-biosynthetic FADs and reconstructed the complete desaturation pathway leading to unsaturated FAs which serve as precursors of minor and major pheromone components including E10,Z12-16:2 and E10,E12,Z14-16:3 which are essential for attracting *M. sexta* males **(C)**. By site-directed mutagenesis of MsexD2 and MsexD3 we have identified a single amino acid residue Ala224 and Ile224, respectively, localized to the predicted fourth transmembrane helix of the FADs, which determines whether the desaturation outcome will be E10,Z12-16:2 or E10,E12,Z14-16:3. In the cut-through model of MsexD2 **(D)** and MsexD3 **(E)** generated by homology modeling using human Z9-FAD structure as a template, Ala224 and Ile224, respectively, is localized to the kink of the substrate binding channel and its surface exposed to the binding channel interior is highlighted in red. The channel is occupied by a hydrocarbon chain of fatty acyl substrate derived from the FAD structure used as a template for structure homology modeling. Adapted from[232].

My contribution

I have analyzed the RNA-seq data and identified the desaturase transcripts; isolated the coding regions of MsexD6 and five variants of MsexD5 and cloned them into yeast expression vectors; prepared part of the MsexD2 and MsexD3 mutants by site-directed mutagenesis and transformed them along with MsexD5s and MsexD6 into yeast strains; cultivated the yeast strains expressing all FADs and their mutants; isolated and analyzed FAME products by GC/MS; applied the isotopically labeled metabolic probes to *M. sexta* PG and analyzed the resulting isotopically labeled FAs and naturally occurring FAs in *M. sexta* PG by GC/MS; performed the phylogenetic analysis of moth FADs; wrote the draft of the manuscript.

3.2 *Publication II:* The role of desaturases in the biosynthesis of marking pheromones in bumblebee males

Background

In the majority of bumblebee species (Hymenoptera: Apidae: *Bombus*), the mate-finding and mating is mediated by so-called marking pheromones (MPs) which are deposited by males on prominent objects to attract conspecific females[123]. MPs are produced by the cephalic part of the male labial gland (LG) which fills large part of the male's head[146,248] and contrasts thus with female bumblebee LGs[249] or male honey bee (*Apis mellifera*) LGs which do not accumulate cephalic LG secretion[250]. MPs generally consist of terpenoids and fatty-acid-derived aliphatic compounds. The presence of unsaturated fatty-acid-derived MP components of various fatty acyl chain lengths which differ among bumblebee species led to hypothesis that these are in bumblebees produced via pheromone-biosynthetic FADs that exhibit species-specific substrate preferences, i.e. a pheromone biosynthetic route analogous to that in moths[251]. Our laboratory initiated efforts to establish male bumblebees as new model organisms for study of molecular basis of pheromone biosynthesis by a search for MP-biosynthetic FADs expressed in LG of three common European bumblebee species which differ substantially in their MP composition. That is, *i) Bombus terrestris*, an established greenhouse pollinator, which uses MP composed mainly of terpenoid compounds, *ii)* its sister species, *B. lucorum* (both *Bombus s.s.*), which uses Z9-14:1-derived ethyl esters (ethyl tetradec-9-enoate), and *iii) B. lapidarius*, representative of further related subgenus *Melanobombus*, which uses predominantly Z9-16:1 and 16:0-derived alcohols (hexadecanol and hexadec-9-enol). A single putative FAD coding region termed BlucNPVE was identified and cloned from *B. lucorum* LG cDNA. The functional characterization of BlucNPVE in yeast expression system demonstrated, that it codes for Z9-FAD which produces preferentially palmitic (Z9-16:1) and oleic acid (Z9-18:1) in the yeast expression system along with trace amounts of Z9-14:1. Production of only trace amount of Z9-14:1 in yeast expression system suggested that BlucNPVE is presumably not responsible for accumulation of Z9-14:1 which serves as a precursor of Z9-14:1-ethylester, the major *B. lucorum* MP component. Instead, it was proposed to be involved in primary metabolism[235]. The pheromone-biosynthetic FADs and the contribution of their distinct specificities to the species-specific MP composition remained elusive.

Summary

By employing RNA sequencing of *B. lucorum* and *B. terrestris* male labial glands and fat bodies (selected as a reference tissue), we identified five paralogous FAD-like genes. Two FAD paralogs were substantially more expressed in LGs than FBs of both species according to the RNA-seq data - BlucNPVE (identical to the FAD previously identified by Matoušková et al.[235]) and BlucSPVE in *B. lucorum*, and BterNPVE and BterSPVE in *B. terrestris*. The differentially high abundance in LGs was confirmed by qRT-PCR analysis. BlapNPVE and BlapSPVE coding regions were isolated from *B. lapidarius* LG cDNA by PCR using combination of degenerated and specific primers designed against conserved FAD regions. FADs from all three investigated species belonging to the NPVE and SPVE groups (named according to the presence of four-amino-acid signature motif) shared over 97% protein sequence identity within the groups and approximately 60% identity between the groups. Functional characterization of FADs in yeast demonstrated that NPVE FADs from the three species were almost identical, all exhibiting Z9-desaturase regioselectivity and highest conversion rate (calculated as ratio of relative abundance of unsaturated FAs to the total relative amount of saturated and unsaturated FAs) with 18:0 (98%), followed by 16:0 (85% - 88%) and 14:0 (62% - 63% in BterNPVE and BlucNPVE, respectively; 47% in BlapNPVE). SPVE FADs produced traces of Z4-14:1 and E4-14:1 as sole products, naturally not present in the LG of the studied bumblebee species and previously not detected in any other insect species. These data indicate that although the desaturase substrate specificities of NPVE FADs does not match the composition of FA-derived MPs, these FADs are the most probable candidate enzymes involved in biosynthesis of Z9-MPs since they are highly abundantly and specifically expressed in LGs. Notably, BterNPVE was one of the most abundant transcripts in *B. terrestris* LG which contrasts with the low abundance of Z9-MP components in *B. terrestris* LG, indicating that the activity of BterNPVE is posttranscriptionally regulated. Together, the experiments indicate that FAD's enzymatic specificities in the studied species did not diverge in the course of evolution and that the species-specific MP composition is not underlined by distinct FAD substrate specificities (Figure 7), i.e. a mechanism of pheromone composition determination common to many moth species does not apply to bumblebees. Rather MP composition is controlled in a species-specific manner by *i)* posttranscriptional regulation of FADs and *ii)* amount and availability of FAs of particular chain lengths which serve as FAD substrates, or *iii)* substrate specificity of downstream MP-biosynthetic enzymes such as fatty acyl reductases or fatty acyl ethyl ester biosynthetic enzymes which can transform UFAs to final MP components.

In ongoing experiments we aim at isolating and characterizing substrate specificities of bumblebee fatty acyl reductases and at comprehensive analysis of fatty acid content in the bumblebee LGs.

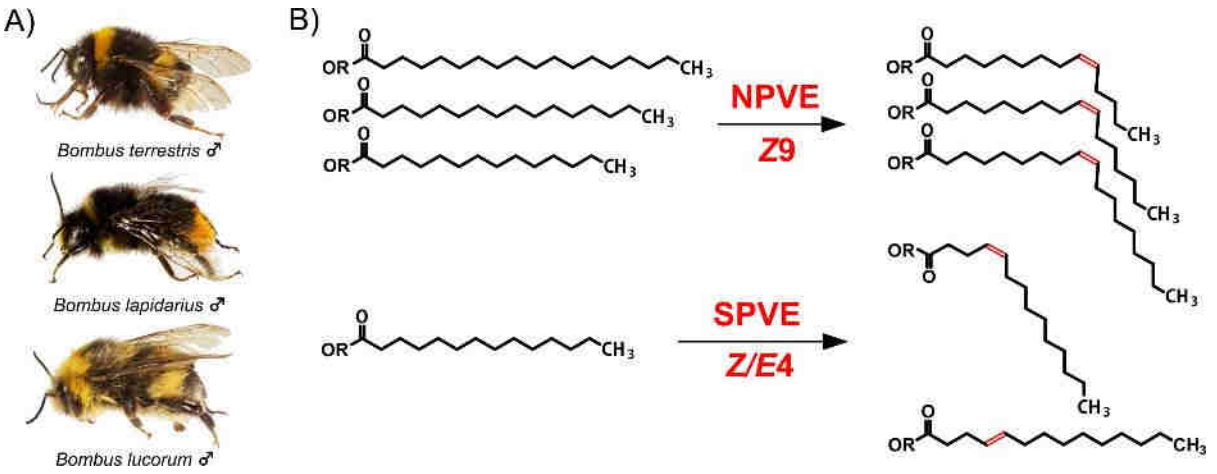

Figure 7: Specificities of mFADs abundantly expressed in labial glands of *Bombus terrestris*, *B. lucorum* and *B. lapidarius*. (A) In the investigated species, **(B)** two mFAD orthologs, NPVE and SPVE, exhibiting Z9 and Z/E4 desaturase specificity and substrate preference for 14:0-18:0 and 14:0, respectively, are abundantly expressed in the labial glands. Adapted from[30].

My contribution

I have analyzed the RNA-seq data and identified there mFAD coding regions; validated LG-specific expression of BlucNPVE and BlucSPVE by qRT-PCR; cloned all FAD coding regions into yeast expression vectors and transformed them into yeast cells, performed all the yeast cultivation experiments, lipid isolations and FA analyses; wrote the draft of the manuscript.

3.3 *Publication III*: Δ12-fatty acid desaturase from *Candida parapsilosis* is a multifunctional desaturase producing a range of polyunsaturated and hydroxylated fatty acids

Background

Fungal FAD research is largely motivated by the search for novel FADs that could be used in metabolic engineering of microorganisms to produce polyunsaturated fatty acids (PUFAs) and other valuable unsaturated fatty acids on an industrial scale[72,252]. Additionally, desaturation, as a part of fungal fatty acid metabolism, has been shown to play a crucial role in the growth and morphogenesis of pathogenic yeast species in plants and humans. Therefore, FADs have been suggested as potential targets for antifungal drugs[74–76,253,254]. Numerous fungal Δ12-, Δ15- and multifunctional membrane fatty acid desaturase genes (FADs) involved in biosynthesis of PUFAs have been already isolated and functionally characterized employing yeast expression system[84,96,255–264]. A range of desaturase regioselectivities dependent on the reference point used by FADs to position the introduced double bond has been described. The main regioselective modes are: (1) the double bond is introduced between specific carbon atoms counted from the carboxy terminus (ΔX) or (2) methyl terminus (ωX) of the fatty acyl substrate, and (3) a subsequent double bond is introduced a specific number of carbon atoms (usually three) counted from the pre-existing double bond (ν+3)[49]. These FAD regioselectivities are not mutually exclusive, and Meesapyodsuk et al. suggested assigning FADs with primary and secondary modes to more precisely describe their regioselectivity[84]. Detailed information on both major and minor FAD diagnostic substrates and products is principal for comprehensive description and classification of these FADs. However, only major PUFA products were analyzed for many of the fungal FADs and studies which re-examined PUFA-producing FADs[257,265] indicates that minor products can be easily neglected[266,267]

Summary

To comprehensively describe enzymatic specificities of PUFA producing FADs, we identified and isolated gene homologs of fungal FADs from opportunistic pathogenic yeast *Candida parapsilosis*. Expression of the *C. parapsilosis* FADs termed CpFAD2 and CpFAD3 in a *Saccharomyces cerevisiae* expression system and detailed analysis of novel minor and major FA products via GC/MS coupled with a range of FA-derivatization techniques enabled us to identify polyunsaturated and hydroxylated products which were previously not described for *Candida albicans* homologs of CpFAD2 and CpFAD3[76].

Overexpression of CpFad3 in *Saccharomyces cerevisiae* strains supplemented with linoleic acid (Δ9, Δ12-18:2) and hexadecadienoic acid (Δ9, Δ12-16:2) led to accumulation of Δ15-PUFAs, i.e., α-linolenic acid (Δ9, Δ12, Δ15-18:3) and hexadecatrienoic acid with terminal double bond (Δ9, Δ12, Δ15-16:3), respectively, which jointly indicate that CpFad3 exhibits Δ15-regioselectivity requiring a preexisting Δ12-double bond and is capable of introducing a terminal double bond.

CpFad2-expressing yeast strains accumulated expected Δ12-PUFAs, i.e. linoleic and hexadecadienoic acid (Δ9, Δ12-16:2), as the expected major PUFAs. However, accompanying Δ15-PUFAs were also detected, namely α-linolenic acid and hexadecatrienoic acid (Δ9, Δ12, Δ15-16:3) and we identified ricinoleic acid (12-hydroxy-9-octadecenoic acid) as an additional product of CpFad2. Based on the PUFA products detected we proposed that the primary regioselective mode of CpFad2 is ν+3 and the secondary mode is Δ12, in accordance with the FAD regioselectivity classification proposed by Meesapyodsuk et al.[84], i.e. that the preexisting double bond serves as a reference point for positioning of the newly introduced double bond and that the Δ12-position is the preferred position of the double bond introduction.

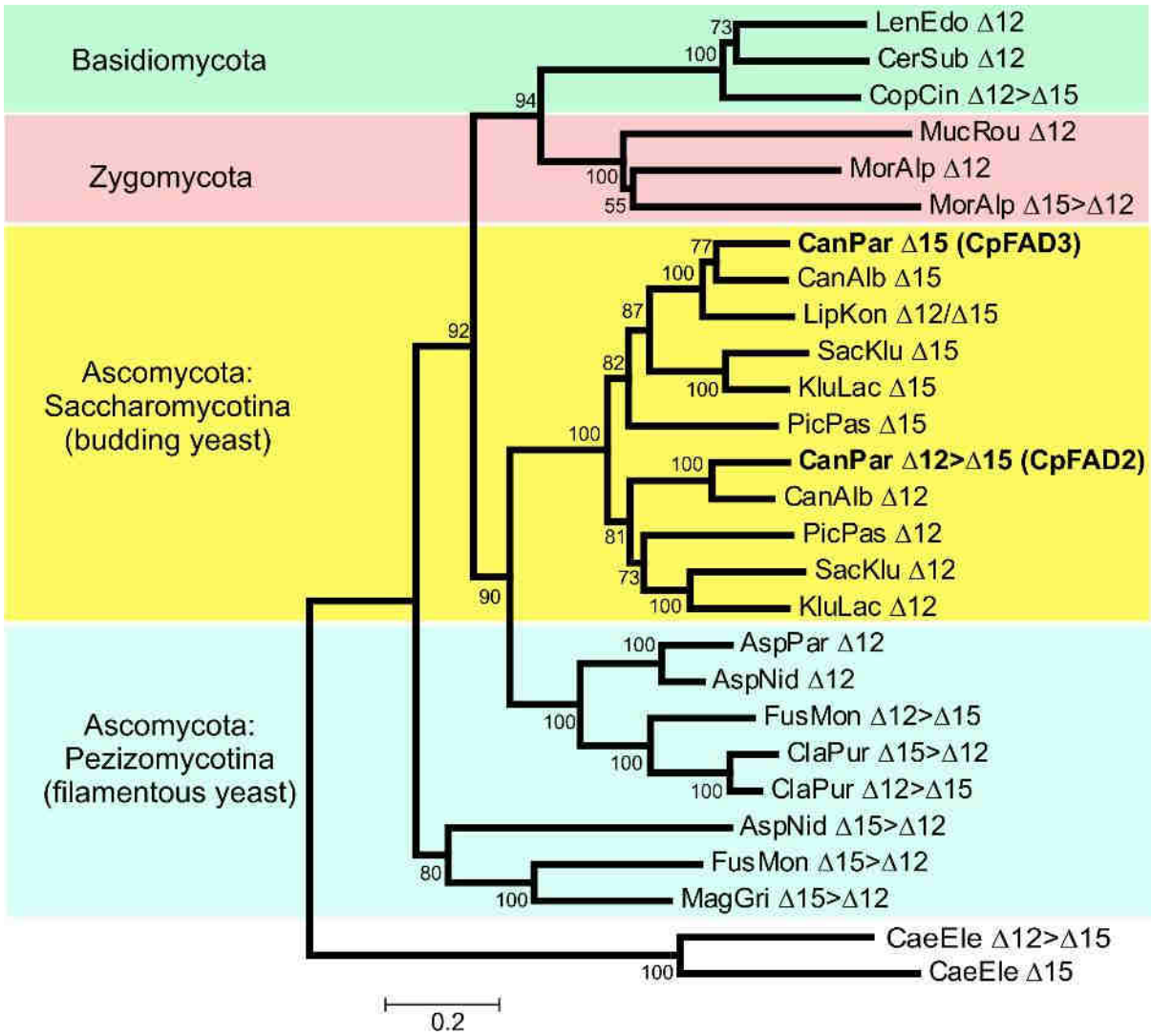

Figure 8: Neighbor-joining gene tree showing relatedness of fungal Δ12- and Δ15-FADs based on their protein sequence. CpFAD2 and CpFAD3 identified and characterized in this work are highlighted in bold. The source species name is abbreviated and followed by experimentally determined desaturase regioselectivity. For multifunctional FADs, preferred regioselectivity is indicated by ‘‘>’’ if available in the literature (e.g., Δ12> Δ15 indicates preferential Δ12-desaturase regioselectivity). Δ12-FAD and Δ15-FAD from the nematode *Caenorhabditis elegans* (CaeEle) were added as an outgroup. Numbers along branches indicate bootstrap percentage support from 1000 replicates. The scale bar shows number of amino acid changes per site. Adapted from[268].

These results also demonstrate that both CpFad2 and CpFad3 are capable of production of multiple PUFAs or hydroxylated FA products which were previously not detected as products of the putative CpFAD2 and CpFAD3 orthologs from budding yeasts (Ascomycota: Saccharomycotina) (Figure 8). This work indicates that detailed analysis of minor FAD products has a potential to uncover a range of otherwise undescribed enzymatic selectivities of Δ12-FADs and Δ15-FADs.

My contribution

I have isolated the coding regions of CpFAD2 and CpFAD3; cloned CpFAD2 and CpFAD3 into yeast expression vectors and transformed them into *S. cerevisiae* yeast strains; cultivated the yeast strains heterologously expressing CpFAD2 and CpFAD3; isolated the total cellular lipids and analyzed their fatty acid methyl ester-, 4,4-dimethyloxazoline-, and trimethylsilyl-derivatives using GC/MS; analyzed the GC/MS data; wrote the draft of the manuscript.

4 Discussion and conclusion

Insect pheromones represent a principal communication channel in many insect species, involving disease vectors and economically important agricultural pests. Understanding pheromone communication of these species is directly motivated by search for novel pest control strategies. But often nature "offers" organisms which are not of imminent economic importance but their remarkable evolutionary life history makes them a convenient model for answering particular biological questions. Arguably, the tobacco hornworm moth (*Manduca sexta*) is such a species. The combination of its large size, facile breeding in laboratory conditions, and its feeding preference for alkaloid-defended Solanaceous plants (such as nicotine-producing tobacco plants) made *M. sexta*, despite its insignificant economic impact as a plant pest species, a favourite model organism for study of herbivore-plant interaction, insect molecular biology, neurophysiology, and biochemistry. *M. sexta* is an exciting species also with respect to its pheromone composition – the female sex pheromone (SP) blend contains triunsaturated fatty acid-derived (3UFA-derived) pheromones which were not identified in related moths (such as the silkworm moth *B. mori*). The potential of *M. sexta* as a model species for investigation of evolution of pheromone communication, however, was untapped, partially due to the missing knowledge on the 3UFA biosynthetic pathway or related genes and, until recently, also due to the missing *M. sexta* genomic information (unpublished *M. sexta* genome is now publicly available at the internet pages of Agricultural pest genomic resources - http://agripestbase.org/).

Our research group ventured into study of *M. sexta* pheromone biosynthesis by searching for membrane fatty acyl desaturase genes (mFADs) abundantly expressed in *M. sexta* female pheromone gland. The absence of *M. sexta* genomic or transcriptomic information at that time necessitated search for mFAD genes using homology-probing PCR approach (employing degenerated primers designed against conserved mFAD motifs) which resulted in identification of MsexD2 mFAD involved in biosynthesis of diunsaturated (2UFA) SP precursors, essential components of *M. sexta* SP. The mFAD involved in 3UFA-derived SP biosynthesis remained elusive at that time[246]. The advent of next-generation sequencing techniques, namely RNA-seq, provided us with a tool to access transcriptomes of *M. sexta* pheromone gland and other tissues. By comparing the transcriptomes across *M. sexta* tissues we identified MsexD3, MsexD5 and MsexD6 mFADs candidates abundantly and preferentially expressed in the female pheromone gland (PG) and by functional characterization of the mFAD gene candidates in yeast expression

system we concluded that MsexD3 and/or MsexD5 produce 3UFAs via desaturation of 2UFA(Publication I). Knowledge on 3UFA-biosynthetic mFADs opened up possibilities for inference of pheromone evolution in the *M. sexta* lineage (see further below).

As a second insect group of interest we selected bumblebees (Hymenoptera: Bombus), namely three common European bumblebee species, *Bombus terrestris*, *B. lucorum*, and *B. lapidarius*. The UFA-derived male marking pheromone (MP) components in these related species substantially qualitatively and quantitatively differ and these species thus represent suitable model organisms for study of entirely unexplored hymenopteran pheromone biosynthetic mFADs and their role in pheromone evolution. Also for these species for which genomic or transcriptomic data were not available until recently[269], the RNA-seq approach enabled us identification of mFAD candidates presumably involved in MP biosynthesis.

As a strategy to confirm the mFAD function we employed characterization of the mFAD enzymatic selectivities in yeast expression system rather than aiming for *in vitro* work with these enzymes, which are due to their transmembrane localization inherently difficult to isolate and characterize. By employing functional characterization of mFADs in yeast, we sacrificed e.g. an option to study mFAD enzymatic kinetics and cofactor requirements - both potentially relevant information for understanding the regulation of pheromone biosynthesis. But the chosen approach enabled us description of regiospecificities and substrate specificities of eight *M. sexta* mFADs and over thirty of their mutants (Publication I and unpublished results), six bumblebee mFADs (Publication II), and two *C. parapsilosis* mFADs (Publication III), a task which we could hardly accomplish by studying the isolated and purified mFAD enzymes *in vitro*.

In the case of study of *M. sexta* pheromone biosynthesis we were admittedly lucky to work with an organism where a functional divergence of mFAD – an evolutionary scenario relatively easily testable by the mFAD functional assay - presumably generated novel SP components.

By contrast, functional divergence of mFADs seems to be not driving the evolution of bumblebee MPS, since all the male bumblebee mFADs are functionally conserved across the three investigated bumblebee species (Publication II). Particularly surprising was highly abundant and preferential expression of Z9-mFADs exhibiting substrate preference towards 16:0 and 18:0 in LGs of *B. terrestris* and *B. lucorum*. This expression pattern is indicative of the role of Z9-mFADs in pheromone biosynthesis, however, these species, in contrast to *B. lapidarius*, do not accumulate larger quantities of Z9-16:1- of Z9-18:1-derived MPs. A possible explanation for the discrepancy between the high Z9-mFAD mRNA abundance and the apparently low activity of the respective enzymes is posttranscriptional downregulation of Z9-

mFADs in *B. terrestris* and *B. lucorum*. This mechanism was proposed to explain the presence of highly abundant yet enzymatically inactive mFAD transcripts in PGs of some moth species[270,271]. Numerous post-transcriptional gene expression regulatory mechanisms, many of them still little understood, are documented across eukaryotic organisms to limit the correlation of measured mRNA quantity and abundance (or activity) of the respective enzyme[272] and further experiments should clarify the proposed role of male bumblebee mFAD posttranscriptional regulation in regulation of MP composition.

Other factors which we propose to influence the species-specific bumblebee MP composition and which remains to be tested are i) differential availability of FA precursors of MP components underlied by the differences in biosynthesis, transport and accumulation of FAs in LG and ii) particular enzymatic specificity of downstream pheromone biosynthetic enzymes such as esterases involved in production of FA-ethyl esters or fatty acyl reductases (FAR) involved in production of FA-derived alcohols. The former hypothesis was addressed by Valterová and collaborators who uncovered contribution of FA transport to MP biosynthesis in *B. terrestris*[273] but the contribution of FA transport to the species-specific MP composition remains to be tested. To address the later hypothesis, we are currently cloning and functionally characterizing bumblebee FARs from the LGs of the three species. Our preliminary results indicate that there are indeed FARs exhibiting distinct substrate specificities which might partially explain the species-specific MP composition (unpublished results).

Another surprising result of bumblebee mFAD survey was the identification of *E*/*Z*4-mFADs in all three species which exclusively desaturate 14:0. The occurrence of the Δ4-monounsaturated FAs is limited in nature. They are present in seeds of Umbelliferae, Araliaceae, and Garryaceae plant species[274] and in the sexually deceptive orchid *Ophrys sphegodes*, in which Δ4-16:1 is a proposed intermediate of alkene biosynthesis[275] but they are absent in the bumblebee LG extracts. The unusual *E*/*Z*4-regiospecificity might be underlined by the presence of the 5th and 6th predicted transmembrane helices, which deviate from the consensual membrane topology of acyl-CoA mFADs. The additional predicted helices likely represent membrane-associated regions, which might play a role in FA substrate recognition, as previously suggested by Diaz et al.[60]. The absence of *E*/*Z*4-14:1 in the bumblebee LG might be explained by the mechanism of *in vivo* posttranscriptional downregulation of the *E*/*Z*4-mFADs proposed above also for Z9-mFADs. To address this question, future development of FAD-specific antibodies or a proteomic approach may unequivocally establish the protein abundances of *Z*9-mFAD and *E*/*Z*4-mFAD across bumblebee tissues.

An alternative tool to validate (or uncover) a biological function of a gene candidate, particularly powerful in non-model organisms for which limited genetic tools are established, is RNA interference (RNAi). In an RNAi experiment, target transcripts are depleted by dsRNA-mediated mRNA degradation and the resulting phenotypic effect on the organism is observed. In insects, the sensitivity to RNAi greatly varies between tissues and species, the most sensitive being beetles (Coleoptera) and the least sensitive flies (Diptera), moths and butterflies (Lepidoptera)[276]. We strived to unravel the contributions of *M. sexta* mFADs to biosynthesis of SPs by impairing the *in vivo* activities of MsexD2 and MsexD3 via injection of dsRNA silencing probes (designed against MsexD2 and MsexD3) into abdomens of *M. sexta* females. However, we observed neither significant decrease in the mFAD transcript levels in the PG nor a change in the UFA content (unpublished results). In the future, overcoming the difficulties of RNAi in Lepidoptera[277] and establishing a reliable RNAi procedure for knock-down of genes expressed in the *M. sexta* PG might provide experimental evidence for the relative contributions of *Msex*D3 and *Msex*D5 to 3UFA biosynthesis. Nevertheless, our results suggest that *Msex*D3 plays the principal role in 3UFA biosynthesis because i) *Msex*D3 transcript is more abundant in the PG compared to *Msex*D5 and ii) the 1:7 ratio of *E*10,*E*12,*E*14-16:3 and *E*10,*E*12,*Z*14-16:3 produced by *Msex*D3 closely resembles the ratio of the respective aldehydic components in the *M. sexta* SP (approx. 1:10) in contrast to the ratio of *Msex*D5 3UFA products (3:1). We speculate that the selection pressure leading to the recruitment of a second, seemingly redundant, 3UFA-biosynthetic mFAD might occur, for example, to secure a sufficiently high production of 3UFA-derived SPs.

RNAi is a promising tool also for uncovering the biological role of bumblebee mFADs, FARs, or other pheromone-biosynthetic gene candidates which we have recently identified as abundantly and preferentially expressed in *B. terrestris* male LG[36].

Our study of PUFA-producing mFADs from the opportunistically pathogenic yeast *Candida parapsilosis* demonstrated previously undiscerned capability of mFADs from budding yeasts (Ascomycota: Saccharomycotina) to act as multifunctional *Z*12/*Z*15-desaturases and to produce hydroxylated products (Publication III). These results contribute to the recognition of mFADs as enzymes inherently exhibiting multiple substrate- and regiospecificities. The switch between the mFAD specificity modes is apparently rather facile and this property of mFADs has, besides implications for evolution of communication mediated by mFAD-produced pheromones, also relevance for the rational engineering of mFADs for biotechnological production of economically interesting UFAs.

Enzymatic plasticity of mFADs was previously experimentally well documented, as I summarized in the introductory part of this thesis. However, no experimental evidence to support the hypothesis that the enzymatic plasticity of SP-biosynthetic mFADs might play a role in shaping the moth SP communication channel was available. Our finding that a single amino acid mutation in SP-producing mFAD has a potential to generate novel SP components in *M. sexta* lineage thus represents the first evidence of the role of mFAD enzymatic plasticity in pheromone communication evolution (Publication I). The finding of the mutation at amino acid position 224 which critically influences the *M. sexta* mFAD specificity and which localizes to the predicted 4th transmembrane helix is in agreement with previous experiments on mFADs from various organisms which suggested the role of transmembrane helices in formation of substrate-binding site. At the time of carrying out the study, the lack of mFAD protein structure however prevented further mechanistic rationalization of the effect of the 224 substitution. By coincidence, two studies providing the first mFAD crystal structures[64,65] were simultaneously published during the final phase of preparation of our manuscript on *M. sexta* mFADs which enabled us to prepare preliminary homology models of MsexD2 and MsexD3 structures. These models uncovered the localization of the 224 amino acid residue to the kink of MsexD2/MsexD3 substrate binding tunnel which presumably plays a key role in conformational restriction and positioning of the fatty acyl substrate moiety with respect to the di-iron active center and provided thus experimental evidence for the proposed critical role of this kink in the determination of mFAD enzymatic specificity (Publication I). The availability of mFAD structures now sets the stage for a next generation of structure-guided mFAD mutagenesis experiments and prompts homology modeling-based re-evaluation of the results of the numerous published mFAD mutagenesis studies. Together, the availability of mFAD structures should mark the shift from identification of mFAD sequence specificity determinants towards the identification of structural specificity determinants and, ultimately, towards understanding of mechanisms of mFAD substrate- and regiospecificity. Still, the computation of reliable homology-based structural models of the mFADs for which experimental structure is not available represents a challenge. Particularly homology modeling of acyl-lipid mFADs which presumably has a different membrane topology than acyl-CoA mFADs[60] and differs also in the form of accepted fatty acyl substrate might prove difficult. Currently, we further pursue the role of the amino acid residue 224 in MsexD2 and MsexD3 by mutating the 224 residue and determining the effect of the mutation on the mFAD substrate- and regiospecificity. According to our preliminary results, a particular side chain volume of 224 residue (alanine or threonine) drives the specificity towards desaturation of 16:0 to Z11-16:1 and subsequent desaturation of

Z11-16:1 to 2UFAs, whereas bulkier side chains (valine or isoleucine) drives the specificity of MsexD2 and MsexD3 towards the desaturation of 2UFAs to 3UFAs. MsexD2 and MsexD3 mutants with 224 amino acid residues with very small and very large amino acid side chains (glycine and phenylalanine, respectively) generally exhibit loss or dramatic decrease of desaturase activity (unpublished results). We are in process of computational modeling of the interactions of various FA substrates with the panel of MsexD2 and MsexD3 mFAD mutants to get insights into mechanistic details of the substrate- and regiospecificity switching. We presume that mutations homologous to the 224 residue might act as a mFAD specificity switch also in non-insect mFADs, a hypothesis which is now particularly amenable to test in mouse or human Z9-mFAD for which the crystal structures are available.

M. sexta mFADs might in future also help to uncover subunit organization and subunit cooperation in mFADs, a little studied aspect of mFAD biochemistry. An experimental evidence based on co-immunoprecipitation and yeast two-hybrid analysis suggests that yeast Z9-mFAD forms dimers *in vivo*[70] and experiments with plant mFADs suggests the they might form heterodimers capable of metabolic channeling, i.e. forwarding of products of one mFAD monomer directly to the second mFAD monomer, thus together physically connecting multiple subsequent desaturation steps into one heterodimer[278]. Given the high sequence similarity of MsexD2 and MsexD3 and their complementary desaturase specificities, we speculate that they might form heterodimers *in vivo* which could effectively produce 3UFA pheromone precursors by connecting the sequential desaturation steps into MsexD2/MsexD3 heterodimer.

The functional plasticity of mFADs is not only fascinating with respect to the general enzyme properties but also has relevance for insect pest management strategies that employ artificial SP baits[279]. The use of SPs in monitoring or mating disruption strategies may impose a selection pressure on the moth mate-finding system and select for a shift in SP composition, as was demonstrated in laboratory conditions for the cabbage looper moth *Trichoplusia ni*[280]. The evolutionary facile functional divergence of the SP composition via mFAD functional divergence might enable the moths to avoid disorientation and thus overcome mating disruption[213].

To gain initial insight into the evolutionary history of 3UFA-derived SP utilization in Sphingidae moths, we analyzed SP precursors in the death head moth, *Acherontia atropos* (Sphingidae: Sphinginae: Acherontiini), a species closely related to *M. sexta* (Sphingidae: Sphinginae: Sphingini) and we identified 3UFAs also there. This finding places the most parsimonious recruitment of 3UFA-producing mFADs to the common ancestor of the Acherontiini and Sphingini tribes - the Sphinginae subfamily. Future sequencing and analysis

of genomes or pheromone gland transcriptomes of *A. atropos* and other moth species related to *M. sexta* coupled with their SP identification should further uncover the evolutionary events which led to the acquisition of 3UFA-derived SPs.

In the thesis we focused on the pheromone producers and genes involved in pheromone biosynthesis. Equally exciting would be to probe the response of *M. sexta*-related moth species to 3UFA-derived SPs to investigate whether these species or some rare males of these species might be "preadapted" to be attracted by 3UFA-derived compounds. Information on mechanisms which underlined the shift of male pheromone preference towards 3UFA-derived pheromones in *M. sexta* lineage would complement our study of the molecular basis of shift in female SP production.

5 References

1. Fabre, J. H. *The Life of the Caterpillar (translated from French original* Souvenirs Entomologique *(1900))*. (Hodder & Stoughton, 1916).
2. Butenandt, von A., Beckmann, R., Stamm, D. & Hecker, E. Über den sexuallockstoff des seidenspinners *Bombyx mori*. Reindarstellung und konstitution. *Z. Naturforsch. B.* **14,** 283–284 (1959).
3. Karlson, P. & Lüscher, M. 'Pheromones': a new term for a class of biologically active substances. *Nature* **183,** 55–56 (1959).
4. Shorey, H. H., Gaston, L. K. & Saario, C. A. Sex pheromones of noctuid moths. XIV. Feasibility of behavioral Control by disrupting pheromone communication in cabbage loopers. *J. Econ. Entomol.* **60,** 1541–1545 (1967).
5. Berger, R. S. Isolation, identification, and synthesis of the sex attractant of the cabbage looper, *Trichoplusia ni*. *Ann. Entomol. Soc. Am.* **59,** 767–771 (1966).
6. Silverstein, R. M., Rodin, J. O. & Wood, D. L. Sex attractants in frass produced by male *Ips confusus* in *Ponderosa* pine. *Science (80-.).* **154,** 509–510 (1966).
7. Carlson, D. A. *et al.* Sex attractant pheromone of the house fly: isolation, identification and synthesis. *Science* **174,** 76–78 (1971).
8. Millar, J. G. in *Gas Chromatogr.* 679–688 (Elsevier Academic Press, 2012).
9. Arn, H., Städler, E. & Rauscher, S. The electroantennographic detector—a selective and sensitive tool in the gas chromatographic analysis of insect pheromones. *Z. Naturforsch* **30c,** 722–725 (1975).
10. Tamaki, Y. in *Compr. insect Physiol. Biochem. Pharmacol.* (Kerkut, G. A. & Gilbert, L. I.) 145–192 (Pergamon, 1985).
11. Ando, T., Inomata, S. & Yamamoto, M. in *Chem. pheromones other Semiochem. I* (Schulz, S.) 51–96 (Springer-Verlag Berlin Heidelberg, 2004). doi:10.1007/b95449
12. El-Sayed. The Pherobase: Database of Pheromones and Semiochemicals. http://www.pherobase.com. (2014).
13. Byers, J. A. Pheromone component patterns of moth evolution revealed by computer analysis of the Pherolist. *J. Anim. Ecol.* **75,** 399–407 (2006).
14. Bjostad, L. B., Wolf, W. A. & Roelofs, W. L. in *Pheromone Biochem.* (Prestwich, G. D. & Blomquist, G. J.) 77–120 (Academic Press, 1987).
15. Bjostad, L. B. & Roelofs, W. L. Sex pheromone biosynthesis in Trichoplusia ni: key steps involve Delta-11 desaturation and chain-shortening. *Science* **220,** 1387–1389 (1983).
16. Roelofs, W. & Bjostad, L. Biosynthesis of lepidopteran pheromones. *Bioorg. Chem.* **12,** 279–298 (1984).
17. Roelofs, W. L. & Wolf, W. A. Pheromone biosynthesis in lepidoptera. *J. Chem. Ecol.* **14,** 2019–2031 (1988).
18. Jurenka, R. A. in *Insect pheromone Biochem. Mol. Biol.* (Blomquist, G. J. & Vogt, R. G.) 53–80 (Elsevier Academic Press, 2003).
19. Blomquist, G. J. & Vogt, R. G. *Insect Pheromone Biochemistry and Molecular Biology*. (Elsevier Academic Press, 2003).
20. Roelofs, W. L. & Knipple, D. C. in *Insect pheromone Biochem. Mol. Biol.* (Blomquist, G. J. & Vogt, R. G.) 81–106 (Elsevier Academic Press, 2003).
21. Blomquist, G. J. & Howard, R. W. in *Insect Pheromone Biochem. Mol. Biol.* (Blomquist, G. J. & Vogt, R. G.) 3–18 (Elsevier Academic Press, 2003).
22. Wolf, W. a. & Roelofs, W. L. Properties of the delta11-desaturase enzyme used in cabbage looper moth sex pheromone biosynthesis. *Arch. Insect Biochem. Physiol.* **3,** 45–52 (1986).
23. Rodriguez, F., Hallahan, D. L., Pickett, J. A. & Camps, F. Characterization of the Δ11-palmitoyl-CoA-desaturase from *Spodoptera littoralis* (lepidoptera: noctuidae). *Insect Biochem. Mol. Biol.* **22,** 143–148 (1992).
24. Thiede, M. A., Ozols, J. & Strittmatter, P. Construction and sequence of cDNA for rat liver stearyl coenzyme A desaturase. *J. Biol. Chem.* **261,** 13230–5 (1986).
25. Stukey, J. E., McDonough, V. M. & Martin, C. E. The *OLE1* gene of *Saccharomyces cerevisiae* encodes

the delta 9 fatty acid desaturase and can be functionally replaced by the rat stearoyl-CoA desaturase gene. *J. Biol. Chem.* **265,** 20144–9 (1990).

26. Knipple, D. C. *et al.* Cloning and functional expression of a cDNA encoding a pheromone gland-specific acyl-CoA Delta11-desaturase of the cabbage looper moth, *Trichoplusia ni*. *Proc. Natl. Acad. Sci. U. S. A.* **95,** 15287–92 (1998).
27. Dallerac, R. *et al.* A delta 9 desaturase gene with a different substrate specificity is responsible for the cuticular diene hydrocarbon polymorphism in *Drosophila melanogaster*. *Proc. Natl. Acad. Sci. U. S. A.* **97,** 9449–9454 (2000).
28. Adams, M. D. The Genome Sequence of *Drosophila melanogaster*. *Science (80-.).* **287,** 2185–2195 (2000).
29. Moto, K. *et al.* Involvement of a bifunctional fatty-acyl desaturase in the biosynthesis of the silkmoth, *Bombyx mori*, sex pheromone. *Proc. Natl. Acad. Sci. U. S. A.* **101,** 8631–6 (2004).
30. Buček, A. *et al.* The role of desaturases in the biosynthesis of marking pheromones in bumblebee males. *Insect Biochem. Mol. Biol.* **43,** 724–31 (2013).
31. Smadja, C. & Butlin, R. K. On the scent of speciation: the chemosensory system and its role in premating isolation. *Heredity (Edinb).* **102,** 77–97 (2009).
32. Metzker, M. L. Sequencing technologies — the next generation. *Genetics* **11,** (2010).
33. Oppenheim, S. J., Baker, R. H., Simon, S. & DeSalle, R. We can't all be supermodels: the value of comparative transcriptomics to the study of non-model insects. *Insect Mol. Biol.* **24,** 139–154 (2015).
34. Misof, B. *et al.* Phylogenomics resolves the timing and pattern of insect evolution. *Science (80-.).* **346,** 763–767 (2014).
35. Antony, B. *et al.* Genes involved in sex pheromone biosynthesis of *Ephestia cautella*, an important food storage pest, are determined by transcriptome sequencing. *BMC Genomics* **16,** 532 (2015).
36. Buček, A. *et al.* Exploring complex pheromone biosynthetic processes in the bumblebee male labial gland by RNA sequencing. *Insect Mol. Biol.* **25,** 295–314 (2016).
37. Jung, C. R. & Kim, Y. Comparative transcriptome analysis of sex pheromone glands of two sympatric lepidopteran congener species. *Genomics* **103,** 308–315 (2014).
38. Gu, S.-H. *et al.* Identification of genes expressed in the sex pheromone gland of the black cutworm *Agrotis ipsilon* with putative roles in sex pheromone biosynthesis and transport. *BMC Genomics* **14,** 636 (2013).
39. Ding, B.-J. & Löfstedt, C. Analysis of the *Agrotis segetum* pheromone gland transcriptome in the light of sex pheromone biosynthesis. *BMC Genomics* **16,** 711 (2015).
40. Groot, A. T., Dekker, T. & Heckel, D. G. The genetic basis of pheromone evolution in moths. *Annu. Rev. Entomol.* **61,** 99–117 (2016).
41. Aguilar, P. S. & de Mendoza, D. Control of fatty acid desaturation: a mechanism conserved from bacteria to humans. *Mol. Microbiol.* **62,** 1507–14 (2006).
42. Los, D. a & Murata, N. Structure and expression of fatty acid desaturases. *Biochim. Biophys. Acta* **1394,** 3–15 (1998).
43. Funk, C. D. Prostaglandins and leukotrienes: advances in eicosanoid biology. *Science* **294,** 1871–1875 (2001).
44. Morgan, D. E. *Biosynthesis in insects*. (RSC Publishing, 2010).
45. Kass, L. R., Brock, D. J. & Bloch, K. Beta-hydroxydecanoyl thioester dehydrase. I. Purification and properties. *J. Biol. Chem.* **242,** 4418–31 (1967).
46. Marrakchi, H., Choi, K.-H. & Rock, C. O. A new mechanism for anaerobic unsaturated fatty acid formation in *Streptococcus pneumoniae*. *J. Biol. Chem.* **277,** 44809–16 (2002).
47. Parsons, J. B. & Rock, C. O. Bacterial lipids: Metabolism and membrane homeostasis. *Prog. Lipid Res.* **52,** 249–276 (2013).
48. Sperling, P., Ternes, P., Zank, T. K. & Heinz, E. The evolution of desaturases. *Prostaglandins. Leukot. Essent. Fatty Acids* **68,** 73–95 (2003).
49. Shanklin, J. & Cahoon, E. B. Desaturation and related modifications of fatty acids. *Annu. Rev. Plant Physiol. Plant Mol. Biol.* **49,** 611–641 (1998).
50. Shanklin, J. & Somerville, C. Stearoyl-acyl-carrier-protein desaturase from higher plants is structurally unrelated to the animal and fungal homologs. *Proc. Natl. Acad. Sci.* **88,** 2510–2514 (1991).
51. López Alonso, D., García-Maroto, F., Rodríguez-Ruiz, J., Garrido, J. A. & Vilches, M. A. Evolution of

the membrane-bound fatty acid desaturases. *Biochem. Syst. Ecol.* **31,** 1111–1124 (2003).

52. Kok, M. *et al.* The *Pseudomonas oleovorans* alkane hydroxylase gene. Sequence and expression. *J. Biol. Chem.* **264,** 5435–41 (1989).
53. Shanklin, J., Whittle, E. & Fox, B. G. Eight histidine residues are catalytically essential in a membrane-associated iron enzyme, stearoyl-CoA desaturase, and are conserved in alkane hydroxylase and xylene monooxygenase. *Biochemistry* **33,** 12787–94 (1994).
54. Zhu, G., Koszelak-Rosenblum, M., Connelly, S. M., Dumont, M. E. & Malkowski, M. G. The crystal structure of an integral membrane fatty acid α-hydroxylase. *J. Biol. Chem.* **290,** 29820–33 (2015).
55. Cahoon, E. B. *et al.* Biosynthetic origin of conjugated double bonds: Production of fatty acid components of high-value drying oils in transgenic soybean embryos. *Proc. Natl. Acad. Sci.* **96,** 12935–12940 (1999).
56. Lee, M. *et al.* Identification of non-heme diiron proteins that catalyze triple bond and epoxy group formation. *Science* **280,** 915–8 (1998).
57. Cahoon, E. B. & Kinney, A. J. Dimorphecolic acid is synthesized by the coordinate activities of two divergent Delta12-oleic acid desaturases. *J. Biol. Chem.* **279,** 12495–12502 (2004).
58. Broun, P., Shanklin, J., Whittle, E. & Somerville, C. Catalytic plasticity of fatty acid modification enzymes underlying chemical diversity of plant lipids. *Science* **282,** 1315–1317 (1998).
59. Aguilar, P. S., Cronan, J. E. & de Mendoza, D. A *Bacillus subtilis* gene induced by cold shock encodes a membrane phospholipid desaturase. *J. Bacteriol.* **180,** 2194–2200 (1998).
60. Diaz, A. R., Mansilla, M. C., Vila, A. J. & de Mendoza, D. Membrane topology of the acyl-lipid desaturase from *Bacillus subtilis*. *J. Biol. Chem.* **277,** 48099–48106 (2002).
61. Mustardy, L., Los, D. A., Gombos, Z. & Murata, N. Immunocytochemical localization of acyl-lipid desaturases in cyanobacterial cells: evidence that both thylakoid membranes and cytoplasmic membranes are sites of lipid desaturation. *Proc. Natl. Acad. Sci. U. S. A.* **93,** 10524–7 (1996).
62. Sayanova, O., Shewry, P. R. & Napier, J. A. Histidine-41 of the cytochrome b(5) domain of the borage Delta(6) fatty acid desaturase is essential for enzyme activity. *Plant Physiol.* **121,** 641–646 (1999).
63. Mitchell, A. G. & Martin, C. E. A novel cytochrome b5-like domain is linked to the carboxyl terminus of the *Saccharomyces cerevisiae* delta-9 fatty acid desaturase. *J. Biol. Chem.* **270,** 29766–72 (1995).
64. Wang, H. *et al.* Crystal structure of human stearoyl–coenzyme A desaturase in complex with substrate. *Nat. Struct. Mol. Biol.* **22,** 581–585 (2015).
65. Bai, Y. *et al.* X-ray structure of a mammalian stearoyl-CoA desaturase. *Nature* **524,** 252–256 (2015).
66. Man, W. C., Miyazaki, M., Chu, K. & Ntambi, J. M. Membrane topology of mouse stearoyl-CoA desaturase 1. *J. Biol. Chem.* **281,** 1251–60 (2006).
67. Sayanova, O. *et al.* Mutagenesis and heterologous expression in yeast of a plant Δ6-fatty acid desaturase. *J. Exp. Bot.* **52,** 1581–1585 (2001).
68. Guy, J. E., Whittle, E., Kumaran, D., Lindqvist, Y. & Shanklin, J. The crystal structure of the ivy Delta(4)-16 : 0-ACP desaturase reveals structural details of the oxidized active site and potential determinants of regioselectivity. *J. Biol. Chem.* **282,** 19863–19871 (2007).
69. Lindqvist, Y., Huang, W. J., Schneider, G. & Shanklin, J. Crystal structure of Delta(9) stearoyl-acyl carrier protein desaturase from castor seed and its relationship to other di-iron proteins. *Embo J.* **15,** 4081–4092 (1996).
70. Lou, Y. & Shanklin, J. Evidence that the yeast desaturase Ole1p exists as a dimer in vivo. *J. Biol. Chem.* **285,** 19384–19390 (2010).
71. The PyMOL Molecular Graphics System, Version 1.2r1, Schrödinger, LLC.
72. Uemura, H. Synthesis and production of unsaturated and polyunsaturated fatty acids in yeast: current state and perspectives. *Appl. Microbiol. Biotechnol.* **95,** 1–12 (2012).
73. Zhang, Z., Dales, N. A. & Winther, M. D. Opportunities and challenges in developing stearoyl-coenzyme A desaturase-1 inhibitors as novel therapeutics for human disease. *J. Med. Chem.* **57,** 5039–56 (2014).
74. Krishnamurthy, S. *et al.* Dosage-dependent functions of fatty acid desaturase Ole1p in growth and morphogenesis of *Candida albicans*. *Microbiology* **150,** 1991–2003 (2004).
75. Nguyen, L. N., Gacser, A. & Nosanchuk, J. D. The stearoyl-coenzyme A desaturase 1 is essential for virulence and membrane stress in *Candida parapsilosis* through unsaturated fatty acid production. *Infect. Immun.* **79,** 136–45 (2011).
76. Murayama, S. Y. *et al.* Construction and functional analysis of fatty acid desaturase gene disruptants in

Candida albicans. *Microbiology* **152,** 1551–8 (2006).
77. Alloatti, A. *et al.* Genetic and chemical evaluation of *Trypanosoma brucei* oleate desaturase as a candidate drug target. *PLoS One* **5,** e14239 (2010).
78. Alloatti, A., Testero, S. A. & Uttaro, A. D. Chemical evaluation of fatty acid desaturases as drug targets in *Trypanosoma cruzi*. *Int. J. Parasitol.* **39,** 985–993 (2009).
79. Tocher, D. R., Leaver, M. J. & Hodgson, P. A. Recent advances in the biochemistry and molecular biology of fatty acyl desaturases. *Prog. Lipid Res.* **37,** 73–117 (1998).
80. Broadwater, J. a, Whittle, E. & Shanklin, J. Desaturation and hydroxylation. Residues 148 and 324 of *Arabidopsis* FAD2, in addition to substrate chain length, exert a major influence in partitioning of catalytic specificity. *J. Biol. Chem.* **277,** 15613–15620 (2002).
81. Buist, P. H. Fatty acid desaturases: selecting the dehydrogenation channel. *Nat. Prod. Rep.* **21,** 249–62 (2004).
82. Reed, D. W., Savile, C. K., Qiu, X., Buist, P. H. & Covello, P. S. Mechanism of 1,4-dehydrogenation catalyzed by a fatty acid (1,4)-desaturase of *Calendula officinalis*. *Eur. J. Biochem.* **269,** 5024–9 (2002).
83. Rodríguez, S., Camps, F. & Fabriàs, G. Synthesis of gem-dideuterated tetradecanoic acids and their use in investigating the enzymatic transformation of (Z)-11-tetradecenoic acid into (E,E)-10,12-tetradecadienoic acid. *J. Org. Chem.* **66,** 8052–8 (2001).
84. Meesapyodsuk, D., Reed, D. W., Covello, P. S. & Qiu, X. Primary structure, regioselectivity, and evolution of the membrane-bound fatty acid desaturases of *Claviceps purpurea*. *J. Biol. Chem.* **282,** 20191–9 (2007).
85. Meesapyodsuk, D. *et al.* Characterization of the regiochemistry and cryptoregiochemistry of a *Caenorhabditis elegans* fatty acid desaturase (FAT-1) expressed in *Saccharomyces cerevisiae*. *Biochemistry* **39,** 11948–54 (2000).
86. Shanklin, J. Exploring the possibilities presented by protein engineering. *Curr. Opin. Plant Biol.* **3,** 243–8 (2000).
87. Spychalla, J. P., Kinney, A. J. & Browse, J. Identification of an animal omega-3 fatty acid desaturase by heterologous expression in *Arabidopsis*. *Proc. Natl. Acad. Sci. U. S. A.* **94,** 1142–1147 (1997).
88. Pugh, E. L. & Kates, M. Direct desaturation of eicosatrienoyl lecithin to arachidonoyl lecithin by rat liver microsomes. *J. Biol. Chem.* **252,** 68–73 (1977).
89. Walenga, R. W. & Lands, W. E. Effectiveness of various unsaturated fatty acids in supporting growth and respiration in *Saccharomyces cerevisiae*. *J. Biol. Chem.* **250,** 9121–9 (1975).
90. Liu, W., Jiao, H., O'Connor, M. & Roelofs, W. L. Moth desaturase characterized that produces both Z and E isomers of delta 11-tetradecenoic acids. *Insect Biochem. Mol. Biol.* **32,** 1489–95 (2002).
91. Hagström, Å. K. *et al.* A novel fatty acyl desaturase from the pheromone glands of *Ctenopseustis obliquana* and *C. herana* with specific Z5-desaturase activity on myristic acid. *J. Chem. Ecol.* **40,** 63–70 (2014).
92. Meesapyodsuk, D. & Qiu, X. Structure determinants for the substrate specificity of acyl-CoA Δ9 desaturases from a marine copepod. *ACS Chem. Biol.* **9,** 922–34 (2014).
93. Libisch, B., Michaelson, L. V, Lewis, M. J., Shewry, P. R. & Napier, J. A. Chimeras of Δ6-fatty acid and Δ8-sphingolipid desaturases. *Biochem. Biophys. Res. Commun.* **279,** 779–785 (2000).
94. Vanhercke, T., Shrestha, P., Green, A. G. & Singh, S. P. Mechanistic and structural insights into the regioselectivity of an Acyl-CoA fatty acid desaturase via directed molecular evolution. *J. Biol. Chem.* **286,** 12860–12869 (2011).
95. Watanabe, K. *et al.* Identification of amino acid residues that determine the substrate specificity of mammalian membrane-bound front-end fatty acid desaturases. *J. Lipid Res.* **57,** 89–99 (2016).
96. Hoffmann, M. *et al.* A small membrane-peripheral region close to the active center determines regioselectivity of membrane-bound fatty acid desaturases from *Aspergillus nidulans*. *J. Biol. Chem.* **282,** 26666–74 (2007).
97. Hongsthong, A., Subudhi, S., Sirijuntarat, M. & Cheevadhanarak, S. Mutation study of conserved amino acid residues of Spirulina delta 6-acyl-lipid desaturase showing involvement of histidine 313 in the regioselectivity of the enzyme. *Appl. Microbiol. Biotechnol.* **66,** 74–84 (2004).
98. Lim, Z. L., Senger, T. & Vrinten, P. Four amino acid residues influence the substrate chain-length and regioselectivity of *Siganus canaliculatus* Δ4 and Δ5/6 desaturases. *Lipids* **49,** 357–67 (2014).
99. Shi, H. *et al.* Molecular mechanism of substrate specificity for delta 6 desaturase from *Mortierella alpina*

and *Micromonas pusilla*. *J. Lipid Res.* **56,** 2309–2321 (2015).

100. Gagné, S. J., Reed, D. W., Gray, G. R. & Covello, P. S. Structural control of chemoselectivity, stereoselectivity, and substrate specificity in membrane-bound fatty acid acetylenases and desaturases. *Biochemistry* **48,** 12298–12304 (2009).
101. Rawat, R., Yu, X. H., Sweet, M. & Shanklin, J. Conjugated fatty acid synthesis: Residues 111 and 115 influence product partitioning of *Momordica charantia* conjugase. *J. Biol. Chem.* **287,** 16230–16237 (2012).
102. Heilmann, I., Pidkowich, M. S., Girke, T. & Shanklin, J. Switching desaturase enzyme specificity by alternate subcellular targeting. *Proc. Natl. Acad. Sci. U. S. A.* **101,** 10266–71 (2004).
103. Guy, J. E. *et al.* Remote control of regioselectivity in acyl-acyl carrier protein-desaturases. *Proc. Natl. Acad. Sci.* **108,** 16594–16599 (2011).
104. Rosenzweig, A. C., Frederick, C. A., Lippard, S. J. & Nordlund, P. Crystal structure of a bacterial non-haem iron hydroxylase that catalyses the biological oxidation of methane. *Nature* **366,** 537–543 (1993).
105. Sazinsky, M. H., Bard, J., Di Donato, A. & Lippard, S. J. Crystal structure of the toluene/o-xylene monooxygenase hydroxylase from *Pseudomonas stutzeri* OX1. Insight into the substrate specificity, substrate channeling, and active site tuning of multicomponent monooxygenases. *J. Biol. Chem.* **279,** 30600–10 (2004).
106. Choi, Y. S., Zhang, H., Brunzelle, J. S., Nair, S. K. & Zhao, H. In vitro reconstitution and crystal structure of p-aminobenzoate N-oxygenase (AurF) involved in aureothin biosynthesis. *Proc. Natl. Acad. Sci.* **105,** 6858–6863 (2008).
107. Nordlund, P., Sjöberg, B.-M. & Eklund, H. Three-dimensional structure of the free radical protein of ribonucleotide reductase. *Nature* **345,** 593–598 (1990).
108. Rather, L. J. *et al.* Structure and mechanism of the diiron benzoyl-coenzyme A epoxidase BoxB. *J. Biol. Chem.* **286,** 29241–8 (2011).
109. Nordlund, P. & Eklund, H. Di-iron—carboxylate proteins. *Curr. Opin. Struct. Biol.* **5,** 758–766 (1995).
110. Wallar, B. J. & Lipscomb, J. D. Dioxygen activation by enzymes containing binuclear non-heme iron clusters. *Chem. Rev.* **96,** 2625–2658 (1996).
111. Shanklin, J., Guy, J. E., Mishra, G. & Lindqvist, Y. Desaturases: emerging models for understanding functional diversification of diiron-containing enzymes. *J. Biol. Chem.* **284,** 18559–18563 (2009).
112. Haas, J. A. & Fox, B. G. Role of hydrophobic partitioning in substrate selectivity and turnover of the *Ricinus communis* stearoyl acyl carrier protein delta(9) desaturase. *Biochemistry* **38,** 12833–40 (1999).
113. Cahoon, E. B., Lindqvist, Y., Schneider, G. & Shanklin, J. Redesign of soluble fatty acid desaturases from plants for altered substrate specificity and double bond position. *Proc. Natl. Acad. Sci. U. S. A.* **94,** 4872–4877 (1997).
114. Whittle, E. & Shanklin, J. Engineering delta 9-16:0-acyl carrier protein (ACP) desaturase specificity based on combinatorial saturation mutagenesis and logical redesign of the castor delta 9-18:0-ACP desaturase. *J. Biol. Chem.* **276,** 21500–5 (2001).
115. Cahoon, E. B. & Shanklin, J. Substrate-dependent mutant complementation to select fatty acid desaturase variants for metabolic engineering of plant seed oils. *Proc. Natl. Acad. Sci.* **97,** 12350–12355 (2000).
116. Whittle, E. J., Tremblay, A. E., Buist, P. H. & Shanklin, J. Revealing the catalytic potential of an acyl-ACP desaturase: Tandem selective oxidation of saturated fatty acids. *Proc. Natl. Acad. Sci.* **105,** 14738–14743 (2008).
117. Wyatt, T. D. *Pheromones and animal behaviour: Communication by smell and taste*. (Cambridge University Press, 2003).
118. Wyatt, T. D. Fifty years of pheromones. *Nature* **457,** 262–263 (2009).
119. Roelofs, W. L. Chemistry of sex attraction. *Proc. Natl. Acad. Sci. U. S. A.* **92,** 44–9 (1995).
120. Tumlinson, J. H. *et al.* Identification of a pheromone blend attractive to *Manduca sexta* (L.) males in a wind tunnel. *Arch. Insect Biochem. Physiol.* **10,** 255–271 (1989).
121. Luxová, A., Urbanová, K., Valterová, I., Terzo, M. & Borg-Karlson, A.-K. Absolute configuration of chiral terpenes in marking pheromones of bumblebees and cuckoo bumblebees. *Chirality* **16,** 228–233 (2004).
122. Blomquist, G. J. *et al.* Pheromone production in bark beetles. *Insect Biochem. Mol. Biol.* **40,** 699–712 (2010).

123. Ayasse, M. & Jarau, S. Chemical ecology of bumble bees. *Annu. Rev. Entomol.* **59,** 299–319 (2014).
124. Pankewitz, F. & Hilker, M. Polyketides in insects: ecological role of these widespread chemicals and evolutionary aspects of their biogenesis. *Biol. Rev.* **83,** 209–226 (2008).
125. Morgan, D. E. in *Biosynth. insects* 146–178 (Royal Society of Chemistry, 2010).
126. Nishida, R. Sequestration of defensive substances from plants by Lepidoptera. *Annu. Rev. Entomol.* **47,** 57–92 (2002).
127. Howard, R. W. & Blomquist, G. J. Ecological, behavioral, and biochemical aspects of insect hydrocarbons. *Annu. Rev. Entomol.* **50,** 371–93 (2005).
128. Zweden, J. S. van & D'Ettorre, P. in *Insect Hydrocarb. Biol. Biochem. Chem. Ecol.* (Blomquist, G. J. & Bagneres, A.-G.) 222–281 (Cambridge University Press, 2010).
129. Vane-Wright, R. I. & Boppre, M. Visual and chemical signalling in butterflies: Functional and phylogenetic perspectives. *Philos. Trans. R. Soc. B Biol. Sci.* **340,** 197–205 (1993).
130. Nieberding, C. M. *et al.* The male sex pheromone of the butterfly *Bicyclus anynana*: towards an evolutionary analysis. *PLoS One* **3,** e2751 (2008).
131. Meer, R. K. Vander, Breed, M. D., Espelie, K. E. & Winston, and M. L. *Pheromone Communication in Social Insects: Ants, Wasps, Bees, and Termites*. (Westview Press, 1998).
132. Trhlin, M. & Rajchard, J. Chemical communication in the honeybee (*Apis mellifera* L.): a review. *Vet. Med. (Praha).* **56,** 265–273 (2011).
133. Slessor, K. N., Winston, M. L. & Le Conte, Y. Pheromone communication in the honeybee (*Apis mellifera* L.). *J. Chem. Ecol.* **31,** 2731–2745 (2005).
134. Plettner, E., Slessor, K. N., Winston, M. L. & Oliver, J. E. Caste-selective pheromone biosynthesis in honeybees. *Science (80-.).* **271,** 1851–1853 (1996).
135. Keeling, C. I., Slessor, K. N., Higo, H. A. & Winston, M. L. New components of the honey bee (*Apis mellifera* L.) queen retinue pheromone. *Proc. Natl. Acad. Sci.* **100,** 4486–4491 (2003).
136. Leoncini, I. *et al.* Regulation of behavioral maturation by a primer pheromone produced by adult worker honey bees. *Proc. Natl. Acad. Sci.* **101,** 17559–17564 (2004).
137. Le Conte, Y., Mohammedi, A. & Robinson, G. E. Primer effects of a brood pheromone on honeybee behavioural development. *Proc. R. Soc. B Biol. Sci.* **268,** 163–168 (2001).
138. Le Conte, Y., Arnold, G., Trouiller, J., Masson, C. & Chappe, B. Identification of a brood pheromone in honeybees. *Naturwissenschaften* **77,** 334–336 (1990).
139. Maisonnasse, A. *et al.* A scientific note on E-β-ocimene, a new volatile primer pheromone that inhibits worker ovary development in honey bees. *Apidologie* **40,** 562–564 (2009).
140. Dani, F. R. *et al.* Nestmate recognition cues in the honey bee: differential importance of cuticular alkanes and alkenes. *Chem. Senses* **30,** 477–489 (2005).
141. Thom, C., Gilley, D. C., Hooper, J. & Esch, H. E. The scent of the waggle dance. *PLoS Biol.* **5,** e228 (2007).
142. Šobotník, J. *et al.* Age-dependent changes in structure and function of the male labial gland in *Bombus terrestris*. *J. Insect Physiol.* **54,** 204–14 (2008).
143. Žáček, P. *et al.* Comparison of age-dependent quantitative changes in the male labial gland secretion of *Bombus terrestris* and *Bombus lucorum*. *J. Chem. Ecol.* **35,** 698–705 (2009).
144. Urbanová, K., Valterová, I., Hovorka, O. & Kindl, J. Chemotaxonomical characterisation of males *Bombus lucorum* (Hymenptera: Apidae) collected in Czech republic. *Eur. J. Entomol.* **127,** 111–115 (2001).
145. Bergström, G., Kullberg, B. J. & Ställberg-Stenhagen, S. Studies on natural odoriferous compounds: VII. Recognition of two forms of *Bombus lucorum* L. (Hymenoptera, Apidae) by analysis of the volatile marking secretion from individual males. *Zoon* **1,** 31–42 (1973).
146. Bergman, P. & Bergström, G. Scent marking, scent origin, and species specificity in male premating behavior of two Scandinavian bumblebees. *J. Chem. Ecol.* **23,** 1235–1251 (1997).
147. Niehuis, O. *et al.* Behavioural and genetic analyses of *Nasonia* shed light on the evolution of sex pheromones. *Nature* **494,** 345–8 (2013).
148. Abdel-latief, M., Garbe, L. A., Koch, M. & Ruther, J. An epoxide hydrolase involved in the biosynthesis of an insect sex attractant and its use to localize the production site. *Proc. Natl. Acad. Sci.* **105,** 8914–8919 (2008).
149. Wicker-Thomas, C. Pheromonal communication involved in courtship behavior in Diptera. *J. Insect*

Physiol. **53,** 1089–1100 (2007).

150. Gemeno, C. & Schal, C. in *Adv. insect Chem. Ecol.* (Cardé, R. T. & Hillar, J. G.) 179–247 (Cambridge University Press, 2004).
151. Seybold, S. J. & Vanderwel, D. in *Insect Biochem. Mol. Biol.* (Blomquist, G. J. & Vogt, R. G.) 137–200 (Elsevier Academic Press, 2003).
152. Leal, W. S. Chemical ecology of phytophagous scarab beetles. *Annu. Rev. Entomol.* **43,** 39–61 (1998).
153. Spikes, A. E. *et al.* First contact pheromone identified for a longhorned beetle (Coleoptera: Cerambycidae) in the subfamily Prioninae. *J. Chem. Ecol.* **36,** 943–54 (2010).
154. Morgan, E. D. in *Biosynth. insects - Adv. Ed.* 66–95 (RSC Publishing, 2010).
155. Liénard, M. A., Strandh, M., Hedenström, E., Johansson, T. & Löfstedt, C. Key biosynthetic gene subfamily recruited for pheromone production prior to the extensive radiation of Lepidoptera. *BMC Evol. Biol.* **8,** 270 (2008).
156. Ma, P. W. K. & Ramaswamy, S. B. in *Insect Pheromone Biochem. Mol. Biol.* (Blomquist, G. J. & Vogt, R.) 19–51 (2003).
157. Tillman, J. a, Seybold, S. J., Jurenka, R. a & Blomquist, G. J. Insect pheromones--an overview of biosynthesis and endocrine regulation. *Insect Biochem. Mol. Biol.* **29,** 481–514 (1999).
158. Liénard, M. A., Hagström, A. K., Lassance, J.-M. & Löfstedt, C. Evolution of multicomponent pheromone signals in small ermine moths involves a single fatty-acyl reductase gene. *Proc. Natl. Acad. Sci. U. S. A.* **107,** 10955–60 (2010).
159. Zhao, C.-H., Lu, F., Bengtsson, M. & Löfstedt, C. Substrate specificity of acetyltransferase and reductase enzyme systems used in pheromone biosynthesis by Asian corn borer,*Ostrinia furnacalis*. *J. Chem. Ecol.* **21,** 1495–1510 (1995).
160. Gu, P., Welch, W. H., Guo, L., Schegg, K. M. & Blomquist, G. J. Characterization of a novel microsomal fatty acid synthetase (FAS) compared to a cytosolic FAS in the housefly, *Musca domestica*. *Comp. Biochem. Physiol. B. Biochem. Mol. Biol.* **118,** 447–56 (1997).
161. Gu, P., Welch, W. H. & Blomquist, G. J. Methyl-branched fatty acid biosynthesis in the German cockroach, *Blatella germanica*: Kinetic studies comparing a microsomal and soluble fatty acid synthetase. *Insect Biochem. Mol. Biol.* **23,** 263–271 (1993).
162. Juárez, M. P. & Fernández, G. C. Cuticular hydrocarbons of triatomines. *Comp. Biochem. Physiol. Part A Mol. Integr. Physiol.* **147,** 711–730 (2007).
163. Ohnishi, A., Hashimoto, K., Imai, K. & Matsumoto, S. Functional characterization of the *Bombyx mori* fatty acid transport protein (BmFATP) within the silkmoth pheromone gland. *J. Biol. Chem.* **284,** 5128–36 (2009).
164. Matsumoto, S. *et al.* Chemical characterization of cytoplasmic lipid droplets in the pheromone-producing cells of the silkmoth, *Bombyx mori*. *Insect Biochem. Mol. Biol.* **32,** 1447–1455 (2002).
165. Du, M., Zhang, S., Zhu, B., Yin, X. & An, S. Identification of a diacylglycerol acyltransferase 2 gene involved in pheromone biosynthesis activating neuropeptide stimulated pheromone production in *Bombyx mori*. *J. Insect Physiol.* **58,** 699–703 (2012).
166. Du, M. *et al.* Identification of lipases involved in PBAN stimulated pheromone production in *Bombyx mori* using the DGE and RNAi approaches. *PLoS One* **7,** e31045 (2012).
167. Millar, J. G. Polyene hydrocarbons and epoxides: a second major class of lepidopteran sex attractant pheromones. *Annu. Rev. Entomol.* **45,** 575–604 (2000).
168. Matsuoka, K. *et al.* Transport of a hydrophobic biosynthetic precursor by lipophorin in the hemolymph of a geometrid female moth which secretes an epoxyalkenyl sex pheromone. *Insect Biochem. Mol. Biol.* **36,** 576–583 (2006).
169. Carot-Sans, G., Muñoz, L., Piulachs, M. D., Guerrero, A. & Rosell, G. Identification and characterization of a fatty acyl reductase from a *Spodoptera littoralis* female gland involved in pheromone biosynthesis. *Insect Mol. Biol.* **24,** 82–92 (2015).
170. Moto, K. *et al.* Pheromone gland-specific fatty-acyl reductase of the silkmoth, *Bombyx mori*. *Proc. Natl. Acad. Sci. U. S. A.* **100,** 9156–61 (2003).
171. Lassance, J.-M. *et al.* Allelic variation in a fatty-acyl reductase gene causes divergence in moth sex pheromones. *Nature* **466,** 486–9 (2010).
172. Teerawanichpan, P., Robertson, A. J. & Qiu, X. A fatty acyl-CoA reductase highly expressed in the head

of honey bee (*Apis mellifera*) involves biosynthesis of a wide range of aliphatic fatty alcohols. *Insect Biochem. Mol. Biol.* **40,** 641–9 (2010).

173. Antony, B. *et al.* Pheromone-gland-specific fatty-acyl reductase in the adzuki bean borer, *Ostrinia scapulalis* (Lepidoptera: Crambidae). *Insect Biochem. Mol. Biol.* **39,** 90–95 (2009).
174. Lassance, J.-M. *et al.* Functional consequences of sequence variation in the pheromone biosynthetic gene pgFAR for *Ostrinia* moths. *Proc. Natl. Acad. Sci. U. S. A.* **110,** 3967–72 (2013).
175. Hagström, A. K., Liénard, M. A., Groot, A. T., Hedenström, E. & Löfstedt, C. Semi-selective fatty acyl reductases from four heliothine moths influence the specific pheromone composition. *PLoS One* **7,** e37230 (2012).
176. Hagström, A. K., Walther, A., Wendland, J. & Löfstedt, C. Subcellular localization of the fatty acyl reductase involved in pheromone biosynthesis in the tobacco budworm, *Heliothis virescens* (Noctuidae: Lepidoptera). *Insect Biochem. Mol. Biol.* **43,** 510–21 (2013).
177. Du, M. *et al.* Glycerol-3-phosphate O-acyltransferase is required for PBAN-induced sex pheromone biosynthesis in *Bombyx mori*. *Sci. Rep.* **5,** 8110 (2015).
178. Zhang, S. D. *et al.* Molecular identification of a pancreatic lipase-like gene involved in sex pheromone biosynthesis of *Bombyx mori*. *Insect Sci.* **21,** 459–468 (2014).
179. Brabcová, J. *et al.* Characterization of neutral lipase BT-1 isolated from the labial gland of *Bombus terrestris* males. *PLoS One* **8,** e80066 (2013).
180. Ohnishi, A. *et al.* Hormone signaling linked to silkmoth sex pheromone biosynthesis involves Ca2+/calmodulin-dependent protein kinase II-mediated phosphorylation of the insect PAT family protein *Bombyx mori* lipid storage droplet protein-1 (BmLsd1). *J. Biol. Chem.* **286,** 24101–24112 (2011).
181. Matsumoto, S. *et al.* Characterization of acyl-CoA-binding protein (ACBP) in the pheromone gland of the silkworm, *Bombyx mori*. *Insect Biochem. Mol. Biol.* **31,** 603–9 (2001).
182. Qiu, Y. *et al.* An insect-specific P450 oxidative decarbonylase for cuticular hydrocarbon biosynthesis. *Proc. Natl. Acad. Sci.* **109,** 14858–14863 (2012).
183. Tillman-Wall, J. A., Vanderwel, D., Kuenzli, M. E., Reitz, R. C. & Blomquist, G. J. Regulation of sex pheromone biosynthesis in the housefly, *Musca domestica*: Relative contribution of the elongation and reductive steps. *Arch. Biochem. Biophys.* **299,** 92–99 (1992).
184. Wicker-Thomas, C. & Chertemps, T. in *Insect Hydrocarb. Biol. Biochem. Chem. Ecol.* 53–74 (2010).
185. Rosell, G., Hospital, S., Camps, F. & Guerrero, A. Inhibition of a chain shortening step in the biosynthesis of the sex pheromone of the Egyptian armyworm *Spodoptera littoralis*. *Insect Biochem. Mol. Biol.* **22,** 679–685 (1992).
186. Jurenka, R. A., Haynes, K. F., Adlof, R. O., Bengtsson, M. & Roelofs, W. L. Sex pheromone component ratio in the cabbage looper moth altered by a mutation affecting the fatty acid chain-shortening reactions in the pheromone biosynthetic pathway. *Insect Biochem. Mol. Biol.* **24,** 373–381 (1994).
187. Jurenka, R. A., Subchev, M., Abad, J.-L., Choi, M.-Y. & Fabrias, G. Sex pheromone biosynthetic pathway for disparlure in the gypsy moth, *Lymantria dispar*. *Proc. Natl. Acad. Sci.* **100,** 809–814 (2003).
188. Millar, J. G. in *Insect Hydrocarb. Biol. Biochem. Chem. Ecol.* 390–447 (2010).
189. Jurenka, R. A. & Roelofs, W. L. Characterization of the acetyltransferase used in pheromone biosynthesis in moths: Specificity for the Z isomer in tortricidae. *Insect Biochem.* **19,** 639–644 (1989).
190. Luxová, A. & Svatoš, A. Substrate specificity of membrane-bound alcohol oxidase from the tobacco hornworm moth (*Manduca sexta*) female pheromone glands. *J. Mol. Catal. B Enzym.* **38,** 37–42 (2006).
191. Fang, N., Teal, P. E. A. & Tumlinson, J. H. Characterization of oxidase (s) associated with the sex pheromone gland in *Manduca sexta* (L.) females. **257,** 243–257 (1995).
192. Teal, P. E. & Tumlinson, J. H. Terminal steps in pheromone biosynthesis by *Heliothis virescens* and *H. zea*. *J. Chem. Ecol.* **12,** 353–66 (1986).
193. Vogel, H., Heidel, A. J., Heckel, D. G. & Groot, A. T. Transcriptome analysis of the sex pheromone gland of the noctuid moth *Heliothis virescens*. *BMC Genomics* **11,** (2010).
194. Tsfadia, O. *et al.* Pheromone biosynthetic pathways: PBAN-regulated rate-limiting steps and differential expression of desaturase genes in moth species. *Insect Biochem. Mol. Biol.* **38,** 552–567 (2008).
195. Alabaster, A. *et al.* Deficiencies in acetyl-CoA carboxylase and fatty acid synthase 1 differentially affect eggshell formation and blood meal digestion in *Aedes aegypti*. *Insect Biochem. Mol. Biol.* **41,** 946–955 (2011).

196. Groot, A. T. *et al.* Experimental evidence for interspecific directional selection on moth pheromone communication. *Proc. Natl. Acad. Sci.* **103,** 5858–5863 (2006).
197. Symonds, M. R. E. & Elgar, M. a. The evolution of pheromone diversity. *Trends Ecol. Evol.* **23,** 220–8 (2008).
198. Higgie, M., Chenoweth, S. & Blows, M. W. Natural selection and the reinforcement of mate recognition. *Science* **290,** 519–21 (2000).
199. Haynes, K. F. & Yeargan, K. V. Exploitation of intraspecific communication systems: Illicit signalers and receivers. *Ann. Entomol. Soc. Am.* **92,** 960–970 (1999).
200. Raffa, K. F. & Dahlsten, D. L. Differential responses among natural enemies and prey to bark beetle pheromones. *Oecologia* **102,** 17–23 (1995).
201. Rouault, J., Capy, P. & Jallon, J. M. Variations of male cuticular hydrocarbons with geoclimatic variables: an adaptative mechanism in *Drosophila melanogaster*? *Genetica* **110,** 117–30 (2000).
202. Rundle, H. D., Chenoweth, S. F., Doughty, P. & Blows, M. W. Divergent selection and the evolution of signal traits and mating preferences. *PLoS Biol.* **3,** e368 (2005).
203. Ferveur, J.-F. Cuticular hydrocarbons: their evolution and roles in *Drosophila* pheromonal communication. *Behav. Genet.* **35,** 279–95 (2005).
204. Paterson, H. E. H. in *Species Speciat.* (Vrba, E. S.) (1985).
205. Wiley, C., Ellison, C. K. & Shaw, K. L. Widespread genetic linkage of mating signals and preferences in the Hawaiian cricket *Laupala*. *Proc. Biol. Sci.* **279,** 1203–9 (2012).
206. Löfstedt, C., Hansson, B. S., Roelofs, W. & Bengtsson, B. O. No linkage between genes controlling female pheromone production and male pheromone response in the European corn borer, *Ostrinia nubilalis* Hübner (Lepidoptera; Pyralidae). *Genetics* **123,** 553–6 (1989).
207. Allison, J. D., Roff, D. A. & Cardé, R. T. Genetic independence of female signal form and male receiver design in the almond moth, *Cadra cautella*. *J. Evol. Biol.* **21,** 1666–1672 (2008).
208. Boake, C. R. Coevolution of senders and receivers of sexual signals: Genetic coupling and genetic correlations. *Trends Ecol. Evol.* **6,** 225–227 (1991).
209. Marcillac, F., Grosjean, Y. & Ferveur, J.-F. A single mutation alters production and discrimination of *Drosophila* sex pheromones. *Proc. R. Soc. B Biol. Sci.* **272,** 303–309 (2005).
210. Bousquet, F. *et al.* Expression of a desaturase gene, *desat1*, in neural and nonneural tissues separately affects perception and emission of sex pheromones in *Drosophila*. *Proc. Natl. Acad. Sci.* **109,** 249–254 (2012).
211. Phelan, P. L. in *Insect Chem. Ecol. An Evol. Approach* (Roitberg, B. D. & Isman, M. B.) 265–314 (Chapman & Hal, 1992).
212. Baker, T. C. Mechanism for saltational shifts in pheromone communication systems. *Proc. Natl. Acad. Sci. U. S. A.* **99,** 13368–13370 (2002).
213. Roelofs, W. L. *et al.* Evolution of moth sex pheromones via ancestral genes. *Proc. Natl. Acad. Sci. U. S. A.* **99,** 13621–6 (2002).
214. Martin, N., Moore, K., Musto, C. J. & Linn, C. E. Flight Tunnel Response of Male European Corn Borer Moths to Cross-Specific Mixtures of European and Asian Corn Borer Sex Pheromones: Evidence Supporting a Critical Stage in Evolution of a New Communication System. *J. Chem. Ecol.* **42,** 51–4 (2016).
215. Löfstedt, C., Herrebout, W. M. & Menken, S. B. J. Sex pheromones and their potential role in the evolution of reproductive isolation in small ermine moths (Yponomeutidae). *Chemoecology* **2,** 20–28 (1991).
216. Symonds, M. R. E. & Gitau-Clarke, C. W. in *Adv. In Insect Phys.* 195–234 (2016).
217. Domingue, M. J., Musto, C. J., Linn, C. E., Roelofs, W. L. & Baker, T. C. Evidence of olfactory antagonistic imposition as a facilitator of evolutionary shifts in pheromone blend usage in *Ostrinia* spp. (Lepidoptera: Crambidae). *J. Insect Physiol.* **53,** 488–496 (2007).
218. Greenfield, M. D. in *Signalers Receiv. Mech. Evol. arthropod Commun.* 22–111 (Oxford University Press, 2002).
219. Galizia, C. G. & Rössler, W. Parallel olfactory systems in insects: anatomy and function. *Annu. Rev. Entomol.* **55,** 399–420 (2010).
220. Tabata, J., Noguchi, H., Kainoh, Y., Mochizuki, F. & Sugie, H. Sex pheromone production and perception in the mating disruption-resistant strain of the smaller tea leafroller moth, *Adoxophyes honmai*. *Entomol.*

Exp. Appl. **122,** 145–153 (2007).
221. Liu, Y. B. & Haynes, K. F. Evolution of behavioral responses to sex pheromone in mutant laboratory colonies of *Trichoplusia ni*. *J. Chem. Ecol.* **20,** 231–8 (1994).
222. Leary, G. P. *et al.* Single mutation to a sex pheromone receptor provides adaptive specificity between closely related moth species. *Proc. Natl. Acad. Sci.* **109,** 14081–14086 (2012).
223. Shirangi, T. R., Dufour, H. D., Williams, T. M. & Carroll, S. B. Rapid evolution of sex pheromone-producing enzyme expression in *Drosophila*. *PLoS Biol.* **7,** e1000168 (2009).
224. Tabata, J. & Ishikawa, Y. Genetic basis to divergence of sex pheromones in two closely related moths, *Ostrinia scapulalis* and *O. zealis*. *J. Chem. Ecol.* **31,** 1111–24 (2005).
225. Roelofs, W. L. & Jurenka, R. A. Biosynthetic enzymes regulating ratios of sex pheromone components in female redbanded leafroller moths. *Bioorg. Med. Chem.* **4,** 461–466 (1996).
226. Gaunt, M. W. & Miles, M. A. An insect molecular clock dates the origin of the insects and accords with palaeontological and biogeographic landmarks. *Mol. Biol. Evol.* **19,** 748–761 (2002).
227. Nei, M. & Rooney, A. P. Concerted and birth-and-death evolution of multigene families. *Annu. Rev. Genet.* **39,** 121–52 (2005).
228. Fang, S. *et al.* Molecular evolution and functional diversification of fatty acid desaturases after recurrent gene duplication in *Drosophila*. *Mol. Biol. Evol.* **26,** 1447–1456 (2009).
229. Knipple, D. C., Rosenfield, C.-L., Nielsen, R., You, K. M. & Jeong, S. E. Evolution of the integral membrane desaturase gene family in moths and flies. *Genetics* **162,** 1737–52 (2002).
230. Liénard, M. A., Wang, H.-L., Lassance, J.-M. & Löfstedt, C. Sex pheromone biosynthetic pathways are conserved between moths and the butterfly *Bicyclus anynana*. *Nat. Commun.* **5,** (2014).
231. Helmkampf, M., Cash, E. & Gadau, J. Evolution of the insect desaturase gene family with an emphasis on social Hymenoptera. *Mol. Biol. Evol.* **32,** 456–71 (2015).
232. Buček, A. *et al.* Evolution of moth sex pheromone composition by a single amino acid substitution in a fatty acid desaturase. *Proc. Natl. Acad. Sci.* **112,** 12586–12591 (2015).
233. Legendre, A., Miao, X.-X., Da Lage, J.-L. & Wicker-Thomas, C. Evolution of a desaturase involved in female pheromonal cuticular hydrocarbon biosynthesis and courtship behavior in *Drosophila*. *Insect Biochem. Mol. Biol.* **38,** 244–255 (2008).
234. Eigenheer, A. L. *et al.* Isolation and molecular characterization of *Musca domestica* delta-9 desaturase sequences. *Insect Mol. Biol.* **11,** 533–542 (2002).
235. Matoušková, P. *et al.* A delta9 desaturase from *Bombus lucorum* males: investigation of the biosynthetic pathway of marking pheromones. *Chembiochem* **9,** 2534–41 (2008).
236. Horne, I., Gibb, N., Damcevski, K., Glover, K. & Haritos, V. S. Two conserved Z9-octadecanoic acid desaturases in the red flour beetle, *Tribolium castaneum*. *Gene* **468,** 41–7 (2010).
237. Riddervold, M. H., Tittiger, C., Blomquist, G. J. & Borgeson, C. E. Biochemical and molecular characterizaton of house cricket (*Acheta domesticus*, Orthoptera: Gryllidae) Delta9 desaturase. *Insect Biochem. Mol. Biol.* **32,** 1731–40 (2002).
238. Zhou, X.-R. *et al.* Isolation and functional characterization of two independently-evolved fatty acid Delta12-desaturase genes from insects. *Insect Mol. Biol.* **17,** 667–76 (2008).
239. Xue, B., Rooney, A. P., Kajikawa, M., Okada, N. & Roelofs, W. L. Novel sex pheromone desaturases in the genomes of corn borers generated through gene duplication and retroposon fusion. *Proc. Natl. Acad. Sci. U. S. A.* **104,** 4467–72 (2007).
240. Wang, H.-L., Liénard, M. a, Zhao, C.-H., Wang, C.-Z. & Löfstedt, C. Neofunctionalization in an ancestral insect desaturase lineage led to rare Δ6 pheromone signals in the Chinese tussah silkworm. *Insect Biochem. Mol. Biol.* **40,** 742–51 (2010).
241. Fujii, T. *et al.* Discovery of a disused desaturase gene from the pheromone gland of the moth *Ascotis selenaria*, which secretes an epoxyalkenyl sex pheromone. *Biochem. Biophys. Res. Commun.* **441,** 849–855 (2013).
242. Groot, A. T. *et al.* Within-population variability in a moth sex pheromone blend: genetic basis and behavioural consequences. *Proc. Biol. Sci.* **281,** 20133054 (2014).
243. Albre, J. *et al.* Sex pheromone evolution is associated with differential regulation of the same desaturase gene in two genera of leafroller moths. *PLoS Genet.* **8,** e1002489 (2012).
244. Albre, J., Steinwender, B. & Newcomb, R. D. The evolution of desaturase gene regulation involved in sex

pheromone production in leafroller moths of the genus *Planotortrix*. *J. Hered.* **104,** 627–638 (2013).

245. Sakai, R., Fukuzawa, M., Nakano, R., Tatsuki, S. & Ishikawa, Y. Alternative suppression of transcription from two desaturase genes is the key for species-specific sex pheromone biosynthesis in two *Ostrinia* moths. *Insect Biochem. Mol. Biol.* **39,** 62–7 (2009).
246. Matoušková, P., Pichová, I. & Svatoš, A. Functional characterization of a desaturase from the tobacco hornworm moth (*Manduca sexta*) with bifunctional Z11- and 10,12-desaturase activity. *Insect Biochem. Mol. Biol.* **37,** 601–610 (2007).
247. Fang, N., Teal, P. E. A., Doolittle, R. E. & Tumlinson, J. H. Biosynthesis of conjugated olefinic systems in the sex pheromone gland of female tobacco hornworm moths, *Manduca sexta* (L.). *Insect Biochem. Mol. Biol.* **25,** 39–48 (1995).
248. Kullenberg, B., Bergstrom, G., Bringer, B., Carlberg, B. & Cederberg, B. Observations on scent marking by *Bombus* Latr. and *Psithyrus* Lep. males (Hym. Apidae) and localization of site of production of the secretion. *Zoon* **1,** 23–30 (1973).
249. Albert, T., Spaethe, J., Grubel, K. & Rossler, W. Royal jelly-like protein localization reveals differences in hypopharyngeal glands buildup and conserved expression pattern in brains of bumblebees and honeybees. *Biol. Open* **3,** 281–288 (2014).
250. Poiani, S. B. & Da Cruz-Landim, C. Morphological changes in the cephalic salivary glands of females and males of *Apis mellifera* and *Scaptotrigona postica* (Hymenoptera, Apidae). *J. Biosci.* **35,** 249–255 (2010).
251. Lanne, B. S., Bergström, G., Wassgren, A.-B. & Törnbäck, B. Biogenetic pattern of straight chain marking compounds in male bumble bees. *Comp. Biochem. Physiol.* **88,** 631–636 (1987).
252. Certik, M. & Shimizu, S. Biosynthesis and regulation of microbial polyunsaturated fatty acid production. *J. Biosci. Bioeng.* **87,** 1–14 (1999).
253. Wilson, R. a, Calvo, A. M., Chang, P.-K. & Keller, N. P. Characterization of the Aspergillus parasiticus delta12-desaturase gene: a role for lipid metabolism in the *Aspergillus*-seed interaction. *Microbiology* **150,** 2881–8 (2004).
254. Calvo, A. M., Gardner, H. W. & Keller, N. P. Genetic connection between fatty acid metabolism and sporulation in *Aspergillus nidulans*. *J. Biol. Chem.* **276,** 25766–25774 (2001).
255. Sakuradani, E., Kobayashi, M., Ashikari, T. & Shimizu, S. Identification of Delta12-fatty acid desaturase from arachidonic acid-producing mortierella fungus by heterologous expression in the yeast *Saccharomyces cerevisiae* and the fungus *Aspergillus oryzae*. *Eur. J. Biochem.* **261,** 812–20 (1999).
256. Huang, Y. S. *et al.* Cloning of delta12- and delta6-desaturases from *Mortierella alpina* and recombinant production of gamma-linolenic acid in *Saccharomyces cerevisiae*. *Lipids* **34,** 649–59 (1999).
257. Sakuradani, E., Abe, T., Iguchi, K. & Shimizu, S. A novel fungal omega3-desaturase with wide substrate specificity from arachidonic acid-producing *Mortierella alpina* 1S-4. *Appl. Microbiol. Biotechnol.* **66,** 648–54 (2005).
258. Damude, H. G. *et al.* Identification of bifunctional delta12/omega3 fatty acid desaturases for improving the ratio of omega3 to omega6 fatty acids in microbes and plants. *Proc. Natl. Acad. Sci. U. S. A.* **103,** 9446–9451 (2006).
259. Wei, D. S., Li, M. C., Zhang, X. X., Zhou, H. & Xing, L. J. A novel Delta12-fatty acid desaturase gene from methylotrophic yeast *Pichia pastoris* GS115. *Acta Biochim. Pol.* **53,** 753–9 (2006).
260. Zhang, X., Li, M., Wei, D. & Xing, L. Identification and characterization of a novel yeast omega3-fatty acid desaturase acting on long-chain n-6 fatty acid substrates from *Pichia pastoris*. *Yeast* **25,** 21–7 (2008).
261. Kainou, K., Kamisaka, Y., Kimura, K. & Uemura, H. Isolation of Delta12 and omega3-fatty acid desaturase genes from the yeast *Kluyveromyces lactis* and their heterologous expression to produce linoleic and alpha-linolenic acids in *Saccharomyces cerevisiae*. *Yeast* **23,** 605–12 (2006).
262. Oura, T. & Kajiwara, S. *Saccharomyces kluyveri* FAD3 encodes an omega3 fatty acid desaturase. *Microbiology* **150,** 1983–90 (2004).
263. Watanabe, K., Oura, T., Sakai, H. & Kajiwara, S. Yeast Delta 12 fatty acid desaturase: gene cloning, expression, and function. *Biosci. Biotechnol. Biochem.* **68,** 721–7 (2004).
264. Yan, Z. *et al.* Clone and identification of bifunctional Δ12/Δ15 fatty acid desaturase LKFAD15 from *Lipomyces kononenkoae*. *Food Sci. Biotechnol.* **22,** 573–576 (2013).
265. Peyou-Ndi, M. M., Watts, J. L. & Browse, J. Identification and characterization of an animal delta(12) fatty acid desaturase gene by heterologous expression in *Saccharomyces cerevisiae*. *Arch. Biochem.*

Biophys. **376,** 399–408 (2000).

266. Zhou, X.-R., Green, A. G. & Singh, S. P. *Caenorhabditis elegans* Delta12-desaturase FAT-2 is a bifunctional desaturase able to desaturate a diverse range of fatty acid substrates at the Delta12 and Delta15 positions. *J. Biol. Chem.* **286,** 43644–50 (2011).
267. Kikukawa, H. *et al.* Characterization of a trifunctional fatty acid desaturase from oleaginous filamentous fungus *Mortierella alpina* 1S-4 using a yeast expression system. *J. Biosci. Bioeng.* **116,** 672–6 (2013).
268. Buček, A., Matoušková, P., Sychrová, H., Pichová, I. & Hrušková-Heidingsfeldová, O. Δ12-Fatty acid desaturase from *Candida parapsilosis* is a multifunctional desaturase producing a range of polyunsaturated and hydroxylated fatty acids. *PLoS One* **9,** e93322 (2014).
269. Sadd, B. M. *et al.* The genomes of two key bumblebee species with primitive eusocial organization. *Genome Biol.* **16,** 76 (2015).
270. Roelofs, W. L. & Rooney, A. P. Molecular genetics and evolution of pheromone biosynthesis in Lepidoptera. *Proc. Natl. Acad. Sci. U. S. A.* **100,** 9179–84 (2003).
271. Park, H. Y., Kim, M. S., Paek, A., Jeong, S. E. & Knipple, D. C. An abundant acyl-CoA (Delta9) desaturase transcript in pheromone glands of the cabbage moth, *Mamestra brassicae*, encodes a catalytically inactive protein. *Insect Biochem. Mol. Biol.* **38,** 581–95 (2008).
272. de Sousa Abreu, R., Penalva, L. O., Marcotte, E. M. & Vogel, C. Global signatures of protein and mRNA expression levels. *Mol. Biosyst.* **5,** 1512–26 (2009).
273. Žáček, P. *et al.* Biosynthetic studies of the male marking pheromone in bumblebees by using labelled fatty acids and two-dimensional gas chromatography with mass detection. *Chempluschem* **80,** 839–850 (2015).
274. Cahoon, E. B., Shanklin, J. & Ohlrogge, J. B. Expression of a coriander desaturase results in petroselinic acid production in transgenic tobacco. *Proc. Natl. Acad. Sci. U. S. A.* **89,** 11184–11188 (1992).
275. Schlüter, P. M. *et al.* Stearoyl-acyl carrier protein desaturases are associated with floral isolation in sexually deceptive orchids. *Proc. Natl. Acad. Sci. U. S. A.* **108,** 5696–701 (2011).
276. Bellés, X. Beyond *Drosophila*: RNAi in vivo and functional genomics in insects. *Annu. Rev. Entomol.* **55,** 111–128 (2010).
277. Terenius, O. *et al.* RNA interference in Lepidoptera: an overview of successful and unsuccessful studies and implications for experimental design. *J. Insect Physiol.* **57,** 231–45 (2011).
278. Lou, Y., Schwender, J. & Shanklin, J. FAD2 and FAD3 desaturases form heterodimers that facilitate metabolic channeling in vivo. *J. Biol. Chem.* **289,** 17996–8007 (2014).
279. Witzgall, P., Kirsch, P. & Cork, A. Sex pheromones and their impact on pest management. *J. Chem. Ecol.* **36,** 80–100 (2010).
280. Evenden, M. L. & Haynes, K. F. Potential for the evolution of resistance to pheromone-based mating disruption tested using two pheromone strains of the cabbage looper, *Trichoplusia ni*. *Entomol. Exp. Appl.* **100,** 131–134 (2001).

6 Supplements (Publications I – III)

I. Buček A, Matoušková P, Vogel H, Šebesta P, Jahn U, Weißflog J, Svatoš A, Pichová I (**2015**) *Evolution of moth sex pheromone composition by a single amino acid substitution in a fatty acid desaturase.* Proc Natl Acad Sci **112**(41): 12586–12591.

II. Buček A, Vogel H, Matoušková P, Prchalová D, Záček P, Vrkoslav V, Šebesta P, Svatoš A, Jahn U, Valterová I, Pichová I (**2013**) *The role of desaturases in the biosynthesis of marking pheromones in bumblebee males.* Insect Biochem Mol Biol **43**(8): 724–31.

III. Buček A, Matoušková P, Sychrová H, Pichová I, Hrušková-Heidingsfeldová O (**2014**) *Δ12-fatty acid desaturase from* Candida parapsilosis *is a multifunctional desaturase producing a range of polyunsaturated and hydroxylated fatty acids.* PLoS One **9**(3):e93322.

Evolution of moth sex pheromone composition by a single amino acid substitution in a fatty acid desaturase

Aleš Buček[a,1], Petra Matoušková[b,1], Heiko Vogel[c], Petr Šebesta[a], Ullrich Jahn[a], Jerrit Weißflog[d], Aleš Svatoš[a,d,2], and Iva Pichová[a,2]

[a]Institute of Organic Chemistry and Biochemistry, Academy of Sciences of the Czech Republic, 166 10 Prague 6, Czech Republic; [b]Faculty of Pharmacy, Charles University in Prague, 500 05 Hradec Králové, Czech Republic; [c]Max Planck Institute for Chemical Ecology, Department of Entomology, D-07745, Jena, Germany; and [d]Max Planck Institute for Chemical Ecology, Mass Spectrometry Group, D-07745, Jena, Germany

Edited by Jerrold Meinwald, Cornell University, Ithaca, NY, and approved September 3, 2015 (received for review July 23, 2015)

For sexual communication, moths primarily use blends of fatty acid derivatives containing one or more double bonds in various positions and configurations, called sex pheromones (SPs). To study the molecular basis of novel SP component (SPC) acquisition, we used the tobacco hornworm (*Manduca sexta*), which uses a blend of mono-, di-, and uncommon triunsaturated fatty acid (3UFA) derivatives as SP. We identified pheromone-biosynthetic fatty acid desaturases (FADs) *Msex*D3, *Msex*D5, and *Msex*D6 abundantly expressed in the *M. sexta* female pheromone gland. Their functional characterization and in vivo application of FAD substrates indicated that *Msex*D3 and *Msex*D5 biosynthesize 3UFAs via *E*/*Z*14 desaturation from diunsaturated fatty acids produced by previously characterized *Z*11-desaturase/conjugase *Msex*D2. Site-directed mutagenesis of sequentially highly similar *Msex*D3 and *Msex*D2 demonstrated that swapping of a single amino acid in the fatty acyl substrate binding tunnel introduces *E*/*Z*14-desaturase specificity to mutated *Msex*D2. Reconstruction of FAD gene phylogeny indicates that *Msex*D3 was recruited for biosynthesis of 3UFA SPCs in *M. sexta* lineage via gene duplication and neofunctionalization, whereas *Msex*D5 representing an alternative 3UFA-producing FAD has been acquired via activation of a presumably inactive ancestral *Msex*D5. Our results demonstrate that a change as small as a single amino acid substitution in a FAD enzyme might result in the acquisition of new SP compounds.

fatty acid desaturase | *Manduca sexta* | sex pheromone biosynthesis | pheromone evolution | substrate specificity

Sex pheromones (SPs) are a diverse group of chemical compounds that are central to mate-finding behavior in insects (1). Variation in SP composition between closely related species and among populations is well documented. Despite this variation, SPs are presumed to be under strong stabilizing selection, and thus the genetic mechanisms driving SP diversification represented an enigma (2). Research on SPs in moths (Insecta: Lepidoptera) helped establish the hypothesis of asymmetric tracking as a major driving force in SP diversification. In this scenario, abrupt changes in female SP composition via a shift in component ratio or the inclusion or loss of a component result in a distinct SP that attracts males with more broadly or differentially tuned SP preference (3). Assortative mating, the preferential mating of females producing a novel SP with males attracted to this SP, restricts gene flow between subpopulations with differing SP compositions. This can ultimately lead to speciation and fixation of novel communication channels (4). Work in insect models such as wasps (5), fruit flies (6), and especially moths (7–9) is helping uncover the genetic basis of SP diversification.

In the majority of moth species, females use species-specific mixtures of SP components (SPCs) consisting of volatile fatty acid (FA) derivatives to attract conspecific males at long range. These SPCs are predominantly long-chain aliphatic (C12–C18) acetates, alcohols, or aldehydes containing zero to three double bonds of various configurations at different positions along the carbon backbone (10). Pheromone biosynthesis involves modifications of fatty acyl substrates, such as chain shortening and elongation, reduction, acetylation, oxidation, and desaturation (11). SP biosynthetic enzymes [i.e., FA reductases (8), FA chain-shortening enzymes (12, 13), and particularly FA desaturases (FADs) (7, 9, 14–17)] are the most commonly discovered traits underlying SP divergence in moths.

Manduca sexta females attract males by releasing an SP containing in addition to mono- and diunsaturated aldehydes, which are typical structural themes in SPs of Bombycoidea moths (10), also uncommon conjugated triunsaturated aldehydes. The production of triunsaturated SPCs represents an easily traceable phenotype, thus making *M. sexta* a convenient yet unexploited model organism for unraveling the mechanisms of chemical communication evolution via novel SPC recruitment. In our previous attempts to decipher the desaturation pathway leading to triunsaturated SPC FA precursors (3UFAs), we identified the *Msex*D2 desaturase, which exhibits *Z*11-desaturase and conjugase (1,4-dehydrogenase) activity and participates in stepwise production of monounsaturated (1UFA) and diunsaturated (2UFA) SPC precursors. The terminal desaturation step resulting in the third conjugated double bond remained, however, elusive (18, 19).

Here, we isolated and functionally characterized FAD genes abundantly and specifically expressed in the pheromone gland

Significance

The diversity of sex pheromones (SPs) is pivotal to insect reproductive isolation and speciation. However, knowledge of molecular mechanisms of pheromone evolution is limited. The *Manduca sexta* SP contains unique triunsaturated fatty acid (3UFA) derivatives and represents thus a suitable model for the investigation of chemical communication evolution via recruitment of novel SP components. Here, we demonstrate that gene duplication and a single amino acid substitution in fatty acid desaturase (FAD) catalyzing production of diunsaturated moth pheromone precursors is sufficient for acquisition of 3UFA SP component precursors. Our study indicates that the potential for change in the moth pheromone composition is underlined by the inherent evolvability of pheromone biosynthetic FADs.

Author contributions: A.B., U.J., A.S., and I.P. designed research; A.B., P.M., H.V., P.S., J.W., and A.S. performed research; A.B., P.M., H.V., A.S., and I.P. analyzed data; and A.B., H.V., U.J., A.S., and I.P. wrote the paper.

The authors declare no conflict of interest.

This article is a PNAS Direct Submission.

Data deposition: The sequences reported in this paper have been deposited in the GenBank database (accession nos. AM158251 and KP890026–KP890030).

[1]A.B. and P.M. contributed equally to this work.

[2]To whom correspondence may be addressed. Email: svatos@ice.mpg.de or iva.pichova@uochb.cas.cz.

This article contains supporting information online at www.pnas.org/lookup/suppl/doi:10.1073/pnas.1514566112/-/DCSupplemental.

(PG) capable of producing 3UFA pheromone precursors and demonstrated the biosynthesis of 3UFAs from 2UFAs. We used site-directed mutagenesis of *M. sexta* FADs and identified a minimal structure motif leading to acquisition of new desaturase specificities. The reconstructed evolutionary relationship of moth FADs demonstrated that the 3UFA pheromone precursors in *M. sexta* were acquired via (*i*) activation of a presumably inactive ancestral FAD gene and/or (*ii*) duplication of an ancestral FAD gene producing 1UFA and 2UFA SPC precursors followed by functional diversification of an FAD duplicate.

Results

Identification of FADs Abundant in the Pheromone Gland. To select candidate FAD genes involved in pheromone biosynthesis, we performed RNA sequencing of *M. sexta* female PGs, the site of pheromone biosynthesis (19), as well as nonpheromone-producing tissues (female fat body, female labial palps, and larval midgut). We identified 14 desaturase transcripts, of which 4 were abundant and enriched in the PG according to normalized expression values (RPKM, reads per kilobase of transcript per million mapped reads): *Msex*D2, a previously characterized Z11-desaturase/conjugase involved in sequential biosynthesis of 1UFA and 2UFA pheromone precursors (18), and three FAD gene products, *Msex*D3, *Msex*D5 and *Msex*D6 (Fig. 1). According to the RPKM values, *Msex*D2 and *Msex*D3 were among the 100 most abundant transcripts in *M. sexta* PG, ranking 12th and 4th, respectively (Dataset S1). A transcript coding for fatty acyl reductase, a gene presumably involved in reduction of fatty acyl pheromone precursors to aldehydic pheromones, was also abundantly expressed (Dataset S1).

The ORF of *Msex*D3 (GenBank accession no. AM158251) encodes a 341-aa protein containing conserved structural features of membrane FADs, that is, three histidine-rich motifs involved in coordination of two iron atoms in the enzyme active site and four transmembrane helices (20, 21). In the *M. sexta* Official Gene Set 2.0 (OGS 2.0; www.agripestbase.org/manduca/), the *Msex*D2 and *Msex*D3 genes are tandemly organized in the genome, located on the same scaffold and separated by 7 kbp (scaffold00070: 983841–985384 and 993705–995505, respectively). Together with the high sequence identity of *Msex*D2 and *Msex*D3 (91% in the homologous 321-aa region, *SI Appendix*, Fig. S1) these data indicate that *Msex*D2 and *Msex*D3 emerged via a recent gene duplication event from an ancestral FAD gene.

Four *Msex*D5 ORF variants (*Msex*D5a–*Msex*D5d) that code for highly similar proteins sharing at least 92% sequence identity were amplified from the *M. sexta* female abdominal tips (ATs) cDNA libraries (GenBank accession nos. KP890027–KP890030) (*SI Appendix*, Fig. S2). These sequences presumably represent allelic variants of a single *Msex*D5 gene, supported by the presence of a single *Msex*D5 gene copy in the *M. sexta* OGS 2.0 (scaffold 00367: 113800–112161). The *Msex*D5 consensus sequence shares moderate protein sequence identity with *Msex*D2 and *Msex*D3 (49.8 and 51.7%, respectively) (*SI Appendix*, Fig. S3).

*Msex*D6 is the least abundantly expressed PG-specific FAD (Fig. 1). Compared with all predicted *M. sexta* FADs, the *Msex*D6 coding region (GenBank accession no. KP890026) exhibits the highest protein sequence identity to *Msex*D2 and *Msex*D3 (68.0 and 71.5%, respectively) (*SI Appendix*, Fig. S3).

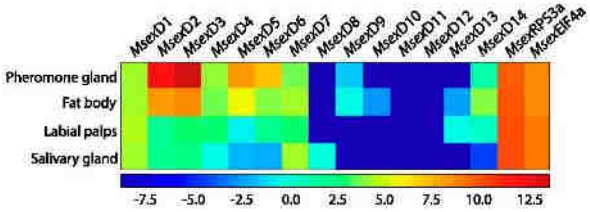

Fig. 1. Heat map indicating transcript abundances of *Msex*D1-*Msex*D14 along with abundances of housekeeping genes Msex-RPS3a and Msex-EIF4a. Transcript abundances are expressed as log2 transformed normalized values (RPKM) across various tissues obtained from virgin *M. sexta* females (pheromone gland, fat body, and labial palps) and from larvae (salivary glands).

Functional Characterization of *Msex*D3, *Msex*D5, and *Msex*D6. We selected *Msex*D3, *Msex*D5a–d, and *Msex*D6 as promising candidate FADs producing 3UFA precursors of SPCs based on their abundant and specific expression in the PG. For functional characterization of FADs, we initially attempted to express the candidate FADs in the *elo1Δ ole1Δ Saccharomyces cerevisiae* strain, which is deficient in the fatty acid desaturation and medium-chain fatty acyl elongation step (22), to eliminate interfering yeast FA metabolites. However, only trace levels of novel unsaturated FAs, detected in the form of FA methyl esters (FAMEs), were biosynthesized in this expression system. Therefore, we characterized FADs in *S. cerevisiae* strain W303, which has a single FAD with *Z*9 specificity and an active FA elongase system. To distinguish the interfering products of natural yeast FA metabolism from the specific products of *M. sexta* FADs, we performed a series of control cultivations of yeast bearing an empty expression plasmid (Fig. 2 and *SI Appendix*, Fig. S4).

To test the ability of *Msex*D3 to produce 3UFAs, we supplemented the yeast cultivation medium with the presumed 3UFA precursor *E*10,*E*12-16:2. This resulted in production of a 1:7 mixture of *E*10,*E*12,*E*14-16:3 and *E*10,*E*12,*Z*14-16:3 (Fig. 2*D*). Monounsaturated FAs were detected as additional specific products of *Msex*D3, that is, *Z*11-16:1, *Z*11-14:1, and *E*11-14:1. *Z*11-16:1, an FA precursor of a monounsaturated pheromone component, was produced in a significantly lower ($P < 0.05$) amount in the *Msex*D3-expressing strain compared with the *Msex*D2-expressing strain ($0.9 \pm 0.5\%$ and $10.6 \pm 0.2\%$, respectively) (Fig. 2). In the *Msex*D3-expressing strain, additional C16:1 and C16:2 FAs with *E*/*Z*13 double bonds were detected. These FAs were biosynthesized not via direct *E*/*Z*13 desaturation but rather by elongation of *E*/*Z*11-14:1, presumably catalyzed by yeast fatty acyl elongase Elo1p (22), followed by a second round of *Z*11 desaturation, as demonstrated by a series of cultivation experiments (*SI Appendix*, Fig. S4). In contrast to *Msex*D2, *Msex*D3 did not exhibit conjugase activity; it did not desaturate the supplemented *Z*11-16:1 to *E*10,*E*12-16:2 or *E*10,*Z*12-16:2 (Fig. 2*C*). MTAD (4-methyl-1,2,4-triazoline-3,5 dione) derivatization was used to confirm the presence or absence of FAMEs with conjugated double bonds (*SI Appendix*, Figs. S4*D* and S5).

The *Msex*D5a–*Msex*D5d variants also produced *E*10,*E*12,*E*14:16-3 and *E*10,*E*12,*Z*14-16:3 (in an ~3:1 ratio) from *E*10,*E*12-16:2 added to the cultivation medium, indicating that all *Msex*D5 variants exhibit *E*/*Z*14-desaturase specificity (Fig. 2*D* and *SI Appendix*, Fig. S6). Therefore, a single FAD variant, *Msex*D5a (hereafter referred to as *Msex*D5), was used in subsequent experiments. *Msex*D5 substrate specificity was assayed by supplementing the cultivation media of *Msex*D5-expressing yeast with *Z*11-16:1-methyl ester. Although no *E*10,*E*12-16:2 or *E*10,*Z*12-16:2 products were detected, we did detect small quantities of *Z*11,*E*13-16:2, demonstrating *E*13 specificity and lack of conjugase activity in *Msex*D5 (Fig. 2*C* and *SI Appendix*, Fig. S4). In contrast to *Msex*D3, *Msex*D5 did not produce *E*11-14:1 or *Z*11-14:1 (Fig. 2*A*), and *Z*11-16:1 was detected in the *Msex*D5-expressing yeast strain at a level comparable to that in the empty strain, indicating that *Msex*D5 lacks *Z*11-desaturase activity with a 16:0 substrate (Fig. 2*B*).

*Msex*D6 did not produce 3UFAs when supplemented with *E*10,*E*12-16:2; however, it produced a substantial amount of *Z*11-18:1 ($12.3 \pm 0.2\%$), an FA with a hydrocarbon backbone identical to the *M. sexta* SPC *Z*11-18:1-aldehyde (*SI Appendix*, Fig. S7). The configuration of the Δ11 double bond was tentatively identified as *Z*11 based on the matching retention time of the *Msex*D6 product with a minor Δ11-18:1 FAME presumably resulting from FA elongation of abundant *Z*9-16:1 in all yeast strains (*SI Appendix*, Fig. S7). Additionally, *Msex*D6 produced $1.3 \pm 0.3\%$ *Z*11-16:1 (Fig. 2*B*).

Analysis of Isotopically Labeled and Natural FAs in *M. sexta* Female AT. To complement the functional characterization of FADs in the yeast expression system and identify the in vivo substrates

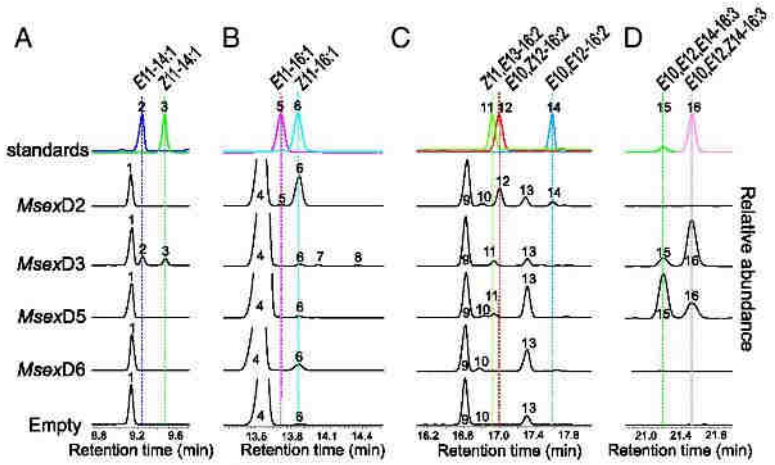

Fig. 2. GC/MS analyses of extracts from yeast cells expressing *M. sexta* desaturases. Extracts from yeasts expressing *Msex*D2, *Msex*D3, *Msex*D5, and *Msex*D6 were compared with extracts from yeasts transformed with an empty plasmid. Chromatograms are displayed as extracted ion chromatograms at (*A*) *m/z* 240, corresponding to the molecular ion ($M^{+\bullet}$) of 14:1; (*B*) *m/z* 268, corresponding to $M^{+\bullet}$ of 16:1; (*C*) *m/z* 266, corresponding to $M^{+\bullet}$ of 16:2; and (*D*) *m/z* 264, corresponding to $M^{+\bullet}$ of 16:3. The specific products of *M. sexta* FADs were identified as *E*11-14:1 (2), *Z*11-14:1 (3), *E*11-16:1 (5), *Z*11-16:1 (6), *Z*11,*E*13-16:2 (11), *E*10,*Z*12-16:2 (12), *E*10,*E*12-16:2 (14), *E*10,*E*12,*E*14-16:3 (15), and *E*10,*E*12,*Z*14-16:3 (16). Additionally, nonspecific, yeast-produced FAs were detected in all yeast strains: *Z*9-14:1 (1), *Z*9-16:1 (4), traces of *Z*11-16:1 (6), and unidentified compounds (10) and (13). In yeast expressing *Msex*D3, *E*13-16:1 (7), *Z*13-16:1 (8), and *Z*11,*E*13-16:2 (11) were identified as products of yeast fatty acid elongase acting on *Z*11-14:1 and *E*11-14:1. Cultivation media for yeasts cultivated for analysis of 14:1 were supplemented with 14:0, media were supplemented with *Z*11-16:1 for analysis of 16:2, and media were supplemented with *E*10,*E*12-16:2 for analysis of 16:3, as described in *Materials and Methods*. For a detailed analysis of nonspecific products, see *SI Appendix*, Fig. S4.

and products of FADs involved in 3UFA-derived SPC biosynthesis, we topically applied metabolic probes in the form of FAs and FAMEs to female *M. sexta* PGs. Deuterium-labeled *E*10,*E*12-16,16,16-$^{2}H_3$-16:2 methyl ester (further referred to as d3-*E*10,*E*12-16:2) applied to PGs was incorporated into two d3-16:3 FAME isomers. Based on the reduction in their retention times compared with the nondeuterated 3UFA methyl ester standards [consistent with the inverse isotopic effect (23)], we identified them as d3-*E*10,*E*12,*E*14-16:3 and d3-*E*10,*E*12,*Z*14-16:3, thus confirming the biosynthesis of 3UFAs from *E*10,*E*12-16:2 in vivo (*SI Appendix*, Figs. S8 and S9).

The identification of *E*11-14:1 and *Z*11-14:1 in the *Msex*D3-expressing yeast strain was confirmed in vivo by incorporation of topically applied 1,2-$^{13}C_2$-tetradecanoic acid into $^{13}C_2$-*Z*11-14:1 and $^{13}C_2$-*E*11-14:1 in the AT. Although they can be biosynthesized in vivo, *Z*11-14:1 and *E*11-14:1 are not naturally present in the *M. sexta* AT, likely due to the low abundance of 14:0 available in AT (*SI Appendix*, Figs. S9 and S10 and ref. 24).

Additionally, we detected *Z*11,*E*13-16:2 in the untreated *M. sexta* AT (*SI Appendix*, Fig. S11), which had not previously been detected in the FA pool of the *M. sexta* PG (24) and which we found to be specifically produced in yeast expressing *Msex*D5 (Fig. 2).

Together, the functional characterization of isolated FADs in our yeast expression system combined with the application of metabolic probes and analysis of FAs indicates that 3UFAs are biosynthesized in *M. sexta* AT by either of the two distinct desaturases *Msex*D3 or *Msex*D5, which share *E*/*Z*14-desaturase specificity but differ in their other desaturase products (Fig. 3).

Reconstruction of the Phylogenetic Relationship Between *M. sexta* and Other Lepidopteran FADs. We reconstructed a FAD gene tree using publicly available sequences of predicted or functionally characterized lepidopteran FADs, 14 FAD genes predicted from the *M. sexta* Official Gene Set 2.0 and additional moth FAD sequences available from in-house sequencing projects (Fig. 4, Dataset S2, and *SI Appendix*, Table S2).

The FAD gene tree exhibits several well-supported clades. The most sequentially and functionally conserved clades are those of Z9-FADs, that is, a clade of FADs that prefer palmitic acid over stearic acid (16:0 > 18:0) that includes the previously characterized *Msex*D1 (18), and a FAD clade that prefers stearic acid (18:0 > 16:0) that includes the predicted *Msex*D4. Both *Msex*D3 and *Msex*D5 cluster within a variable clade of SP-biosynthetic FADs herein termed "Z11-like," which encompasses highly functionally diverse pheromone biosynthetic FADs (25), in addition to numerous FADs with Z11-desaturase specificity. Of note, the closest putative *Msex*D5 ortholog is desat1 from *Ascotis selenaria*, which is proposed to be a nonfunctional FAD (26). Putative orthologs of *Msex*D5 are predicted also in other moth species that do not possess 3UFA SPCs (e.g., the pine caterpillar moth *Dendrolimus punctatus* and the silkworm moth *Bombyx mori*) (Fig. 4).

The closest homolog of *Msex*D3 is *Msex*D2, indicating that the duplication event leading to the tandemly arranged gene pair of *Msex*D2 and *Msex*D3 occurred after separation of the *B. mori* and *M. sexta* lineages. Alternatively, *B. mori* could have lost the FAD gene orthologous to *Msex*D3. The former scenario, which proposes a more recent gene duplication event, is further supported by the high sequence identity of *Msex*D2 and *Msex*D3.

The phylogenetic reconstruction yielded six additional strongly supported clades (I–VI, Fig. 4). Typically, FADs from *M. sexta* and *B. mori* that are presumably not involved in SP biosynthesis are in clades orthologous to moth FADs for which involvement in SP biosynthesis was implied based on their experimentally determined desaturase specificity. The tree topology provides strong support for the hypothesis that biosynthetically inactive members of the FAD gene family are retained in the moth genomes and in the course of evolution can be activated and recruited for novel SPC biosynthesis (11).

Based on these results, we propose that the recruitment of *Msex*D3 and *Msex*D5 genes for SPC biosynthesis occurred after separation of the *M. sexta* and *B. mori* lineages and led to the acquisition of 3UFA SPC precursors in *M. sexta*, thus extending

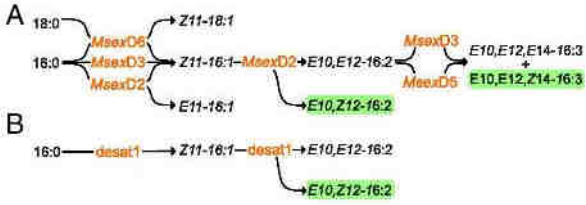

Fig. 3. The reconstructed desaturation pathway of *M. sexta* SPC precursors compared with that of *B. mori*. (*A*) In *M. sexta*, the desaturation pathway is extended by an *E*/*Z*14-desaturation step catalyzed by *Msex*D3 and/or *Msex*D5, which leads to 3UFA SPC precursors. Desaturase specificities of *Msex*D2 and *Msex*D6 contribute to additional precursors of minor SPCs. (*B*) Biosynthesis of the SPC precursor *E*10,*Z*12-16:2 in *B. mori* (44). Precursors of SPCs essential for triggering the full range of male premating responses are framed in green (27, 45).

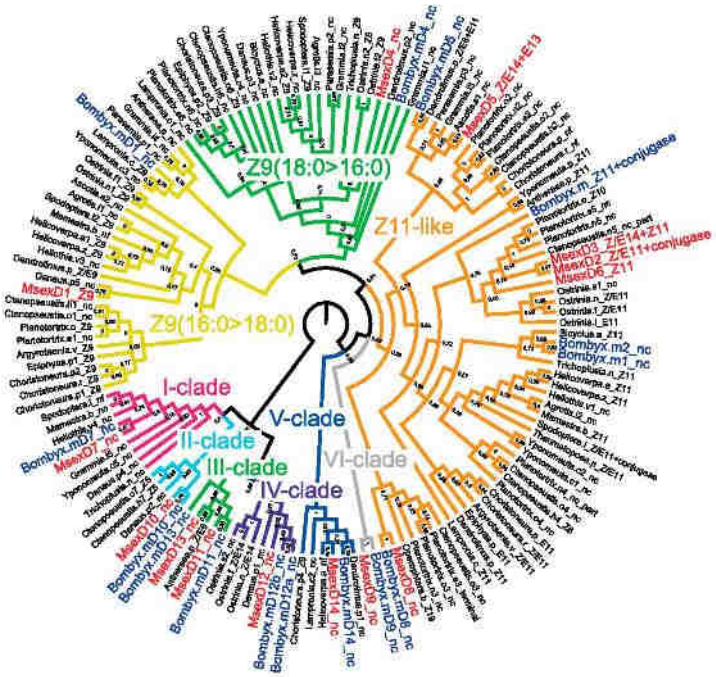

Fig. 4. Phylogenetic tree showing the relationships between lepidopteran FADs. *M. sexta* desaturases are highlighted in red. *B. mori* desaturases are highlighted in blue. Eight highly supported clades are colored and named. FADs are named by the genus and a single letter abbreviation of the source species name followed by designation of the FAD specificity, when available, or by "nc" for FADs that have not been functionally characterized or "nf" for FADs that were functionally assayed but no desaturase activity was detected. Numbers along branches indicate branch support calculated by approximate likelihood ratio test (aLRT, minimum of SH-like and Chi2-based values). For GenBank sequence accession numbers and full species names, see *SI Appendix*, Table S2.

the SP biosynthetic pathway by an additional *E*/*Z*-14 desaturation step compared with *B. mori* (Fig. 3).

We identified 3UFAs also in the AT of the death head moth, *Acherontia atropos* (Sphinginae: Acherontiini; *SI Appendix*, Fig. S12 and *SI Appendix*, *SI Materials and Methods*). This finding places the most parsimonious recruitment of 3UFA-producing FADs in the common ancestor of the Acherontiini and Sphingiini tribes, the Sphinginae subfamily (*SI Appendix*, Fig. S13 and Table S3).

Identification of the Sequence Determinants of *E*/*Z*14-Desaturase Specificity in *Msex*D3. To identify the domains, structural motifs, and amino acid residues critical for the distinct specificities of *Msex*D2 and *Msex*D3, we prepared a set of truncated, domain-swapped and single-amino acid-swapped mutants of *Msex*D2 and *Msex*D3 (Fig. 5*A*). Mutated FADs were expressed in *S. cerevisiae*, and total yeast cell FAs were analyzed. To assess the effect of individual mutations on the desaturase specificity, we determined the relative amounts of major pheromone precursors (*Z*11-16:1, *E*10, *Z*12-16:2, *E*10,*E*12-16:2, *E*10,*E*12,*E*14-16:3, and *E*10,*E*12,*Z*14-16:3) produced by the *Msex*D2 and *Msex*D3 mutants.

To test the role of variable N- and C-terminal regions on desaturase specificity, we prepared a set of truncation mutants. The identification of 3UFA products in the *Msex*D3-C20 mutant, truncated by 20 amino acids from the C terminus, indicated the dispensability of this extension for *E*/*Z*14-desaturase specificity. Additional 20 amino acids truncation (*Msex*D3-C40) led, however, to complete loss of both *Z*11- and *Z*/*E*14-desaturase activities, suggesting that the extensive deletion affected the general desaturase activity of *Msex*D3 (Fig. 5). The truncation of both desaturases by 14 amino acids at the N terminus (*Msex*D2-N14, *Msex*D3-N14) did not change the spectrum of desaturase products (Fig. 5).

Besides the N- and C-terminal regions, the protein sequence divergence between *Msex*D2 and *Msex*D3 is concentrated in the hydrophobic region between the first two histidine motifs (HR, Leu98–Val118) and in the fourth putative transmembrane domain (TM4, Trp210–Ala231) (*SI Appendix*, Fig. S1). Therefore, we reciprocally swapped the HR and TM4 regions, resulting in chimeric FADs (Fig. 5*A*). The exchange of the HR region did not change the desaturase product spectrum in the chimeras *Msex*D2-HR and *Msex*D3-HR (Fig. 5). However, the exchange of the *Msex*D2 TM4 domain with TM4 of *Msex*D3 (*Msex*D2-TM4 chimera) led to a fundamental change in *Msex*D2-TM4 products compared with *Msex*D2; the conjugase and *Z*11-desaturase specificity was almost completely abolished ($P < 0.05$). Notably, traces of *E*10,*E*12,*E*14-16:3 and *E*10,*E*12,*Z*14-16:3 were detected, indicating a gain of *E*/*Z*14-desaturase specificity in *Msex*D2-TM4 (Fig. 5). Together, these results indicate that the exchange of TM4 in *Msex*D2-TM4 led to an overall shift in desaturase specificity toward *Msex*D3. In a reciprocal fashion, *Msex*D3-TM4 exhibited an increase of *Z*11-16:1 production ($P < 0.05$) to a level of *Z*11-16:1 produced by *Msex*D2 (Fig. 5*B*), the acquisition of conjugase activity (Fig. 5*C*), and loss of *E*/*Z*14 specificity as indicated by loss of 3UFA products (Fig. 5*D*). Thus, *Msex*D3-TM4 displayed the full spectrum of *Msex*D2 products.

To determine the contribution of individual amino acid residues to the observed reciprocal exchange of desaturase specificities in TM4 mutants, we swapped individual nonconserved amino acids and generated mutants *Msex*D2-216, *Msex*D3-216, *Msex*D2-219, *Msex*D3-219, *Msex*D2-220, *Msex*D3-220, *Msex*D2-223, *Msex*D3-223, *Msex*D2-224, and *Msex*D3-224. The mutations at amino acid positions 216, 219, 220, and 223 either led to a decrease in desaturase activity ($P < 0.05$) or did not significantly change the overall desaturase activity ($P > 0.05$) and did not lead to production of novel desaturase products (Fig. 5). However, the exchange of alanine and isoleucine at residue 224 led to a reciprocal exchange of desaturase specificities similar to that observed for the TM4 exchange (Fig. 5). Notably, *Msex*D2-224Ile lost conjugase activity (Fig. 5*C*) and gained *E*/*Z*14-desaturase specificity, as indicated by production of *E*10,*E*12,*E*14-16:3 and *E*10,*E*12,*Z*14-16:3 (Fig. 5*D*), whereas *Msex*D3-224Ala completely lost the ability to produce 3UFAs (Fig. 5*D*) but acquired conjugase activity (Fig. 5*C*).

To control for the influence of different protein expression levels of *Msex*D2-224Ile- and *Msex*D3-224Ala- on specificity changes, we cloned these mutants in-frame with the N-terminal His6tag and detected their levels in yeast lysates using anti-His6tag antibodies. The FADs were produced at comparable levels and exhibited also reciprocal exchange of desaturase specificities (*SI Appendix*, Fig. S14).

Using homology modeling with mammalian FADs as a template (20, 21) we generated structural models of *Msex*D2 and *Msex*D3,

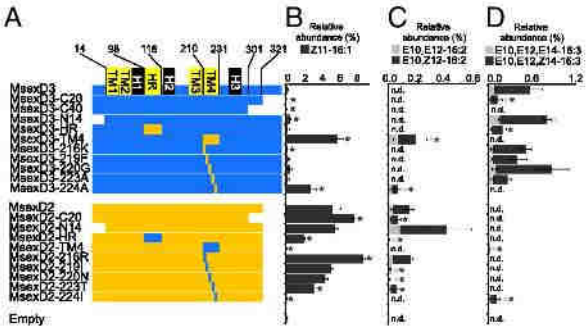

Fig. 5. Identification of sequence determinants of *Msex*D2 and *Msex*D3 desaturase specificities by site-directed mutagenesis. (*A*) Overview of truncated, domain-swapped, and single-amino-acid-swapped mutants. Predicted transmembrane helices (TM1–TM4), the hydrophobic region (HR), and conserved histidine motifs (H1–H3) are highlighted, and the amino acid positions of swapped or truncated regions are marked with numbers. (*B*) Relative amounts of *Z*11-16:1 accumulated in yeast strains expressing *Msex*D2 and *Msex*D3 mutants. (*C*) Relative amounts of *E*10,*E*12-16:2 and *E*10,*Z*12-16:2 accumulated in yeast strains expressing *Msex*D2 and *Msex*D3 mutants cultivated in the presence of *Z*11-16:1. (*D*) Relative amounts of *E*10,*E*12,*E*14-16:3 and *E*10,*E*12,*Z*14-16:3 accumulated in yeast strains expressing *Msex*D2 and *Msex*D3 mutants cultivated in the presence of *E*10,*E*12-16:2. The relative abundances of individual FAMEs were calculated from the peak areas in GC/MS chromatograms. Bars represent means ± SD of relative FAME abundances in three cultivation replicates. *Significant difference compared with the parental wild-type FAD (two-sample *t* test, $P < 0.05$, gray and black asterisks indicate the significant differences for each of the FAME isomers). n.d., FAME not detected. Empty, control yeast strain transformed with an empty plasmid.

which indicate that the residue 224 is contributing to the formation of the kink in fatty acyl substrate binding tunnel (*SI Appendix*, Fig. S15).

Together, these findings provide evidence that a single amino acid substitution in *Msex*D2 is sufficient to abolish the original desaturase specificities and introduce an *E*/*Z*14-desaturase specificity, leading to the production of 3UFA SPC precursors.

Discussion

Using next-generation sequencing of *M. sexta* female PG and reference tissues, we identified a set of highly abundant and PG-enriched FAD transcripts, including *Msex*D2, a previously described FAD involved in biosynthesis of mono- and diunsaturated SPC precursors (18), and previously unidentified *Msex*D3, *Msex*D5, and *Msex*D6 FADs. The 3UFA precursor of the essential *M. sexta* SPC *E*10,*E*12,*Z*14-16:3-aldehyde (27), along with *E*10,*E*12,*E*14-16:3, was produced by *Msex*D3 and *Msex*D5 in our yeast expression system.

Under the hypothesis that both *Msex*D3 and *Msex*D5 are biosynthetically active in vivo, the biosynthesis of 3UFA precursors of SPC would be redundantly catalyzed by two evolutionarily distinct enzymes, a feature that has not been previously described in SP-biosynthetic FADs. The selection pressure leading to the recruitment of a second, seemingly redundant, 3UFA-biosynthetic FAD might occur, for example, to secure a sufficiently high production of 3UFA-derived SPCs. However, our results suggest that *Msex*D3 plays the principal role in 3UFA biosynthesis because (*i*) *Msex*D3 transcript is more abundant in the PG compared with *Msex*D5 and (*ii*) the 1:7 ratio of *E*10,*E*12,*E*14-16:3 and *E*10,*E*12,*Z*14-16:3 produced by *Msex*D3 closely resembles the ratio of the respective aldehydic components in the *M. sexta* SP (approximately 1:10) (27), in contrast to the ratio of *Msex*D5 3UFA products (3:1).

The evolutionary events leading to the acquisition of *Msex*D5 are uncovered by the FAD gene family tree, which indicates several putative orthologs of *Msex*D5 across moth species. None of the orthologs exhibits *E*/*Z*14-desaturase specificity. Rather, they (*i*) are presumably not active in SP biosynthesis, such as desat1 from the Japanese giant looper *Ascotis selenaria* (26), (*ii*) exhibit distinct desaturase specificity, such as FAD from *Dendrolimus punctatus* (28), or (*iii*) have not been functionally characterized, such as putative FADs from *Grammia incorrupta* and *Parasemia plantaginis*. The reconstructed FAD gene tree suggests that *Msex*D5 was acquired by activation of an inactive FAD gene. This is further supported by the topology of the FAD gene tree containing well-supported clades I–VI, which typically encompass (in addition to presumably nonfunctional FADs or FADs not involved in SP biosynthesis) FADs exhibiting unique desaturase specificities. The rich FAD multigene family would thus serve as a reservoir from which novel SP-biosynthetic FADs can be recruited (7, 11).

Our finding of a single amino acid residue 224 that critically influences desaturase specificity of *Msex*D2 and *Msex*D3 is consistent with results obtained for other FADs from across kingdoms (20, 29–31), indicating high enzymatic plasticity of FADs, that is, susceptibility to shifts in their enzymatic specificities following a small number of amino acid substitutions. Homology models of *Msex*D2 and *Msex*D3 localizing the amino acid residue 224 (Ala and Ile, respectively) to position of conserved Thr257 in Z9-FADs, which contributes to formation of the kink in the FA substrate binding tunnel (20, 21), suggest that the kink determines the desaturase substrate specificity by positioning the fatty acyl chain in respect to the diiron active center (*SI Appendix*, Fig. S15). Future studies should show whether this mechanism of desaturase substrate selectivity is shared across FADs from various organisms. Additionally, our results together with the observed influence of one amino acid substitution on specificity of SP-biosynthetic FA reductases (8) and SP-receptor (32) in *Ostrinia* moths suggest an evolutionary significant effect of a single amino acid substitution in key proteins involved in pheromone communication on moth speciation.

In summary, we show that two distinct *E*/*Z*14-FADs (*Msex*D3 and *Msex*D5) are capable of biosynthesis of unique 3UFA SPC precursors in *M. sexta*. The *E*/*Z*14-desaturase specificity of *Msex*D3 could have evolved abruptly via a single amino acid mutation in a gene duplicate of 1UFA- and 2UFA-producing *Msex*D2. Alternatively, 3UFA SPCs might have been acquired in *M. sexta* via activation of presumably inactive ancestral *Msex*D5. These results indicate that the presence of inactive FAD genes in moth genomes and the susceptibility of FAD enzymes to changes of the desaturase specificity underlie an evolutionary facile recruitment of novel compounds for the SP communication channel.

Materials and Methods

For detailed descriptions see *SI Appendix, SI Materials and Methods*.

RNA Isolation. *M. sexta* females were reared under conditions described by Große-Wilde et al. (33). Total RNA was extracted from each of the adult and larval tissue samples.

Illumina Sequencing, Transcriptome Assembly, and Annotation. Tissue-specific transcriptome sequencing of four different mRNA pools was carried out on an Illumina HiSeq2000 Genome Analyzer platform. The transcriptome was annotated using BLAST, Gene Ontology and InterProScan searches using BLAST2GO PRO v2.6.1 (www.blast2go.de/) as described (34).

Digital Gene Expression Analysis. Digital gene expression analysis was carried out by using QSeq software (DNAStar Inc.). Biases in the sequence datasets and different transcript sizes were corrected using the RPKM algorithm.

Sequence Analysis. Desaturase topology was predicted using the web-based program TMHMM 2.0 (35). Maximum-likelihood phylogenetic analysis was performed in the web-based pipeline Phylogeny.fr (36) using protein sequences of lepidopteran FADs retrieved from the EMBL database, ManducaBase (www.agripestbase.org), SilkBase (silkbase.ab.a.u-tokyo.ac.jp), and in-house sequencing projects.

Desaturase Cloning. A cDNA library used for isolation of FAD ORFs was prepared from total RNA extracted from ATs, consisting of PG, papillae anales, and intersegmental membranes, of female *M. sexta*. FAD ORFs were cloned into the pYES2 (Invitrogen) or pYEXTHS-BN vector. pYEXTHS-BN plasmids encoded FADs with N-terminal His6tags. Vectors bearing mutated *Msex*D2 or *Msex*D3 were constructed as described in detail in *SI Appendix, SI Materials and Methods*.

Functional Expression in Yeast. Yeasts transformed with pYES2 and pYEXTHS-BN were cultivated in liquid YNB medium lacking uracil. Heterologous FAD expression in pYEXTHS-BN transformed yeasts was monitored by Western blotting using anti-His6tag antibodies (37). Total cellular lipids were transesterified to FAMEs (18). When indicated, yeast strains were cultivated with FAMEs supplemented to a final concentration of 0.25 mM in cultivation medium.

GC/MS Analysis. The FAME extracts were analyzed by GC/MS (MasSpec-Micromass; EI at 70 eV) using DB-5MS and DB-WAX capillary columns (both from J&W Scientific). The double-bond positions of the FAMEs were determined by concordance of retention times and mass spectra of FAMEs in analyzed yeast extracts with that of synthetic UFA standards and by derivatization with MTAD and dimethyldisulfide.

Chemical Synthesis. The synthesis of methyl *E*10,*E*12,*Z*14-hexadecatrienoate was performed by a single-step Suzuki–Miyaura coupling (38). Methyl Z11,E13-hexadecadienoate was prepared by a Wittig reaction (39). Methyl *E*10,*E*12-hexadecadienoate was prepared by coupling methyl 11-undecynoate and (*E*)-iodo pentene (40). Methyl *E*10,*E*12-16,16,16-trideuteriohexadecadienoate was prepared by coupling methyl 11-undecynoate with (*E*)-2-((4-iodobut-3-enyl)oxy)tetrahydro-2H-pyran (41).

Application of Metabolic Probes to *M. sexta* AT. One microliter of *E*10,*E*12-16,16,16-$^{2}H_{3}$-16:2-methyl ester (50 μg/μL) or 1,2-$^{13}C_{2}$-14:0 acid (50 μg/μL; Sigma-Aldrich) in dimethyl sulfoxide/water/ethanol (7/2/1) was applied topically to *M. sexta* ATs. ATs were dissected after 24 h, extracted, and analyzed by GC/MS (42).

Homology Modeling. The structures of *Msex*D2 and *Msex*D3 were generated using homology modeling module in YASARA (43) with default parameters. Structures of mammalian FADs (PDB ID codes 4YMK and 4ZYO) were used as templates.

ACKNOWLEDGMENTS. We thank Sylke Dietel and Christopher Koenig for *M. sexta* rearing, Jan Doubský for assistance in fatty acid methyl ester organic synthesis (all Max Planck Institute for Chemical Ecology), Rikard Unelius (Linnaeus University) for providing *Z*11,*E*13-16:2 standard, Vladimír Vrkoslav for technical assistance with GC/MS analyses and Michal Doležal (both Institute of Organic Chemistry and Biochemistry) for generating the FAD homology models, Caterina Holz for providing the pYEXTHS-BN plasmid, and Hillary Hoffman for language consulting. This research was financially supported by project RVO 61388963 from Academy of Sciences of the Czech Republic, project LO 1302 from Ministry of Education of the Czech Republic and by the Max Planck Society. P.M. was supported by the European Social Fund and the state budget of the Czech Republic (Project CZ.1.07/2.3.00/30.0022).

1. Johansson BG, Jones TM (2007) The role of chemical communication in mate choice. *Biol Rev Camb Philos Soc* 82(2):265–289.
2. Paterson HEH (1985) The recognition concept of species. *Species and Speciation*, ed Vrba ES (Transvaal Museum, Pretoria, South Africa).
3. Phelan PL (1992) Evolution of sex pheromones and the role of asymmetric tracking. *Insect Chemical Ecology: An Evolutionary Approach*, eds Roitberg BD, Isman MB (Chapman & Hall, New York), pp 265–314.
4. Smadja C, Butlin RK (2009) On the scent of speciation: The chemosensory system and its role in premating isolation. *Heredity (Edinb)* 102(1):77–97.
5. Niehuis O, et al. (2013) Behavioural and genetic analyses of *Nasonia* shed light on the evolution of sex pheromones. *Nature* 494(7437):345–348.
6. Shirangi TR, Dufour HD, Williams TM, Carroll SB (2009) Rapid evolution of sex pheromone-producing enzyme expression in *Drosophila*. *PLoS Biol* 7(8):e1000168.
7. Roelofs WL, et al. (2002) Evolution of moth sex pheromones via ancestral genes. *Proc Natl Acad Sci USA* 99(21):13621–13626.
8. Lassance J-M, et al. (2013) Functional consequences of sequence variation in the pheromone biosynthetic gene pgFAR for *Ostrinia* moths. *Proc Natl Acad Sci USA* 110(10):3967–3972.
9. Groot AT, et al. (2014) Within-population variability in a moth sex pheromone blend: Genetic basis and behavioural consequences. *Proc Biol Sci* 281(1779):20133054.
10. El-Sayed (2014) The Pherobase: Database of Pheromones and Semiochemicals. Available at www.pherobase.com.
11. Roelofs WL, Rooney AP (2003) Molecular genetics and evolution of pheromone biosynthesis in Lepidoptera. *Proc Natl Acad Sci USA* 100(16):9179–9184.
12. Jurenka RA, Haynes KF, Adlof RO, Bengtsson M, Roelofs WL (1994) Sex pheromone component ratio in the cabbage looper moth altered by a mutation affecting the fatty acid chain-shortening reactions in the pheromone biosynthetic pathway. *Insect Biochem Mol Biol* 24(4):373–381.
13. Tabata J, Ishikawa Y (2005) Genetic basis to divergence of sex pheromones in two closely related moths, *Ostrinia scapulalis* and *O. zealis*. *J Chem Ecol* 31(5):1111–1124.
14. Wang H-L, Liénard MA, Zhao CH, Wang CZ, Löfstedt C (2010) Neofunctionalization in an ancestral insect desaturase lineage led to rare Δ6 pheromone signals in the Chinese tussah silkworm. *Insect Biochem Mol Biol* 40(10):742–751.
15. Xue B, Rooney AP, Kajikawa M, Okada N, Roelofs WL (2007) Novel sex pheromone desaturases in the genomes of corn borers generated through gene duplication and retroposon fusion. *Proc Natl Acad Sci USA* 104(11):4467–4472.
16. Fujii T, et al. (2011) Sex pheromone desaturase functioning in a primitive *Ostrinia* moth is cryptically conserved in congeners' genomes. *Proc Natl Acad Sci USA* 108(17):7102–7106.
17. Albre J, et al. (2012) Sex pheromone evolution is associated with differential regulation of the same desaturase gene in two genera of leafroller moths. *PLoS Genet* 8(1):e1002489.
18. Matoušková P, Pichová I, Svatoš A (2007) Functional characterization of a desaturase from the tobacco hornworm moth (*Manduca sexta*) with bifunctional Z11- and 10,12-desaturase activity. *Insect Biochem Mol Biol* 37(6):601–610.
19. Fang N, Teal PEA, Doolittle RE, Tumlinson JH (1995) Biosynthesis of conjugated olefinic systems in the sex pheromone gland of female tobacco hornworm moths, *Manduca sexta* (L.). *Insect Biochem Mol Biol* 25(1):39–48.
20. Bai Y, et al. (2015) X-ray structure of a mammalian stearoyl-CoA desaturase. *Nature* 524(7564):252–256.
21. Wang H, et al. (2015) Crystal structure of human stearoyl-coenzyme A desaturase in complex with substrate. *Nat Struct Mol Biol* 22(7):581–585.
22. Schneiter R, Tatzer V, Gogg G, Leitner E, Kohlwein SD (2000) Elo1p-dependent carboxy-terminal elongation of C14:1Delta(9) to C16:1Delta(11) fatty acids in *Saccharomyces cerevisiae*. *J Bacteriol* 182(13):3655–3660.
23. Shi B, Davis BH (1993) Gas chromatographic separation of pairs of isotopic molecules. *J Chromatogr A* 654(2):319–325.
24. Tumlinson JH, Teal PE, Fang N (1996) The integral role of triacyl glycerols in the biosynthesis of the aldehydic sex pheromones of *Manduca sexta* (L). *Bioorg Med Chem* 4(3):451–460.
25. Knipple DC, Rosenfield C-L, Nielsen R, You KM, Jeong SE (2002) Evolution of the integral membrane desaturase gene family in moths and flies. *Genetics* 162(4):1737–1752.
26. Fujii T, et al. (2013) Discovery of a disused desaturase gene from the pheromone gland of the moth *Ascotis selenaria*, which secretes an epoxyalkenyl sex pheromone. *Biochem Biophys Res Commun* 441(4):849–855.
27. Tumlinson JH, et al. (1989) Identification of a pheromone blend attractive to *Manduca sexta* (L.) males in a wind tunnel. *Arch Insect Biochem Physiol* 10(4):255–271.
28. Liénard MA, et al. (2010) Elucidation of the sex-pheromone biosynthesis producing 5,7-dodecadienes in *Dendrolimus punctatus* (Lepidoptera: Lasiocampidae) reveals Delta 11- and Delta 9-desaturases with unusual catalytic properties. *Insect Biochem Mol Biol* 40(6):440–452.
29. Lim ZL, Senger T, Vrinten P (2014) Four amino acid residues influence the substrate chain-length and regioselectivity of Siganus canaliculatus Δ4 and Δ5/6 desaturases. *Lipids* 49(4):357–367.
30. Meesapyodsuk D, Qiu X (2014) Structure determinants for the substrate specificity of acyl-CoA Δ9 desaturases from a marine copepod. *ACS Chem Biol* 9(4):922–934.
31. Rawat R, Yu XH, Sweet M, Shanklin J (2012) Conjugated fatty acid synthesis: Residues 111 and 115 influence product partitioning of *Momordica charantia* conjugase. *J Biol Chem* 287(20):16230–16237.
32. Leary GP, et al. (2012) Single mutation to a sex pheromone receptor provides adaptive specificity between closely related moth species. *Proc Natl Acad Sci USA* 109(35):14081–14086.
33. Große-Wilde E, et al. (2010) Sex-specific odorant receptors of the tobacco hornworm *manduca sexta*. *Front Cell Neurosci* 4:7.
34. Vogel H, Badapanda C, Knorr E, Vilcinskas A (2014) RNA-sequencing analysis reveals abundant developmental stage-specific and immunity-related genes in the pollen beetle *Meligethes aeneus*. *Insect Mol Biol* 23(1):98–112.
35. Krogh A, Larsson B, von Heijne G, Sonnhammer EL (2001) Predicting transmembrane protein topology with a hidden Markov model: application to complete genomes. *J Mol Biol* 305(3):567–580.
36. Dereeper A, et al. (2008) Phylogeny.fr: Robust phylogenetic analysis for the non-specialist. *Nucleic Acids Res* 36(Web Server issue):W465–W469.
37. Buček A, Matoušková P, Sychrová H, Pichová I, Hrušková-Heidingsfeldová O (2014) Δ12-Fatty acid desaturase from *Candida parapsilosis* is a multifunctional desaturase producing a range of polyunsaturated and hydroxylated fatty acids. *PLoS One* 9(3):e93322.
38. Frost CG, Penrose SD, Gleave R (2008) Rhodium catalysed conjugate addition of a chiral alkenyltrifluoroborate salt: the enantioselective synthesis of hermitamides A and B. *Org Biomol Chem* 6(23):4340–4347.
39. Oonishi Y, Mori M, Sato Y (2007) Rhodium(I)-catalyzed intramolecular hydroacylation of 4,6-dienals: Novel synthesis of cycloheptenones. *Synthesis (Stuttg)* 2007(15):2323–2336.
40. Gagnon D, Lauzon S, Godbout C, Spino C (2005) Sterically biased 3,3-sigmatropic rearrangement of azides: Efficient preparation of nonracemic α-amino acids and heterocycles. *Org Lett* 7(21):4769–4771.
41. Stille JK, Simpson JH (1987) Stereospecific palladium-catalyzed coupling reactions of vinyl iodides with acetylenic tin reagents. *J Am Chem Soc* 109(10):2138–2152.
42. Svatoš A, Kalinová B, Boland W (1999) Stereochemistry of lepidopteran sex pheromone biosynthesis: A comparison of fatty acid-CoA Δ11-(Z)-desaturases in *Bombyx mori* and *Manduca sexta* female moths. *Insect Biochem Mol Biol* 29(3):225–232.
43. Krieger E, et al. (2009) Improving physical realism, stereochemistry, and side-chain accuracy in homology modeling: Four approaches that performed well in CASP8. *Proteins* 77(Suppl 9):114–122.
44. Moto K, et al. (2004) Involvement of a bifunctional fatty-acyl desaturase in the biosynthesis of the silkmoth, *Bombyx mori*, sex pheromone. *Proc Natl Acad Sci USA* 101(23):8631–8636.
45. Butenandt A, Beckmann R, Stamm D, Hecker E (1959) Über den sexuallockstoff des seidenspinners *Bombyx mori*. Reindarstellung und konstitution. *Z Naturforsch B* 14:283–284.

Insect Biochemistry and Molecular Biology 43 (2013) 724–731

Contents lists available at SciVerse ScienceDirect

Insect Biochemistry and Molecular Biology

journal homepage: www.elsevier.com/locate/ibmb

The role of desaturases in the biosynthesis of marking pheromones in bumblebee males

Aleš Buček [a], Heiko Vogel [b], Petra Matoušková [a], Darina Prchalová [a], Petr Žáček [a], Vladimír Vrkoslav [a], Petr Šebesta [a], Aleš Svatoš [a,b], Ullrich Jahn [a], Irena Valterová [a], Iva Pichová [a,*]

[a] Institute of Organic Chemistry and Biochemistry, Academy of Sciences of the Czech Republic, v.v.i. Flemingovo n. 2, 166 10 Prague 6, Czech Republic
[b] Max Planck Institute for Chemical Ecology, Hans-Knöll-Str. 8, D-07745 Jena, Germany

ARTICLE INFO

Article history:
Received 1 February 2013
Received in revised form
7 May 2013
Accepted 10 May 2013

Keywords:
Fatty acid desaturase
Bumblebee
Hymenoptera
Pheromone
RNA-seq
Functional expression

ABSTRACT

Bumblebee males (Hymenoptera) produce species-specific labial gland secretions called marking pheromones (MPs). MPs generally consist of terpenoids and fatty-acid-derived aliphatic compounds with various chain lengths predominantly containing one or no double bonds. The unsaturated fatty-acid-derived MP components were hypothesized to be produced by fatty acid desaturases (FADs) that exhibit diverse substrate specificities. To address this hypothesis, we isolated and functionally characterized FADs from three bumblebee species: *Bombus lucorum*, *Bombus terrestris*, and *Bombus lapidarius*. By employing RNA sequencing of the male labial glands and fat bodies of *B. lucorum* and *B. terrestris*, we identified five paralogous FAD-like sequences but only two FAD lineages were abundant and differentially expressed in the labial glands. We found that abundant FAD lineages were also expressed in the labial gland and fat body of *Bombus lapidarius*. Functional characterization of FADs in a yeast expression system confirmed that Δ4-FADs exhibited a unique Δ4-desaturase activity exclusively on 14-carbon fatty acyls and Δ9-FADs displayed Δ9-desaturase activity on 14- to 18-carbon fatty acyls. These results indicate that Δ9-FADs are involved in the biosynthesis of major unsaturated components of MPs in *B. lucorum* and *B. lapidarius* despite the diverse MP composition of these bumblebee species. The contribution of lipases, acyltransferases, esterases, and fatty acid reductases to production of the species-specific MP composition is also discussed in light of the transcriptomic data obtained in this study.

1. Introduction

In the majority of bumblebee species (Hymenoptera: Apidae: *Bombus*), males exhibit the unique premating behavior of marking prominent objects with pheromones to attract a conspecific female (reviewed by Goulson, 2010). This so-called marking pheromone (MP) is a secretion of the cephalic part of the male labial gland (LG) (Kullenberg et al., 1973; Bergman and Bergstrom, 1997). MPs consist of a mixture of terpenoids or fatty-acid-derived (FA-derived) compounds; their composition is species-specific and can be a valuable taxonomic tool in discriminating bumblebee species and subspecies (e.g., Bertsch et al., 2005; Rasmont et al., 2005; Coppée et al., 2008). Lanne et al. (1987) hypothesized that the biosynthesis of unsaturated FA-derived components of MPs is analogous to the biosynthesis of lepidopteran sex pheromones and that it involves mainly Δ9-fatty acid desaturases (FADs), which introduce a double bond at the Δ9 position of fatty acyl carbon chains. To test this hypothesis, Δ9-FAD from *Bombus lucorum* was cloned and functionally characterized; however, this enzyme was proposed to be involved in primary metabolism rather than MP biosynthesis (Matoušková et al., 2008).

FADs are ubiquitous membrane enzymes localized in the endoplasmic reticulum of all eukaryotic organisms. They play a crucial role in the maintenance of cell membrane structures *via* desaturation of fatty acids in membrane lipids (reviewed by Los and Murata, 1998). The FAD gene family presumably expanded in insects before the divergence of the lepidopteran and dipteran lineages (Roelofs and Rooney, 2003). Many lepidopteran species possess FAD's gene orthologs but extensive functional

Abbreviations: MP, marking pheromone; FAD, fatty acid desaturase; FA, fatty acid; RPKM, reads per kilobase of exon model per million mapped reads; DMDS, dimethyl disulfide; GC/MS, gas chromatography – mass spectrometry; ORF, open reading frame; LG, labial gland; FB, fat body; FAEE, fatty acid ethyl ester; FAR, fatty acid reductase; TM, trans-membrane; qPCR, real-time quantitative PCR; Me, methylester; Et, ethyl ester; MP, marking pheromone.

* Corresponding author. Tel.: +420 220 183 251.
E-mail addresses: iva.pichova@uochb.cas.cz, iva.pichova@seznam.cz (I. Pichová).

0965-1748/$ – see front matter © 2013 Elsevier Ltd. All rights reserved.
http://dx.doi.org/10.1016/j.ibmb.2013.05.003

characterization of almost 50 lepidopteran FADs indicated that FADs displaying Δ9 function are conserved across this insect order and diversification in sequence and function proceeds preferentially in Δ11 subfamily, which is not present in other insect classes (Knipple et al., 2002; Roelofs and Rooney, 2003; Liénard et al., 2008). Particularly in moths, this subfamily of FADs (further referred to as Δ11-FADs-like subfamily) evolved a broad range of specificities toward: (1) fatty acid chain length, (2) position of the introduced double bond, and (3) double bond configuration. This range enables production of the species-specific FA-derived sex pheromones.

In other insect classes, FADs have received much less attention. To date, very few nonlepidopteran FADs involved in sex pheromone production have been identified; such FADs have been reported in the fruit fly (Diptera) (Dallerac et al., 2000) and the housefly (Diptera) (Eigenheer et al., 2002). Δ9-FADs involved in primary metabolism from the red flour beetle (Coleoptera) (Horne et al., 2010) and the house cricket (Orthoptera) (Riddervold et al., 2002) have been cloned and functionally characterized. We previously cloned and functionally characterized the first hymenopteran Δ9-FAD from the bumblebee *B. lucorum* (Matoušková et al., 2008).

Our current study focuses on three bumblebee species that produce substantially different MPs. The MP of *B. lucorum* (*Bombus s.s.*) predominantly consists of C14-FA-derived ethyl esters (ethyl tetradec-9-enoate) (Bergström et al., 1973; Urbanová et al., 2001). In contrast, the MP of *Bombus terrestris* (*Bombus s.s.*) contains mainly terpenoid compounds (Kullenberg et al., 1970; Šobotník et al., 2008) but no unsaturated FA-derived compounds. In *Bombus lapidarius*, which is representative of the related subgenus *Melanobombus*, the MP is almost exclusively composed of C16-FA-derived alcohols (hexadecanol and hexadec-9-enol) (Kullenberg et al., 1970; Luxová et al., 2003).

In the present work, we describe the isolation, functional characterization, and transcript quantification of two FADs with Δ9- and Δ4-desaturase activity, respectively, from *B. lucorum*, *B. terrestris*, and *B. lapidarius*.

2. Material and methods

2.1. Tissue collection and total RNA isolation

Bombus lucorum, *Bombus terrestris*, and *Bombus lapidarius* males (0–5 days old) were obtained from laboratory colonies established as described by Šobotník et al. (2008). Carefully dissected LGs and fat bodies (FBs) were stored in TRIzol (Invitrogen) at −80 °C prior to RNA isolation. Total RNA was isolated using TRIzol according to the manufacturer's instructions. Genomic DNA contaminants were digested with TURBO DNase (Ambion) at 37 °C for 1 h. The RNA quantity was assessed by NanoDrop ND-100 UV/Vis spectrophotometer (Thermo Scientific) and RNA integrity was confirmed using Agilent 2100 Bioanalyzer (Agilent Technologies).

2.2. RNA-seq data generation, assembly, and annotation

RNA-seq was performed with dissected LGs and FBs from both *Bombus lucorum* and *Bombus terrestris*, using 5 μg total RNA isolated from each sample. RNA-seq was outsourced to Fasteris (www.fasteris.com) and was performed using the HiSeqTM 2000 Sequencing System from Illumina (www.illumina.com), multiplexing the four indexed samples in one lane and utilizing single read 100 bp technology. CLC Genomics Workbench (Version 5.0.1) was used for sequence backbone assembly of the resulting 35 Mio sequence reads for both *Bombus lucorum* tissues and 56 Mio sequence reads for both *Bombus terrestris* tissues. First, sequences were trimmed for length and quality with standard settings. Subsequently, they were assembled using the following CLC parameters: nucleotide mismatch cost = 2; insertion/deletion costs = 2; length fraction = 0.3; similarity = 0.9; and any conflict among the individual bases was resolved by voting for the base with highest frequency. Contigs shorter than 250 bp were removed from the final analysis, resulting in a final *de novo* reference assembly (backbone) of 36,162 contigs for *Bombus lucorum* and 38,564 contigs for *Bombus terrestris*. The digital gene expression analysis was performed with QSeq Software (DNAStar Inc.), utilizing the respective mapping tools. Each Illumina sequence was mapped to the obtained reference backbone sequences, which were then used to estimate expression levels and fold-change differences between tissues. The correction for biases in the sequence datasets and different transcript sizes was addressed by using the RPKM (reads per kilobase of exon model per million mapped reads) algorithm (Mortazavi et al., 2008). Due to the lack of a reference genome, exon model information was replaced with contigs derived from the respective transcriptome assemblies (reads per kilobase of contig per million mapped reads). Homology searches (BLASTx and BLASTn) of unique sequences and functional annotation by gene ontology terms (GO; www.geneontology.org), InterPro terms (InterProScan, EBI), enzyme classification codes (EC), and metabolic pathways (KEGG, Kyoto Encyclopedia of Genes and Genomes) were determined using the BLAST2GO software suite v2.4.1 (www.blast2go.de).

2.3. Real-time quantitative PCR

Total RNA (0.25 μg) extracted from LGs and FBs of three-day-old *B. lucorum* and *B. terrestris* males (three biological replicates) served as templates for cDNA synthesis using SuperScript III Reverse Transcriptase (Invitrogen) and random hexamer primers according to the manufacturer's instructions. Real-time quantitative PCR (qPCR) was performed using a LightCycler 480 Real-Time PCR System (Roche). PCR reactions were carried out using Dynamo HS SYBR Green qPCR Master Mix (Finnzymes), 0.625 μM of each primer, and 1 μl of cDNA template. Ten-fold dilutions of cDNA mixture were analyzed to calculate the reaction efficiency for each primer pair. All samples were examined in two technical replicates, and data were exported from the LightCycler 480 SW 1.5 into Microsoft Excel and analyzed using GenEx software (www.multid.se). Relative gene expression was normalized to phospholipase A2 (PLA2) and elongation factor 1α (EEF1A) (Horňáková et al., 2010). qPCR primers for SPVE and NPVE FADs were designed using Primer3 (Rozen and Skaletsky, 2000). Detailed parameters of qPCR analysis and qPCR primer sequences are described in Supplementary Materials and Methods.

2.4. Sequence analysis

The nucleotide sequences of predicted FADs were aligned using the Muscle algorithm (Edgar, 2004) and trimmed manually. Desaturase topology was predicted using the freely available web-based program TMHMM 2.0 (Krogh et al., 2001). The phylogenetic trees were reconstructed with MEGA5 software (Tamura et al., 2011) using the neighbor-joining method, Jones-Taylor-Thorton (JTT) substitution model (Jones et al., 1992) and 1000 bootstrap replicates as a measure of statistical reliability. The publicly available genetic sequence database GenBank (www.ncbi.nlm.nih.gov/genbank) was searched using the BLAST algorithm and was used to retrieve the FADs sequences. Complete and partial coding sequences of FADs reported in this work were deposited in GenBank under accession numbers KC437326–KC437333.

2.5. Cloning of FADs and heterologous expression in S. cerevisiae

The central fragments of Δ9-Blap and Δ9-Bter were isolated using homology-probing PCR according to the procedure described by Matoušková et al. (2008). Briefly, cDNA libraries prepared from total RNA extracted from *B. lapidarius* and *B. terrestris* LGs and FBs were screened using degenerate primers designed against the conserved histidine-rich motifs of membrane FADs. The 3′ and 5′ ends were obtained by rapid amplification of cDNA-ends (RACE) PCR and the composed full-length sequences were verified by sequencing. The SPVE_Blap coding sequence from *B. lapidarius* was obtained using specific primers designed against conserved 3′ and 5′ noncoding regions of Δ4-Bter and Δ4-Bluc obtained from RNA-seq (Table S1).

To construct expression vectors, the open reading frames (ORFs) were amplified from LG cDNA libraries using specific expression primers (Table S1) and ligated in-frame with an N-terminal hexahistidine tag into the pYEXTHS-BN vector under control of the CUP1 promoter (Holz et al., 2002). The resulting expression vectors were verified by sequencing. Desaturase- and elongase-deficient *Saccharomyces cerevisiae* cells (MAT**a** *elo1:HIS3 ole1:LEU2 ade2 his3 leu2 ura3*) (Schneiter et al., 2000) were transformed with expression vectors or an empty pYEXTHS-BN vector (control) using the *S.c.* EasyComp transformation kit (Invitrogen) according to the manufacturer's instructions. Transformed colonies were selected on YNB agar plates lacking uracil (YNB-U: 0.67% yeast nitrogen base without amino acids, 2% glucose, 2% agarose, supplemented with Brent supplement mix without uracil (ForMedium) according to the manufacturer's instructions) and inoculated into 20 ml of YNB-U liquid medium supplemented with 0.5 mM $CuSO_4$ for induction of FAD expression. When indicated, methyl myristate, methyl laurate, palmitoleic acid, or oleic acid were added to a final concentration of 0.3 mM, together with 1% tergitol as a solubilizer. The yeast cells were cultivated at 30 °C for 3 days until the late stationary growth phase was reached. To evaluate heterologous protein expression, yeast cells were harvested by centrifugation (3 min, 3000 g, room temperature), resuspended in lysis buffer (50 mM Tris, pH 6.8, containing 1.5% β-mercaptoethanol, 2% SDS, 10% glycerol, and bromophenol blue) and sonicated. Cellular extracts corresponding to 100 μl of yeast culture were separated by SDS–PAGE (12% gel). His-tagged FADs were detected by Western blot using anti-poly-histidine peroxidase-conjugated antibodies (1:2000) (Sigma–Aldrich) and West Femto chemiluminescent substrate (Thermo Scientific) according to the manufacturer's instructions.

2.6. FAME preparation, DMDS derivatization, and GC/MS analysis

S. cerevisiae cells were harvested by centrifugation (3 min, 3000 g, room temperature) and washed with 0.1% tergitol solution and water. The cell pellet was lyophilized and extracted by shaking with 1 ml of a dichloromethane:methanol solution (2:1) and 0.3 g of glass beads (1 h, room temperature). Fatty acid methyl esters (FAMEs) were prepared from the extract of total cellular lipids using the transesterification procedure described by Matoušková et al. (2008). The resulting FAMEs were extracted with 600 μl of hexane and analyzed by gas chromatography coupled with mass spectrometric detection (GC/MS) under the conditions described below.

The double bond position in all detected unsaturated FAs was identified using dimethyl disulfide (DMDS) derivatization of FAME extracts according to the procedure described by Murata et al. (1978). The retention behavior and mass spectra were compared with those of synthetic standards of methyl myristoleate (Sigma–Aldrich), methyl palmitoleate (Sigma–Aldrich), methyl oleate (Sigma–Aldrich), a 92:8 mixture of methyl *Z*4-tetradecenoate and methyl *E*4-tetradecenoate (prepared as described below). The FAME extracts and corresponding DMDS adducts were analyzed with a 7890A gas chromatograph coupled to a 5975C mass spectrometer equipped with electron ionization (EI) and a quadruple analyzer (Agilent Technologies) using DB-5MS or DB-WAX capillary columns (both J&W Scientific; 30 m × 0.25 mm, film thickness 0.25 mm). Conditions for analysis were as follows: carrier gas: He at a flow rate of 1 ml/min; split ratio: 1:10; injection volume: 2 μl; injector temperature: 220 °C; and thermal gradient: 140 °C–245 °C at 3 °C/min, then 8 °C/min to 280 °C, and final temperature held for 5 min. The temperature program was terminated at 245 °C and held for 10 min when the DB-WAX column was used.

2.7. Synthesis of a (4Z)- and (4E)-methyl tetradec-4-enoate mixture (Z4-14:1Me/E4-14:1Me)

A 92:8 mixture of *Z*4-14:1Me and *E*4-14:1Me was synthesized by a Wittig reaction of methyl 4-oxobutanoate with decyltriphenylphosphorane, prepared from the reaction of decyltriphenylphosphonium bromide with butyllithium in tetrahydrofuran (THF). The configuration of the major double bond isomer *Z*4-14:1Me was determined from the ^{1}H NMR spectrum (doublet of triplets at 5.42 ppm, with a coupling constant of 10.8 Hz).

n-Butyllithium (1.6 M in hexane, 0.25 ml, 0.400 mmol) was added dropwise at −78 °C to a suspension of decyltriphenylphosphonium bromide (200 mg, 0.414 mmol) in dry THF (2 ml) under a nitrogen atmosphere, and the resulting deep orange mixture was stirred at −78 °C for 30 min. The cooling bath was removed, the reaction mixture was warmed to room temperature and stirred for 10 min, whereupon almost all salt dissolved. The reaction mixture was again cooled to −78 °C, and a concentrated solution of methyl 4-oxobutanoate (46 mg, 0.4 mmol) in THF (0.2 ml) was added slowly. During the addition of the aldehyde, the color of the reaction mixture discharged. The reaction mixture was stirred for 5 min, then warmed to room temperature and stirred for an additional 3 h. The reaction was quenched by addition of a half-saturated ammonium chloride solution (2 ml). Diethyl ether (5 ml) was added, and the organic layer was separated. The aqueous phase was extracted with diethyl ether (2 × 2 ml). The combined organic layers were washed with brine (5 ml) and dried over magnesium sulfate. The solvent was removed *in vacuo*. Flash column chromatography (20:1 pentane:diethyl ether) afforded an inseparable 92:8 mixture of (4*Z*)- and (4*E*)-methyl tetradec-4-enoate (41 mg, 43%) as a colorless oil. Spectroscopic data are shown in the Supplementary Materials and Methods.

3. Results

3.1. Description of predicted FAD sequences

We utilized system based on four-amino-acid (aa) signature motif (Knipple et al., 2002), i.e., GPTE, KPTE, LPQD, NPVE, and SPVE (Fig. 1) for initial analysis of FAD lineages from transcriptomic data, since little was known about FAD specificities from hymenopteran *species*. We predicted five paralogous FAD lineages in *B. lucorum* and *B. terrestris* LG and FB. The FAD orthologs from *B. terrestris* and *B. lucorum* were highly conserved, sharing over 98% aa sequence similarity. The abundances of predicted FAD transcripts were assessed according to the calculated RPKM values.

GPTE_Bluc and GPTE_Bter FAD transcripts had low abundance and were present at comparable levels in both LG and FB cDNA libraries. A partial transcript termed KPTE_Bter was sequenced in low abundance only in *B. terrestris* LG and FB libraries, but we were able to amplify a KPTE_Bluc ortholog from the *B. lucorum* cDNA

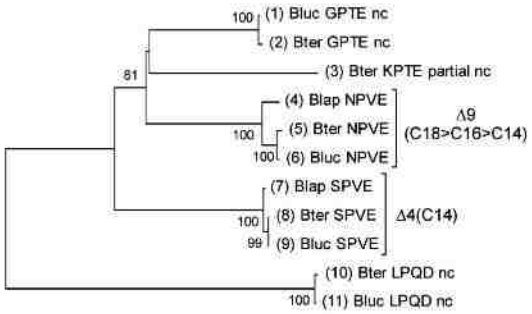

Fig. 1. Phylogenetic relationship between FAD amino acid sequences predicted from RNA-seq of LG and FB cDNA libraries from *B. lucorum* and *B. terrestris*. NPVE_Blap and SPVE_Blap sequences were obtained by PCR using *B. lapidarius* FB and LG cDNA libraries. Accession numbers are as follows: (1) KC437331, (2) KC437330, (3) KC437329, (4) CAT01313, (5) CAW34805, (6) CAM96720, (7) KC437327, (8) KC437328, (9) KC437326, (10) KC437332, and (11) KC437333. Numbers along branches indicate bootstrap percentage support from 1000 replicates. Bootstrap support values <50% are not shown. nc, not characterized.

library using PCR primers designed against KPTE_Bter. The KPTE_Bluc sequence was not obtained in RNA-seq, probably due to its low abundance in the *B. lucorum* LG. The presence of a KPTE_Bluc amplicon indicates that the KPTE lineage is not specific for *B. terrestris* (data not shown). Additional predicted partially sequenced FAD transcripts were designated LPQD_Bluc and LPQD_Bter and were significantly more abundant in the fat body than in the labial gland (data not shown). The full-length sequences of LPQD_Bter and LPQD_Bluc were obtained using PCR with gene-specific primers (data not shown). Their sequences did not contain the catalytically essential third histidine-rich motif of membrane FADs (Shanklin et al., 1994). This finding suggests that LPQD transcript might not encode functional FAD or might code for an enzyme with other than desaturase activity.

The two remaining FAD lineages, designated NPVE and SPVE, were significantly more abundant in LGs than FBs, according to RNA-seq data. The NPVE_Bluc and NPVE_Bter transcripts were 43-fold and 14-fold, respectively, more abundant in LGs than FBs of the corresponding bumblebee species. SPVE_Bluc and SPVE_Bter were 12-fold and 29-fold, respectively, more abundant in LGs than FBs. The differentially high abundance in LGs was confirmed by qPCR analysis (Fig. 2). We therefore selected NPVE and SPVE FADs, along

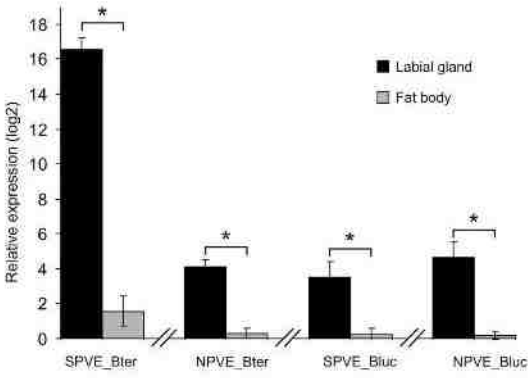

Fig. 2. Relative abundance of Bluc_SPVE, Bter_SPVE, Bluc_NPVE, and Bter_NPVE transcripts in labial glands (LG) and fat bodies (FB) quantified by qPCR. Data are shown as mean ± SD of three biological replicates. $^{*}p < 0.05$.

with the NPVE and SPVE orthologs from *B. lapidarius* obtained by PCR amplification of the respective LG cDNA library, for further characterization.

3.2. Sequence analysis of NPVE and SPVE FADs

The NPVE_Bluc sequence obtained in this study was identical to that of the previously characterized Δ9-FAD from *B. lucorum* (Matoušková et al., 2008). Both the NPVE_Blap and NPVE_Bter ORFs encode proteins with 351 aa residues. These proteins are almost identical to the sequence of Δ9-FAD from *B. lucorum*, sharing 97% and 98% aa sequence similarity, respectively. The most similar functionally characterized non-bumblebee sequence found in GenBank was a Z9-FAD from the house cricket *Acheta domesticus* that prefers an 18-carbon fatty acyl substrate (80% and 81% aa sequence similarity, respectively, NCBI GenBank: AAK25796, Riddervold et al., 2002).

The SPVE_Bluc and SPVE_Bter ORFs encode an identical protein with 368 aa residues, further referred to as SPVE_Bluc/Bter, which is almost identical to the 368-aa SPVE_Blap protein (99% aa similarity). The SPVE-Bluc/Bter and SPVE_Blap proteins share high sequence similarity with a Z9-desaturase from the housefly *Musca domestica* that produces a 1:1 ratio of Z9-16:1 and Z9-18:1 (64% and 66% aa sequence similarity, respectively, NCBI GenBank: AAN31393, Eigenheer et al., 2002) and Z9-FADs from *A. domesticus* (66% and 64% aa sequence similarity, respectively). Topology predictions indicate the presence of four transmembrane helices in NPVE FADs, whereas six transmembrane helices are predicted in SPVE FADs (Fig. S1).

NPVE and SPVE FAD orthologs from *B. lucorum*, *B. terrestris*, and *B. lapidarius* share high aa sequence similarities with uncharacterized hymenopteran FADs, e.g., those from the bumblebee *Bombus impatiens* (over 97% aa sequence similarity; NCBI RefSeq: XP_003492439 and XP_003492440), the leafcutter bee *Megachile rotundata* (over 85% aa sequence similarity; XP_003703958 and XP_003703934), the European honeybee *Apis mellifera* (over 86% aa sequence similarity; XP_624557 and XP_395629), and several ant species, such as the leafcutter ant *Acromyrmex echinatior* (over 80% aa sequence similarity; EGI70555 and EGI70557).

3.3. NPVE FADs display Δ9-desaturase specificity

To test the enzymatic properties of NPVE_Blap, NPVE_Bter, and NPVE_Bluc, their ORFs were cloned with an N-terminal hexahistidine tag into the pYEXTHS-BN plasmid under control of the Cu^{2+}-inducible CUP1 promoter. The desaturase- and elongase-deficient *elo1*Δ *ole1*Δ yeast strain was transformed with the resulting NPVE vectors or an empty pYEXTHS-BN vector (control). Only the strains transformed with vectors bearing NPVE ORFs grew well without addition of unsaturated fatty acids to the cultivation medium, indicating the complementation of unsaturated FA auxotrophy by the NPVE ORFs. Western blot analysis demonstrated that His-tagged NPVE FADs with a molecular weight of ~40 kDa were expressed in the NPVE transformants (Fig. 3). GC/MS analysis of transesterified lipidic extracts showed almost identical FAME profiles for all NPVE strains with dominant peaks of methyl palmitoleate (Z9-16:1Me) and methyl oleate (Z9-18:1Me), along with a minor peak of methyl myristoleate (Z9-14:1Me). Accordingly, the NPVE FADs were termed Δ9-FADs. As the relative amount of myristic acid (14:0) in the yeast strains accounted for less than 1%, its concentration was increased by supplementing the cultivation medium with 0.3 mM methyl myristate (Fig. 4A). The conversion rates of myristic acid, palmitic acid, and stearic acid to their corresponding Z9-unsaturated products were calculated as the ratio of relative abundance of unsaturated FAs to the total relative amount

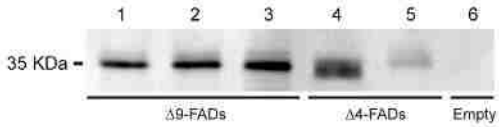

Fig. 3. Expression of Δ9-FADs and Δ4-FADs in yeast strains monitored by Western blot. Cell lysates prepared from 100 μl of yeast culture were separated by SDS–PAGE, and the histidine-tagged FADs were detected by anti-poly-histidine antibodies. Lane 1, Δ9-Bter; lane 2, Δ9-Bluc; lane 3, Δ9-Blap; lane 4, Δ4-Bter/Bluc; lane 5, Δ4-Blap; lane 6, yeast strain bearing empty plasmid (control). The molecular weight marker is shown on the left.

of saturated and unsaturated FAs. All Δ9-FADs desaturated 18:0 with the highest conversion rate (98%), followed by 16:0 (85%–88%) and 14:0 (62%–63% in Δ9-Bter and Δ9-Bluc, respectively; 47% in Δ9-Blap) (Fig. 4B).

3.4. SPVE FADs display Δ4-desaturase specificity

Because the protein sequences encoded by SPVE_Bter and SPVE_Bluc ORFs were identical, only the SPVE_Bter ORF was amplified and ligated into the pYEXTHS-BN vector, and the resulting expression vector is further referred to as the SPVE_Bter/Bluc vector. The enzymatic properties of SPVE_Bter/Bluc and SPVE_Blap FADs were tested analogously as the NPVE FAD activities and specificities. However, SPVE transformants did not grow in the YNB-U − $CuSO_4$ cultivation medium. To investigate whether the SPVE FADs possess any desaturation activity, the transformants were cultivated in the presence of a mixture of Z9-16:1 and Z9-18:1 (1:1) to maintain their growth. Western blot analysis revealed that both SPVE FADs were expressed in the yeast system, although SPVE_Blap was expressed in lower amounts than SPVE_Bter/Bluc (Fig. 3). GC/MS analysis of FAME extracts revealed trace amounts of unsaturated 14:1Me (0.01%) as a sole novel product of SPVE FADs. In order to increase its amount, the yeast cultivation medium was supplemented with methyl myristate, the presumed precursor of 14:1Me. Under these conditions, the amount of 14:1Me increased to 0.19% and 0.22% in SPVE_Bter/Bluc and SPVE_Blap transformants, respectively.

The double bond position was determined to be Δ4 using DMDS derivatization, based on the presence of characteristic fragments at *m/z* 147 and 187. Δ4-14:1Me was partially separated into two isomers with identical mass spectra using a non-polar DB5 column. The comparison with the retention behavior of synthetic Z4-14:1Me containing minor amounts of E4-14:1Me indicated that both the Z4- and E4-isomers are present in the extract from SPVE transformed strains in an approximately 5:1 ratio (Fig. 5).

To further test the specificity of Δ4-FADs toward a short chain fatty acyl substrate, the cultivation medium was supplemented with methyl laurate (12:0). However, no novel desaturation products of 12:0 were detected (data not shown), indicating that Δ4-FADs exclusively desaturate myristate.

3.5. Phylogenetic analysis

To infer the evolutionary relationship between insect FADs, we constructed a phylogenetic tree based on sequences comprising functionally characterized insect Δ9-FADs; representatives of the moth Δ11-FADs-like lineage; the bumblebee Δ9 (NPVE) and Δ4 (SPVE) FADs reported here; and their homologs from *B. impatiens*, *A. mellifera*, *M. rotundata*, and *A. echinatior* (Fig.S2). The hymenopteran FADs formed a Δ9-lineage clustering with insect Δ9-FADs, and a novel Δ4-lineage. The lepidopteran lineage of Δ9(C18 > C16)-FADs with preference for stearate and Δ9(C16 > C18)-FADs with preference for palmitate were well separated (Knipple et al., 2002; Rooney, 2009). The bumblebee Δ9- lineage was not statistically supported to cluster with the lepidopteran Δ9(C18 > C16) or Δ9(C16 > C18) lineages (Fig. S2).

4. Discussion

MP biosynthesis in *B. lucorum*, *B. terrestris*, and *B. lapidarius* was previously studied *in vivo* and *in vitro* by tracking the incorporation of labeled precursors into MP components. Enzymatic activities such as FA reduction, FA esterification, *de novo* terpenoid synthesis, triacylglycerol hydrolysis, or FA desaturation were detected in the investigated species (Luxová et al., 2003; Matoušková et al., 2008; Žáček et al., 2013). The most detailed study on the biosynthesis of FA-derived MPs was performed in *B. lucorum*, but no desaturase activity was detected during the *in vitro* experiments, thus preventing the determination of LG FAD specificities (Luxová et al., 2003; Matoušková et al., 2008; Žáček et al., 2013). Although Δ9-desaturation was observed during *in vivo* experiments after applying palmitic acid to the abdomen or head capsule of *B. lucorum* males, transport of fatty acyls occurred between the FB and LG; therefore, it could not be established whether LG or FB is the site of Δ9-desaturation (Luxová et al., 2003).

The desaturase multigene family evolution is well described in Lepidoptera. The desaturase family originated before split among Lepidoptera, Diptera, and Orthoptera (Roelofs and Rooney, 2003).

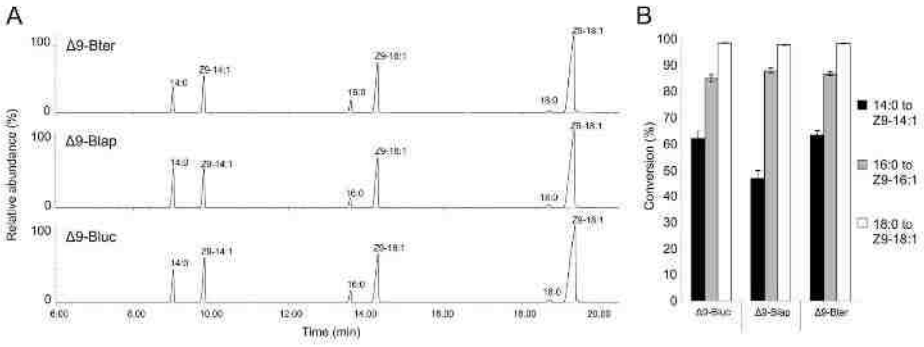

Fig. 4. GC/MS analysis of the FAME extracts of yeast strains expressing Δ9-FADs. (A) Chromatograms represent FAMEs prepared from total lipidic extracts of strains expressing Δ9-Bter, Δ9-Blap, and Δ9-Bluc using a DB-WAX column. (B) Conversion rates of myristic (14:0), palmitic (16:0), and stearic (18:0) acids to their corresponding monounsaturated fatty acids (Z9-14:1, Z9-16:1, and Z9-18:1, respectively) calculated from relative abundances of individual FAMEs produced in the yeast strains. Bars represent mean ± S.D. of three cultivation replicates. The cultivation medium was supplemented with 0.3 mM methyl myristate.

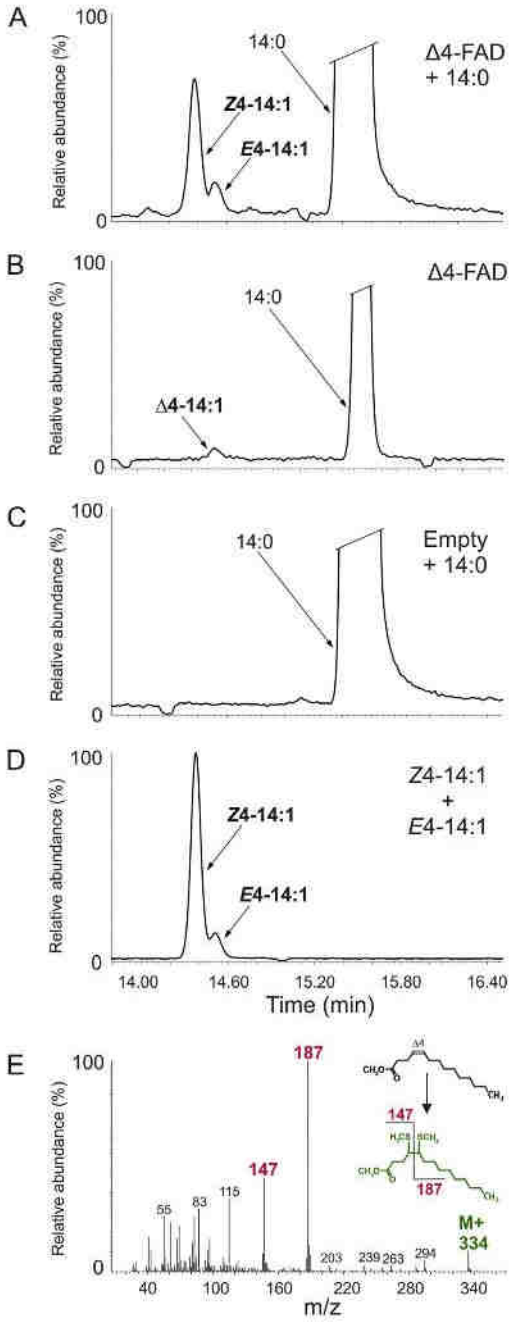

Fig. 5. GC/MS analysis of FAME extracts from yeast strains expressing Δ4-FADs. Sections of chromatograms represent analysis of FAMEs prepared from strains expressing Δ4-FADs (A and B) and a control strain transformed with an empty plasmid (C), which were cultivated in the presence (indicated as "+14:0") or absence of supplemental methyl myristate. The profile and quantity of FAMEs isolated from strains expressing Δ4-Bluc/Bter and Δ4-Blap were virtually identical, and for clarity, only the chromatogram obtained from GC/MS analysis of the Δ4-Blap strain is shown. (D) Chromatogram of a mixture of Z4-14:1Me and E4-14:1Me synthetic standards. (E) The mass spectrum of a DMDS adduct of 14:1Me present in the extract of SPVE yeast strains. Characteristic fragments and molecular ions are highlighted. A DB-5 column was used in all analyses.

This family is composed from at least five gene clusters that are correlated with desaturase functions (Roelofs and Rooney, 2003; Liénard et al., 2008; Rooney, 2009). In this study, we identified five distinct transcripts encoding putative FADs in the LG transcriptomes of *B. lucorum* and *B. terrestris*. Two FAD genes with the signature motif NPVE and SPVE were significantly more highly expressed in LGs than in FBs. We therefore selected these as candidate genes possibly involved in the biosynthesis of FA precursors of MPs.

The heterologous expression of NPVE_Bter, NPVE_Blap, and the previously characterized NPVE_Bluc (Matoušková et al., 2008) provided evidence that all NPVE FADs are Δ9-FADs. The substrate preference of Δ9-FADs was highly conserved, with 18:0 being the preferred substrate, followed by 16:0 and 14:0. Previously, we functionally characterized Δ9-Bluc in an *ole1*Δ yeast strain using an expression vector with a galactose-inducible promoter. In that expression system, 14:0 was desaturated to Z9-14:1 with a low conversion rate. This observation led to the hypothesis that Δ9 NPVE_Bluc participates mainly in the primary metabolism of C16 and C18 fatty acids (Matoušková et al., 2008). However, the experiments presented in this work indicated a higher conversion of 14:0, along with increased conversion rates of 16:0 and 18:0, compared with rates in the previously employed expression system. We attribute these observed differences to the use of the Cu^{2+}-induced expression of Δ9-Bluc and the use of the *elo1*Δ *ole1*Δ yeast strain, which presumably resulted in higher desaturase production and activity.

We propose that Δ9-FADs are involved in the production of MPs in *B. lucorum* and *B. lapidarius* because: (1) Δ9-FAD transcripts are highly abundant in the LG of *B. lucorum* and also present in the *B. lapidarius* LG (not quantified), and (2) in the yeast expression system, Δ9-FADs produced Δ9-14:1 and Δ9-16:1, which are presumed precursors of major MP components in *B. lucorum* and *B. lapidarius*, respectively. However, the species-specific composition of MP is apparently not determined by the specificity of FADs but rather by the selectivity of other enzymes involved in preferential transport of 14:0 in LGs or in *de novo* biosynthesis of 14:0 in LGs, as ethyl tetradec-9-enoate is the major component (53%) of *B. lucorum* MP. Additional MPs are present here in lower concentrations: ethyl dodecanoate (6%), ethyl hexadec-9-enoate (4%), ethyl tetradecanoate (2%), and ethyl octadec-9-enoate (2%) (Bergström et al., 1973; Urbanová et al., 2001). The composition of FA ethyl esters found in the LG extract correlates well with the content of free FAs, with Z9-14:1 being the major free FA in LGs (Matoušková et al., 2008). Given the low abundance of Z9-14:1 in *B. lucorum* FBs (Cvacka et al., 2006), we initially presumed that a Δ9-FAD with preference for 14:0 was expressed exclusively in the *B. lucorum* LG and was responsible for the major content of Z9-14:1Et in *B. lucorum* MP. Indeed, pheromone-specific FADs exhibiting a substrate preference toward 14:0 were identified in the fruit fly (Dallerac et al., 2000) and numerous moth species (e.g., Liu et al., 2002; Fujii et al., 2011). Nevertheless, our results provide evidence that the Δ9-Bluc enzyme, whose transcript is highly abundant in the LG, does not prefer 14:0 as a substrate but rather exhibits broad substrate specificity toward 18:0, 16:0, and 14:0.

Myristic acid (14:0) can be transported to LGs from FBs in the form of diacylglycerols and then cleaved by a selective enzyme (Žáček et al., 2013). Simultaneously, 14:0 can be desaturated in the LG to Z9-14:1 *via* abundant NPVE_Bluc, resulting in accumulation of Z9-14:1 and depletion of 14:0. Low content of 14:0 in the LG was indeed observed by Matoušková et al. (2008). Importantly, the proposed biosynthetic pathway would lead to the accumulation of Z9-14:1 without the necessity of a 14:0-specific FAD.

Our preliminary analysis of *B. lucorum* transcriptomic data supports both the "*de novo*" and "selective transport" hypotheses of

supplying the LG with a sufficient amount of 14:0 substrate for MP biosynthesis. In the transcriptomic data, we found that lipase and acyltransferase transcripts were highly abundant and differentially expressed in *B. lucorum* LGs, which could indicate an association with FA transport and storage (reviewed by Arrese et al., 2001; Yen et al., 2008; respectively). Lipase and acyltransferase are promising candidates for enzymes involved in the selective release and accumulation, respectively, of 14:0 in *B. lucorum* LGs (Table S2 and Supplementary List S1).

In *B. lucorum*, the terminal biosynthetic reaction is fatty acid ethyl esterification. The specificity of this reaction step toward a 14-carbon-long FA substrate may further contribute to the prevalence of ethyl myristoleate in *B. lucorum* MP (Matoušková et al., 2008). Recently, α/β-3 and EsLi enzymes from the honeybee (*A. mellifera*) were shown to exhibit FA ethyl ester synthase activity and to produce ethyl oleate, a honeybee prime pheromone (Castillo et al., 2012). The preliminary transcriptomic data analysis indicates the presence of homologs of α/β-3 and EsLi in *B. lucorum* LGs and FBs. However, these enzymes are not differentially expressed in the LG, and therefore they are likely not the principal enzymes of LG-localized biosynthesis of ethyl esters (data not shown).

In the *B. lapidarius* LG, the content of major free FAs correlated reasonably well with the content of volatile alcohol components of MP. The dominant free FA in LG is Z9-16:1 (90%), followed by minor amounts of Z11-18:1 (7%) and 16:0 (2%) (Fig.S3 and Supplementary Materials and Methods). Although we demonstrated that Δ9-Blap exhibits a significantly decreased preference toward 14:0 compared with Δ9-Bluc and Δ9-Bter, this shift in desaturase specificity toward longer FA substrates alone does not explain the dominant content of free Z9-16:1 in LGs. More likely, the composition of free FAs in the *B. lapidarius* LG suggests a specific mechanism responsible for the accumulation of Z9-16:1 and 16:0 in LGs, analogous to the accumulation of C14 fatty acids in the *B. lucorum* LG discussed above. The observation that C16 fatty acids are the major constituents of triacylglycerols in the FB of *B. lapidarius* and the major fatty acyl chains of MP volatiles led to the hypothesis that Z9-16:1 and 16:0 could be transported from the FB to the LG in the form of diacylglycerol and serve there as MP precursors (Cvacka et al., 2006). Alternatively, 16:0 could be the major transported FA, which undergoes rapid desaturation in the LG by Δ9-Blap to give rise to the specific MP composition of *B. lapidarius*.

The proposed terminal step of MP biosynthesis in *B. lapidarius* is FA reduction catalyzed by a fatty acid reductase (FAR). The strict specificity of the *B. lapidarius* FAR toward C16 fatty acids could explain the fact that Z11-18:1 is present as a free FA in the LG but that the corresponding alcohol is absent in the MP. An analogous mechanism of determination of pheromone blend composition was proposed for several moth FARs, which exhibit preferences for the chain length and double bond position of the sex pheromone precursor FAs (Moto et al., 2003; Lassance et al., 2013).

In *B. terrestris*, GC analysis of the LG extract coupled with electroantennographic detection indicated that Δ9-unsaturated fatty acid derivatives were not present as active components of the extract (Šobotník et al., 2008). In contrast to this previous observation, the NPVE_Bter transcript encoding Δ9-FAD is highly abundant in the *B. terrestris* LG. One possible explanation is post-transcriptional downregulation of Δ9-Bter. This mechanism was proposed to explain the presence of highly abundant yet enzymatically inactive desaturase transcripts in moth pheromone glands (Roelofs and Rooney, 2003; Park et al., 2008). Post-transcriptional downregulation might result in the low abundance of the Δ9-Bter enzyme and explain the absence of Δ9-unsaturated compounds in the *B. terrestris* LG. However, Δ9-Bter mRNA is one of the most abundant transcripts in the *B. terrestris* LG (data not shown), and further experiments will be required to explain the apparent discrepancy between high abundance of Δ9-Bter transcript and absence of Δ9-FA-derived compounds in MP of *B. terrestris*.

Identification of desaturase with Δ4-specificity was surprising because occurrence of the Δ4-monounsaturated FAs (Δ4-16:1) is limited in nature. It is present in seeds of *Umbelliferae*, *Araliaceae*, and *Garryaceae* plant species (Cahoon et al., 1992) and in the sexually deceptive orchid *Ophrys sphegodes*, in which Δ4-16:1 is a proposed intermediate of alkene biosynthesis (Schlüter et al., 2011). The unusual Δ4-specificity might be underlined by the presence of the 5th and 6th predicted transmembrane (TM) helices, which deviates from the expected membrane topology of acyl-CoA desaturases (Stukey et al., 1990; Man et al., 2006). The additional predicted helices likely represent membrane-associated regions, which might play a role in FA substrate recognition, as previously suggested by Diaz et al. (2002). Concerning the highly unusual Δ4-FAD activity, it cannot be excluded that the enzymatic activity of Δ4-FADs in bumblebee tissue differs from the Δ4-desaturase activity observed in the yeast expression system. Based on the conserved histidine-rich motifs $HX_{3-4}H$, $HX_{2-3}HH$, and $(H/Q)X_{2-3}HH$ (reviewed by Shanklin and Cahoon, 1998), the Δ4-FADs belong to the large family of non-heme iron enzymes. This gene family comprises not only enzymes that introduce double bonds into fatty acyl chains but also FA hydroxylases and sphingolipid-modifying enzymes (Shanklin and Cahoon, 1998). However, none of the previously described non-heme iron-containing enzymes was found to be homologous to Δ4-FADs (data not shown). The absence of Δ4-14:1 in the bumblebee LG might be explained by the mechanism of post-transcriptional downregulation of Δ4-FADs discussed above. To address this question, future development of FAD-specific antibodies may unequivocally establish the abundance of Δ9-FAD and Δ4-FAD enzymes across bumblebee tissues.

5. Conclusion

Next-generation sequencing of the *B. terrestris* and *B. lucorum* LG and FB transcriptomes enabled the identification of five paralogous FAD-like sequences and selection of two candidate FADs paralogs, which are differentially and abundantly expressed in the LGs and therefore presumably involved in MP biosynthesis. Functional characterization of Δ4-FADs and Δ9-FADs from *B. terrestris* and *B. lucorum*, along with their homologs from *B. lapidarius*, revealed that FAD substrate specificities and amino acid sequences are highly conserved across bumblebee species, even though the FA compositions of bumblebee MPs are diverse. Although *B. terrestris* contains Δ9-FADs and Δ4-FADs, which display *in vitro* activities, only trace amounts of desaturated FA-derived compounds are present in the pheromone blend of this bumblebee. These desaturases are likely post-transcriptionally downregulated in this species. Our data further indicate that Δ9-FADs are involved in the biosynthesis of MPs in *B. lapidarius* and *B. lucorum*; however, their substrate specificities do not regulate the species-specific composition of the MPs. Specific MP composition may instead be determined by enzymes that participate in accumulation of FAs with a particular chain length in the bumblebee LGs, e.g., by fatty acyl lipases and acyltransferases. Additionally, enzymes involved in terminal step of pheromone biosynthesis, i.e. fatty-acyl reductases in *B. lapidarius* and fatty acid esterases in *B. lucorum* might further contribute to the species specific MP composition.

Acknowledgments

We are grateful to R. Schneiter for providing the yeast strain *elo1*Δ *ole1*Δ, C. Holz for providing the pYEXTHS-BN plasmid, A. Bučánková for providing the reared bumblebees, J. Kindl for

dissecting bumblebee tissues, H. Hoffman for proof-reading of the manuscript. This study was financially supported by the Czech Science Foundation (203/09/1446), by the research project RVO: 613 88 963, and by Max Planck Society.

Appendix A. Supplementary data

Supplementary data related to this article can be found at http://dx.doi.org/10.1016/j.ibmb.2013.05.003.

References

Arrese, E.L., Canavoso, L.E., Jouni, Z.E., Pennington, J.E., Tsuchida, K., Wells, M.A., 2001. Lipid storage and mobilization in insects: current status and future directions. Insect Biochem. Mol. Biol. 31, 7–17.

Bergman, P., Bergström, G., 1997. Scent marking, scent origin, and species specificity in male premating behavior of two Scandinavian bumble bees. J. Chem. Ecol. 23, 1235–1251.

Bergström, G., Kullberg, B.J., Ställberg-Stenhagen, S., 1973. Studies on natural odoriferous compounds: VII. Recognition of two forms of *Bombus lucorum* L. (Hymenoptera, Apidae) by analysis of the volatile marking secretion from individual males. Zoon 1 (Suppl.1), 31–42.

Bertsch, A., Schweer, H., Titze, A., Tanaka, H., 2005. Male labial gland secretions and mitochondrial DNA markers support species status of *Bombus cryptarum* and *B. magnus* (*Hymenoptera, Apidae*). Insectes Soc. 52, 45–54.

Cahoon, E.B., Shanklin, J., Ohlrogge, J.B., 1992. Expression of a coriander desaturase results in petroselinic acid production in transgenic tobacco. Proc. Natl. Acad. Sci. USA 89, 11184–11188.

Castillo, C., Chen, H., Graves, C., Maisonnasse, A., Le Conte, Y., Plettner, E., 2012. Biosynthesis of ethyl oleate, a primer pheromone, in the honey bee (*Apis mellifera* L.). Insect Biochem. Mol. Biol. 42, 404–416.

Coppée, A., Terzo, M., Valterova, I., Rasmont, P., 2008. Intraspecific variation of the cephalic labial gland secretions in *Bombus terrestris* (L.) (Hymenoptera: Apidae). Chem. Biodiversity 5, 2654–2661.

Cvacka, J., Hovorka, O., Jiros, P., Kindl, J., Stránský, K., Valterová, I., 2006. Analysis of triacylglycerols in fat body of bumblebees by chromatographic methods. J. Chromatogr. A. 1101, 226–237.

Dallerac, R., Labeur, C., Jallon, J.M., Knipple, D.C., Roelofs, W.L., Wicker-Thomas, C., 2000. A Δ9 desaturase gene with a different substrate specificity is responsible for the cuticular diene hydrocarbon polymorphism in *Drosophila melanogaster*. Proc. Natl. Acad. Sci. USA 97, 9449–9454.

Diaz, A.R., Mansilla, M.C., Vila, A.J., De Mendoza, D., 2002. Membrane topology of the acyl-lipid desaturase from *Bacillus subtilis*. J. Biol. Chem. 277, 48099–48106.

Edgar, R.C., 2004. MUSCLE: multiple sequence alignment with high accuracy and high throughput. Nucleic Acids Res. 32, 1792–1797.

Eigenheer, A.L., Young, S., Blomquist, G.J., Borgeson, C.E., Tillman, J.A., Tittiger, C., 2002. Isolation and molecular characterization of *Musca domestica* delta-9 desaturase sequences. Insect Mol. Biol. 11, 533–542.

Fujii, T., Ito, K., Tatematsu, M., Shimada, T., Katsuma, S., Ishikawa, Y., 2011. Sex pheromone desaturase functioning in a primitive *Ostrinia moth* is cryptically conserved in congeners' genomes. Proc. Natl. Acad. Sci. USA, 108, 7102–7106.

Goulson, D., 2010. Bumblebees – Behaviour, Ecology and Conservation. Oxford University Press, New York, pp. 45–52.

Holz, C., Hesse, O., Bolotina, N., Stahl, U., Lang, C., 2002. A micro-scale process for high-throughput expression of cDNAs in the yeast *Saccharomyces cerevisiae*. Protein Expr. Purif. 25, 372–378.

Horne, I., Gibb, N., Damcevski, K., Glover, K., Haritos, V.S., 2010. Two conserved Z9-octadecanoic acid desaturases in the red flour beetle, *Tribolium castaneum*. Gene 468, 41–47.

Horňáková, D., Matoušková, P., Kindl, J., Valterová, I., Pichová, I., 2010. Selection of reference genes for real-time polymerase chain reaction analysis in tissues from *Bombus terrestris* and *Bombus lucorum* of different ages. Anal. Biochem. 397, 118–120.

Jones, D.T., Taylor, W.R., Thorton, J.M., 1992. The rapid generation of mutation data matrices from protein sequences. Comput. Appl. Biosci. 8, 275–282.

Knipple, D.C., Rosenfield, C.-L., Nielsen, R., You, K.M., Jeong, S.E., 2002. Evolution of the integral membrane desaturase gene family in moths and flies. Genetics 162, 1737–1752.

Krogh, A., Larsson, B., Von Heijne, G., Sonnhammer, E.L., 2001. Predicting transmembrane protein topology with a hidden Markov model: application to complete genomes. J. Mol. Biol. 305, 567–580.

Kullenberg, B., Bergström, G., Ställberg-Stenhagen, S., 1970. Volatile components of the cephalic marking secretion of male bumble bees. Acta Chem. Scand. 24, 1481–1485.

Kullenberg, B., Bergstrom, G., Bringer, B., Carlberg, B., Cederberg, B., 1973. Observations on scent marking by *Bombus* Latr. and *Psithyrus* Lep. males (Hym. Apidae) and localization of site of production of the secretion. Zoon 1 (Suppl.1), 23–30.

Lanne, B.S., Bergström, G., Wassgren, A.-B., Törnbäck, B., 1987. Biogenetic pattern of straight chain marking compounds in male bumble bees. Comp. Biochem. Physiol. 88, 631–636.

Lassance, J.-M., Liénard, M.A., Antony, B., Qian, S., Fujii, T., Tabata, J., Ishikawa, Y., Löfstedt, C., 2013. Functional consequences of sequence variation in the pheromone biosynthetic gene pgFAR for Ostrinia moths. Proc. Natl. Acad. Sci. USA 110, 3967–3972.

Liénard, M.A., Strandh, M., Hedenström, E., Johansson, T., Löfstedt, C., 2008. Key biosynthetic gene subfamily recruited for pheromone production prior to the extensive radiation of Lepidoptera. BMC Evol. Biol. 8, 270.

Liu, W., Jiao, H., O'Connor, M., Roelofs, W.L., 2002. Moth desaturase characterized that produces both Z and E isomers of Δ11-tetradecenoic acids. Insect Biochem. Mol. Biol. 32, 1489–1495.

Los, D.A., Murata, N., 1998. Structure and expression of fatty acid desaturases. Biochim. Biophys. Acta 1394, 3–15.

Luxová, A., Valterová, I., Stránský, K., Hovorka, O., Svatoš, A., 2003. Biosynthetic studies on marking pheromones of bumblebee males. Chemoecology 87, 81–87.

Man, W.C., Miyazaki, M., Chu, K., Ntambi, J.M., 2006. Membrane topology of mouse stearoyl-CoA desaturase 1. J. Biol. Chem. 281, 1251–1260.

Matoušková, P., Luxová, A., Matoušková, J., Jiroš, P., Svatoš, A., Valterová, I., Pichová, I., 2008. A Δ9 desaturase from *Bombus lucorum* males: investigation of the biosynthetic pathway of marking pheromones. ChemBioChem. 9, 2534–2541.

Mortazavi, A., Williams, B.A., McCue, K., Schaeffer, L., Wold, B., 2008. Mapping and quantifying mammalian transcriptomes by RNA-Seq. Nat. Methods 5, 621–628.

Moto, K., Yoshiga, T., Yamamoto, M., Takahashi, S., Okano, K., Ando, T., Nakata, T., Matsumoto, S., 2003. Pheromone gland-specific fatty-acyl reductase of the silkmoth, *Bombyx mori*. Proc. Natl. Acad. Sci. USA 100, 9156–9161.

Murata, T., Ariga, T., Araki, E., 1978. Determination of double bond positions of unsaturated fatty acids by a chemical ionization mass spectrometry computer system. J. Lipid Res. 19, 172–176.

Park, H.Y., Kim, M.S., Paek, A., Jeong, S.E., Knipple, D.C., 2008. An abundant acyl-CoA (Δ9) desaturase transcript in pheromone glands of the cabbage moth, *Mamestra brassicae*, encodes a catalytically inactive protein. Insect Biochem. Mol. Biol. 38, 581–595.

Rasmont, P., Terzo, M., Aytekin, A.M., Hines, H., Urbanova, K., Cahlikova, L., Valterova, I., 2005. Cephalic secretions of the bumblebee subgenus *Sibiricobombus* Vogt suggest *Bombus niveatus* Kriechbaumer and *Bombus vorticosus* Gerstaecker are conspecific (Hymenoptera, Apidae, *Bombus*). Apidologie 36, 571–584.

Riddervold, M.H., Tittiger, C., Blomquist, G.J., Borgeson, C.E., 2002. Biochemical and molecular characterizaton of house cricket (*Acheta domesticus*, Orthoptera: Gryllidae) Δ9 desaturase. Insect Biochem. Mol. Biol. 32, 1731–1740.

Roelofs, W.L., Rooney, A.P., 2003. Molecular genetics and evolution of pheromone biosynthesis in Lepidoptera. Proc. Natl. Acad. Sci. USA 100, 9179–9184.

Rooney, A.P., 2009. Evolution of moth sex pheromone desaturases. Ann. N.Y. Acad. Sci. 1170, 506–510.

Rozen, S., Skaletsky, H., 2000. Primer3 on the WWW for general users and for biologist programmers. Methods Mol. Biol. 132, 365–386.

Schlüter, P.M., Xu, S., Gagliardini, V., Whittle, E., Shanklin, J., Grossniklaus, U., Schiestl, F.P., 2011. Stearoyl-acyl carrier protein desaturases are associated with floral isolation in sexually deceptive orchids. Proc. Natl. Acad. Sci. USA 108, 5696–5701.

Schneiter, R., Tatzer, V., Gogg, G., Leitner, E., Kohlwein, S.D., 2000. Elo1p-dependent carboxy-terminal elongation of C14:1Δ9 to C16:1Δ11 fatty acids in *Saccharomyces cerevisiae*. J. Bacteriol. 182, 3655–3660.

Shanklin, J., Cahoon, E.B., 1998. Desaturation and related modifications of fatty acids. Annu. Rev. Plant Physiol. Plant Mol. Biol. 49, 611–641.

Shanklin, J., Whittle, E., Fox, B.G., 1994. Eight histidine residues are catalytically essential in a membrane-associated iron enzyme, stearoyl-CoA desaturase, and are conserved in alkane hydroxylase and xylene monooxygenase. Biochemistry 33, 12787–12794.

Stukey, J.E., McDonough, V.M., Martin, C.E., 1990. The *OLE1* gene of *Saccharomyces cerevisiae* encodes the Δ9 fatty acid desaturase and can be functionally replaced by the rat stearoyl-CoA desaturase gene. J. Biol. Chem. 265, 20144–20149.

Tamura, K., Peterson, D., Peterson, N., Stecher, G., Nei, M., Kumar, S., 2011. MEGA5: molecular evolutionary genetics analysis using maximum likelihood, evolutionary distance, and maximum parsimony methods. Mol. Biol. Evol. 28, 2731–2739.

Urbanová, K., Valterová, I., Hovorka, O., Kindl, J., 2001. Chemotaxonomical characterisation of males *Bombus lucorum* (Hymenptera: Apidae) collected in Czech Republic. Eur. J. Entomol. 127, 111–115.

Yen, C.-L.E., Stone, S.J., Koliwad, S., Harris, C., Farese, R.V., 2008. Thematic review series: glycerolipids. DGAT enzymes and triacylglycerol biosynthesis. J. Lipid Res. 49, 2283–2301.

Šobotník, J., Kalinová, B., Cahlíková, L., Weyda, F., Ptáček, V., Valterová, I., 2008. Age-dependent changes in structure and function of the male labial gland in *Bombus terrestris*. J. Insect Physiol. 54, 204–214.

Žáček, P., Prchalová, D., Tykva, R., Kindl, J., Vogel, H., Svatoš, A., Pichová, I., Valterová, I., 2013. De novo biosynthesis of sexual pheromone in the labial gland of bumblebee males. ChemBioChem. 14, 361–371.

Δ12-Fatty Acid Desaturase from *Candida parapsilosis* Is a Multifunctional Desaturase Producing a Range of Polyunsaturated and Hydroxylated Fatty Acids

Aleš Buček[1], Petra Matoušková[1], Hana Sychrová[2], Iva Pichová[1]*, Olga Hrušková-Heidingsfeldová[1]*

1 Institute of Organic Chemistry and Biochemistry, Academy of Sciences of the Czech Republic, Prague, Czech Republic, **2** Institute of Physiology, Academy of Sciences of the Czech Republic, Prague, Czech Republic

Abstract

Numerous Δ12-, Δ15- and multifunctional membrane fatty acid desaturases (FADs) have been identified in fungi, revealing great variability in the enzymatic specificities of FADs involved in biosynthesis of polyunsaturated fatty acids (PUFAs). Here, we report gene isolation and characterization of novel Δ12/Δ15- and Δ15-FADs named *Cp*Fad2 and *Cp*Fad3, respectively, from the opportunistic pathogenic yeast *Candida parapsilosis*. Overexpression of *Cp*Fad3 in *Saccharomyces cerevisiae* strains supplemented with linoleic acid (Δ9,Δ12-18:2) and hexadecadienoic acid (Δ9,Δ12-16:2) leads to accumulation of Δ15-PUFAs, *i.e.*, α-linolenic acid (Δ9,Δ12,Δ15-18:3) and hexadecatrienoic acid with an unusual terminal double bond (Δ9,Δ12,Δ15-16:3). *Cp*Fad2 produces a range of Δ12- and Δ15-PUFAs. The major products of *Cp*Fad2 are linoleic and hexadecadienoic acid (Δ9,Δ12-16:2), accompanied by α-linolenic acid and hexadecatrienoic acid (Δ9,Δ12,Δ15-16:3). Using GC/MS analysis of trimethylsilyl derivatives, we identified ricinoleic acid (12-hydroxy-9-octadecenoic acid) as an additional product of *Cp*FAD2. These results demonstrate that *Cp*FAD2 is a multifunctional FAD and indicate that detailed analysis of fatty acid derivatives might uncover a range of enzymatic selectivities in other Δ12-FADs from budding yeasts (Ascomycota: Saccharomycotina).

Citation: Buček A, Matoušková P, Sychrová H, Pichová I, Hrušková-Heidingsfeldová O (2014) Δ12-Fatty Acid Desaturase from *Candida parapsilosis* Is a Multifunctional Desaturase Producing a Range of Polyunsaturated and Hydroxylated Fatty Acids. PLoS ONE 9(3): e93322. doi:10.1371/journal.pone.0093322

Editor: Vishnu Chaturvedi, California Department of Public Health, United States of America

Received November 19, 2013; **Accepted** March 3, 2014; **Published** March 28, 2014

Funding: This study was funded by project TA01011461 from Technology Agency of the Czech Republic and by the research project RVO 613 88 963. The funders had no role in study design, data collection and analysis, decision to publish, or preparation of the manuscript.

Competing Interests: The authors have declared that no competing interests exist.

* E-mail: iva.pichova@uochb.cas.cz (IP); olga-hh@uochb.cas.cz (OHH)

Introduction

Unsaturated fatty acids (UFAs) play a key role in maintenance of optimal physical and biological properties of cell membranes [1]. UFAs are biosynthesized from saturated fatty acids by two evolutionary unrelated classes of fatty acid desaturases: soluble fatty acid desaturases, which are expressed exclusively in plant plastids, and membrane-bound fatty acid desaturases (subsequently referred to as FADs), which are widespread in eukaryotes and some prokaryotes [2].

FADs are highly specific towards their fatty acyl substrates (either acyl-CoA or acyl-lipid) and towards the position and geometric configuration of the newly introduced double bond. A range of desaturase regioselectivities dependent on the reference point used by FADs to position the introduced double bond has been described. The main regioselective modes are: (1) the double bond is introduced between specific carbon atoms counted from the carboxy terminus (ΔX) or (2) methyl terminus (ωX) of the fatty acyl substrate, and (3) a subsequent double bond is introduced a specific number of carbon atoms (usually three) counted from the pre-existing double bond (v+3) [3]. However, these FAD regioselectivities are not mutually exclusive, and Meesapyodsuk *et al.* [4] suggested assigning them primary and secondary modes to more precisely describe FAD regioselectivity. For example, multifunctional FADs preferentially producing Δ9,Δ12-18:2 and Δ9,Δ12-16:2 from Δ9-UFAs but also capable of producing minor amounts of Δ9,Δ12,Δ15-18:3 and Δ9,Δ12,Δ15-16:3 might be termed as v+3 (Δ12), indicating that the primary desaturase regioselectivity is v+3 and the preferred regioselectivity is Δ12. However, this nomenclature may require detailed information on FAD diagnostic substrates and products, which are often not available in the literature. Therefore, we will adhere to nomenclature designating FADs as Δ12- and/or Δ15-FADs.

In fungal species such as *Saccharomyces cerevisiae* or *Candida glabrata*, the main UFAs are Δ9-UFAs. By contrast, in numerous Basidiomycota, Zygomycota and Ascomycota fungal species, such as *Coprinus cinereus* [5], *Mortierella alpina* [6–8], *Fusarium moniliforme* [9], *Aspergillus nidulans* [10], *Pichia pastoris* [11,12], *Kluyveromyces lactis* [13], *Saccharomyces kluyveri* [14,15] and the majority of *Candida* species [16], Δ12- and Δ15-FADs can desaturate Δ9-UFAs to polyunsaturated fatty acids (PUFAs).

Bifunctional Δ12/Δ15-FADs have been characterized in Ascomycota [4,9,10,17], Basidiomycota [5] and the protozoon *Acanthamoeba castellan* [18]. Additionally, bi- or multifunctional FADs that had previously been identified as FADs with a single desaturase regioselectivity [8,19] were recently reported [20,21]. As a result of the similarity between desaturation and hydroxylation reaction pathways, FADs from different kingdoms additionally produce minor amounts of hydroxy fatty acids [22–24].

The role of Δ9-FADs in pathogenic *Candida* sp. has been demonstrated in *C. albicans*, in which partial repression of Ole1p

Δ9-FAD blocks hyphae and chlamydospore formation [25]. In *C. parapsilosis*, gene deletion of OLE1 impaired invasive growth, pseudohyphae formation and virulence in mice and increased susceptibility to macrophages and various stress factors such as SDS, salts and H_2O_2 [26].

The role of PUFAs is more elusive than that of Δ9-UFAs, and PUFAs are probably not essential under all growth conditions. Murayama *et al.* [27] demonstrated that the loss of PUFA production in *C. albicans via* targeted disruptions of the Δ12- and Δ15-FAD genes *Ca*FAD2 and *Ca*FAD3, respectively, did not lead to any changes in growth rate under low temperature, chlamydospore formation, hyphal formation or virulence under the conditions tested. In contrast, the hyphal form of *C. albicans* is enriched in PUFAs compared to the yeast form which suggests a specific role for PUFAs in *C. albicans* morphogenesis [28].

In this study, we isolated the coding regions *Cp*FAD2 and *Cp*FAD3, homologs of fungal Δ12- and Δ15-FADs, respectively, from *C. parapsilosis*, an emerging fungal pathogen [29]. We expressed these FADs in a *Saccharomyces cerevisiae* expression system and identified a broad range of novel polyunsaturated and hydroxylated FA products, including an unusual Δ9,Δ12,Δ15-16:3 with a terminal double bond.

Methods

Strains, media and growth conditions

Saccharomyces cerevisiae strain BY4741 (MATa his3Δ1 leu2Δ met15Δ ura3Δ; EUROSCARF, Germany) was cultivated in liquid medium lacking uracil (YNBglc-U: 0.67% yeast nitrogen base without amino acids, 2% glucose, supplemented with Brent supplement mix without uracil according to the manufacturer's instructions). In cultivation media, 2% glucose was used as the carbon source. Heterologous protein expression was induced in YNB-U media containing 2% galactose as the sole carbon source (YNBgal-U). When indicated, media were supplemented with 0.5 mM linoleic acid (Sigma-Aldrich), 0.25 mM hexadecadienoic acid (Δ9,Δ12-16:2; Larodan), 1% tergitol and 0.65 M NaCl. *C. parapsilosis* (clinical isolate P-69 obtained from the mycological collection of the Faculty of Medicine, Palacky University, Olomouc, Czech Republic) was cultivated prior to lipid extraction in YNBglc medium at 37°C until the culture reached a stationary growth phase.

Sequence and phylogenetic analysis

The assembly of shotgun reads of *C. parapsilosis* genome publicly available in Candida Genome database was searched using the BLAST tool (http://www.candidagenome.org/cgi-bin/compute/blast_clade.pl) with previously characterized Δ12- and Δ15-FADs as a query.

Amino acid sequences of FADs were aligned using the Muscle algorithm [30], and the phylogeny of FADs was reconstructed with MEGA5 software [31] by neighbor-joining method with calculated bootstrap support from 1,000 bootstrap replicates as a measure of statistical reliability. Desaturase topology was predicted using the programs TMHMM 2.0 [32] and HMMTOP [33]. Pairwise sequence alignment was performed using the EMBOSS Needle web-based tool (http://www.ebi.ac.uk/Tools/psa/emboss_needle/).

Known FAD sequences were retrieved from GenBank. The FAD sequences reported here were deposited into GenBank under accession numbers FN386265 and FN386266.

Heterologous expression in *Saccharomyces cerevisiae*

Total cellular DNA was extracted from *C. parapsilosis* strain CP-69 and served as a template for PCR amplification of the *Cp*FAD2 coding region using the following primers: *Cp*FAD2-5′ (CTG GAG CTC *ATG* TCT TCA GCC ACA ACT TC) and *Cp*FAD2-3′ (CTG CTC GAG *TTA* TTT CTC TTT CTT TGG GT) (*Sac*I and *Xho*I restriction sites are underlined; start and stop codons are italicized). The *Cp*FAD3 coding region was amplified using the primers *Cp*FAD3-5′ (CAG GAG CTC *ATG* AGT ACG GTC CAT GCA TC) and *Cp*FAD3-3′ (CTG CTC GAG *CTA* GTT TCT TGG TTT GAC AC). The resulting fragments were cloned into the vector pYES2 (Invitrogen) under control of the galactose-inducible *GAL1* promoter, generating plasmids *Cp*FAD2-pYES and *Cp*FAD3-pYES. The constructs were verified by sequencing.

S. cerevisiae strain BY4741 was transformed with *Cp*FAD2-pYES, *Cp*FAD3-pYES and empty pYES2 plasmid by electroporation. The resulting *Cp*FAD2, *Cp*FAD3 and Empty yeast strains were selected on YNBglc-U agar plates. Single colonies were inoculated into 20 ml of YNBglc-U and cultivated in a rotary shaker (30°C, 220 RPM). At the early stationary phase, yeast cells were harvested by centrifugation (3 min, 1000 g, 20°C), washed with 20 ml of YNBgal-U and transferred into 20 ml of fresh YNBgal-U (optionally supplemented with linoleic acid, hexadecadienoic acid and tergitol). Yeast strains were cultivated for 72 h.

Lipid extraction and fatty acid methyl ester preparation

Yeast cells were harvested and total cellular lipids were extracted as described by Buček *et al.* [34], and fatty acid methyl esters (FAMEs) were prepared according to Matoušková *et al.* [35]. The resulting FAMEs were extracted with hexane (600 µl), and the extracts were analyzed by gas chromatography coupled to mass spectrometry (GC/MS) using the conditions described below. The relative abundances of individual fatty acids were calculated from the peak areas in GC/MS total ion current chromatograms.

DMOX derivatization

Fatty acid 4,4-dimethyloxazoline (DMOX) derivatives were prepared from FAME extracts according to Fay and Richli [36]. Briefly, hexane solvent was evaporated under a stream of nitrogen, and FAMEs were heated at 180°C overnight with 0.5 g 2-amino-2-methylpropanol. After cooling, the DMOX derivatives were dissolved in 5 ml dichloromethane and washed three times with 2 ml distilled water. The dichloromethane phase was dried over anhydrous $MgSO_4$, evaporated under a stream of nitrogen and redissolved in hexane. DMOX derivatives were analyzed using GC/MS under the conditions described below and identified by comparing their mass spectra to previously described spectra and using inferred empirical rules [37].

TMS derivatization

Hydroxy FAs were analyzed in the form of their trimethylsilyl (TMS) derivatives by treating the FAME extracts with excess *N,O*-bis(trimethylsilyl)acetamide (Sigma-Aldrich) in acetonitrile (10 min, 40°C), evaporated under a gentle stream of N_2 and redissolved in chloroform [24]. Freshly prepared TMS derivatives were analyzed using GC/MS under the conditions described below, and their mass spectra and retention behavior were compared to the previously published mass spectra of FAME TMS derivatives [24] and to that of a TMS derivative prepared from 1 mg methyl ricinoleate (methyl 12-hydroxyoleate, Sigma-Aldrich).

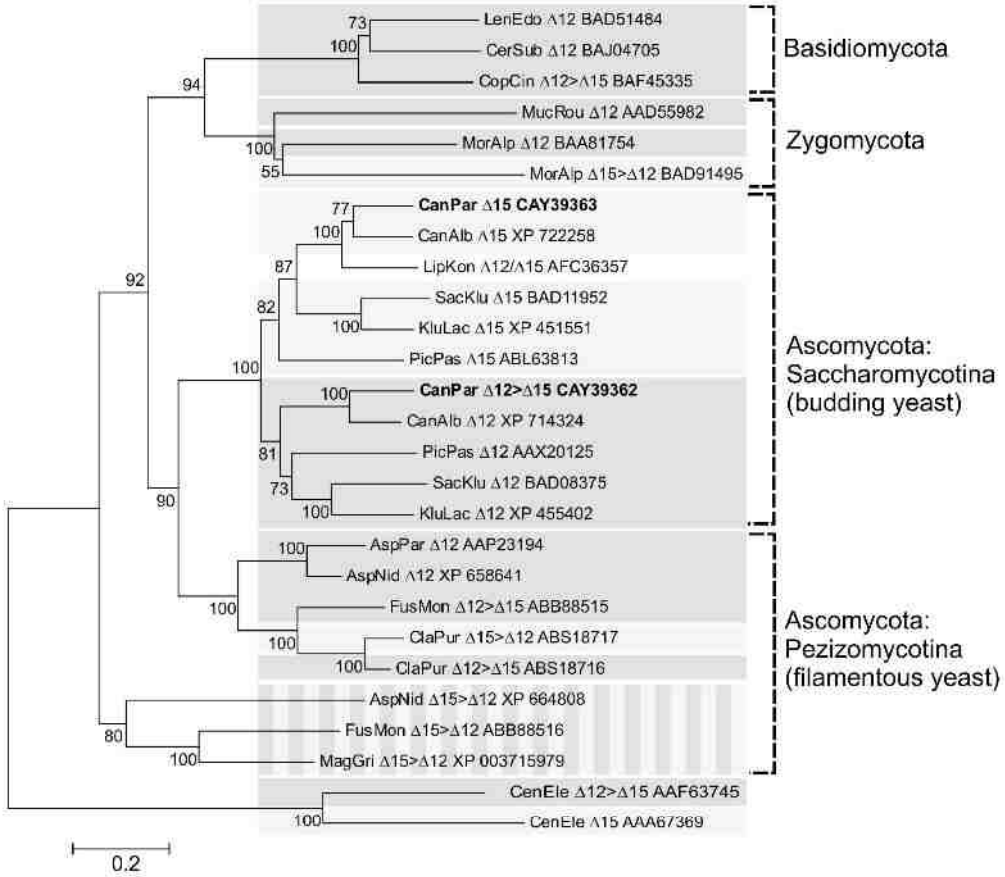

Figure 1. Phylogenetic tree of fungal Δ12- and Δ15-FADs. The species name is abbreviated and followed by experimentally determined desaturase regioselectivity and GenBank protein accession number. For multifunctional FADs, regioselectivity is indicated by ">" (e.g., Δ12>Δ15 indicates a preference for Δ12-desaturation) if available in the literature. Dark grey background denotes Δ12-FADs and Δ12>Δ15-FADs, light grey background denotes Δ15-FADs and Δ15>Δ12-FADs and striped background highlights a clade of bifunctional Δ15>Δ12-FADs. *Cp*FAD2 and *Cp*FAD3 are highlighted in bold. Δ12-FAD and Δ15-FAD from the nematode *Caenorhabditis elegans* were added as an outgroup.
doi:10.1371/journal.pone.0093322.g001

GC/MS analysis

The FAME extracts and respective DMOX and TMS derivatives were analyzed with a 7890A gas chromatograph coupled to a 5975C mass spectrometer, equipped with electron ionisation and quadruple analyser (Agilent Technologies, Santa Clara, CA, USA) using DB-5MS or DB-WAX capillary columns (both J&W Scientific, Folsom, CA, USA; 30 m×0.25 mm, film thickness 0.25 mm); the electron ionisation was set at 70 eV.

Conditions for the analysis of FAMEs and DMOX derivatives were as follows: carrier gas, He: 1 ml/min; 10:1 split ratio, injection volume 2 µl; injector temperature 220°C; thermal gradient 140°C to 245°C at 3°C/min, then at 8°C/min to 280°C and temperature held for 5 min. The temperature program was terminated at 245°C and held at this temperature for 10 min when the DB-WAX column was used. The TMS derivatives were analyzed on a DB-5MS column using the following thermal gradient: 50°C to 140°C at 10°C/min, then 1°C/min to 198°C, 3°C/min to 320°C and temperature held for 3 min.

Results

Sequence and phylogenetic analysis of *Cp*FAD2 and *Cp*FAD3 open reading frames

In the genome database of *C. parapsilosis* [38], we found two open reading frames (ORFs) homologous to fungal FAD2 and FAD3 desaturases and termed them *Cp*FAD2 and *Cp*FAD3, respectively. *Cp*Fad2 shares high amino acid (aa) sequence identity with *C. albicans* Δ12-FAD (80%) [27] and other Δ12-FADs from budding yeasts (Saccharomycotina) (>59%). *Cp*Fad2 shares lower sequence identity with Δ12-FADs from filamentous Ascomycota (Pezizomycotina) (>44%), Basidiomycota (>33%) and Zygomycota (>32%). *Cp*FAD3 shares high sequence identity (79%) with Δ15-FAD from *C. albicans* and with Δ15-FADs from other budding yeasts (61%). *Cp*FAD2 also shares lower sequence identity with bifunctional Δ15>Δ12-FADs from filamentous Ascomycota (> 36%) and Zygomycota *Mortierella alpina* (34%).

The *Cp*FAD2 sequence encodes a 426-aa putative polypeptide; *Cp*FAD3 encodes a 432-aa putative polypeptide. *Cp*Fad2 and *Cp*Fad3 share 57% identity and 74% similarity and contain up to six predicted transmembrane helices and a tripartite conserved

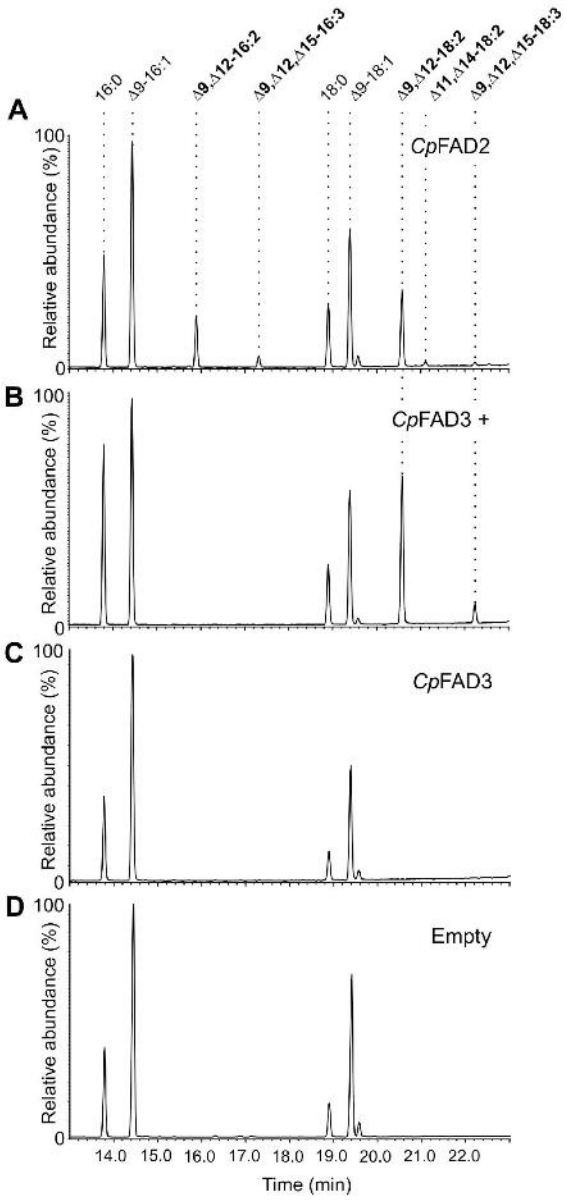

Figure 2. GC chromatograms of FAME extracts from *S. cerevisiae* strains. Analysis of extracts from (**A**) strain expressing *Cp*Fad2, (**B**) strain expressing *Cp*Fad3 grown in media supplemented with 0.5 mM linoleic acid and 1% tergitol, (**C**) strain expressing *Cp*Fad3 and (**D**) strain bearing empty pYES2 plasmid.
doi:10.1371/journal.pone.0093322.g002

histidine-rich motif $HX_{3\ 4}H$, $HX_{2\ 3}HH$, $(H/Q)X_{2\ 3}HH$, which indicates that these proteins belong to a non-heme iron enzyme family [3] (Fig. S1).

In the reconstructed phylogenetic tree of functionally characterized fungal Δ12- and Δ15-FADs, all FADs cluster into clades according to the class or subphylum of the source organism, with the exception of FADs from the filamentous yeasts *Aspergillus nidulans*, *Fusarium moniliforme* and *Magnaporthe grisea*, which create a group of multifunctional Δ15/Δ12 FADs [9]. Within the clades, FADs cluster generally into "Δ12-FAD" subclades and "Δ15-FAD" subclades. *Cp*Fad2 clusters within a subclade of strictly monofunctional Δ12-FADs, whereas *Cp*Fad3 belongs to a subclade of Δ15-FADs (Fig. 1.).

Functional characterization of *Cp*FAD2 and *Cp*FAD3 in *S. cerevisiae*

We designed two pairs of specific primers to amplify the *Cp*FAD2 and *Cp*FAD3 ORFs, and we obtained a single amplicon for each primer pair from genomic DNA isolated from *C. parapsilosis*. Sequencing of *Cp*FAD2 and *Cp*FAD3 confirmed that the nucleotide sequences of the amplified coding regions are identical to those obtained from the *C. parapsilosis* genome database.

The sequence comparison of *Cp*Fad2 and *Cp*Fad3 with previously characterized FADs strongly suggests that *Cp*Fad2 is a Δ12-FAD, whereas *Cp*Fad3 is a Δ15-FAD. However, the homology-based functional annotation of FADs may fail to predict FAD substrate specificity [39] or regioselectivity [14]. To experimentally determine the specificities and regioselectivities of *Cp*Fad2 and *Cp*Fad3, we cloned their coding regions into the pYES2 vector under control of a galactose-inducible promoter. We transformed the resulting plasmids into *S. cerevisiae*, generating the *Cp*FAD2 and *Cp*FAD3 strains.

The total lipidic extracts of galactose-induced *Cp*FAD2 and *Cp*FAD3 strains were transesterified, and the resulting fatty acid methyl esters (FAMEs) were compared to the FAME extract from a control strain transformed with an empty plasmid (Empty strain).

In the FAME extract from the induced *Cp*FAD2 strain, we detected multiple PUFAs that were not present in the FAME extract from the control strain (Fig. 2 and Table 1). The double bond position of all detected PUFAs was confirmed by the presence of characteristic MS fragment ions of DMOX derivatives (Fig. 3). In the *Cp*FAD2 strain, the most abundant novel PUFAs were linoleic acid (Δ9,Δ12-18:2; 11.88% ± 0.99%) and hexadecadienoic acid (Δ9,Δ12-16:2; 5.25% ± 0.65%). Traces of an octadecadienoic acid isomer with a characteristic 12 atomic mass unit gap between m/z 224 to 236 and 264 to 276 were detected, which is indicative of a Δ11,Δ14 double bond position (Fig. S2). We presume that Δ11,Δ14-18:2 is an elongation product of Δ9,Δ12-16:2. Unexpectedly, we also detected α-linolenic acid (Δ9,Δ12,Δ15-18:3; 0.12% ± 0.11%) in the *Cp*FAD2 strain, which indicates that the α-linolenic acid is synthesized from linoleic acid *via* minor Δ15-desaturase activity of *Cp*FAD2 desaturase (Fig. 2).

Additionally, a hexadecatrienoate (0.77% ± 0.09%) with double bonds in position Δ9 and Δ12 and a third double bond in either the Δ14- or Δ15-position was identified in the *Cp*FAD2 strain (Fig. 2). The DMOX derivatives of FAMEs with terminal double bonds do not produce the characteristic fragmentation pattern exhibiting a 12 atomic mass unit gap [40]. However, we could unambiguously identify the triunsaturated product of *Cp*Fad2 as Δ9,Δ12,Δ15-16:3 with terminal (n-1) double bond by comparing its spectrum to that of Δ9,Δ12,Δ15-16:3 methylester [41] (Fig. S3) and to the mass spectrum of a previously described DMOX derivative of Δ9,Δ12,Δ15-16:3 [18,21] (Fig. 3B). To confirm the production of Δ9,Δ12,Δ15-16:3 *via* desaturation of Δ9,Δ12-16:2, the *Cp*FAD2 strain was supplemented with Δ9,Δ12-16:2. The increase in relative abundance of Δ9,Δ12,Δ15-16:3 in the supplemented *Cp*FAD2 strain indicated that Δ9,Δ12,Δ15-16:3 is produced by Δ15-desaturation (Fig. 4B, C).

In the *Cp*FAD3 strain, supplementing the cultivation medium with linoleic acid led to production of α-linolenic acid (3.62% ± 0.15%). No polyunsaturated products were detected in the

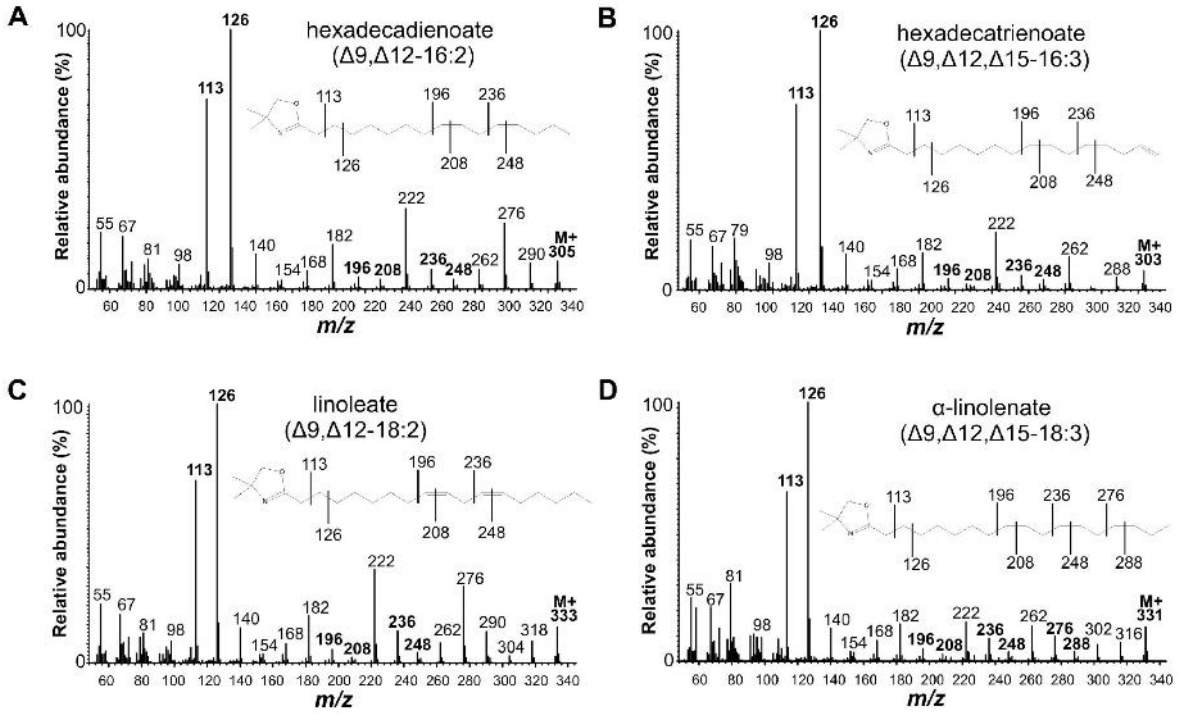

Figure 3. Mass spectra of DMOX derivatives of PUFAs detected in FAME extracts from *Cp*FAD2 and *Cp*FAD3 yeast strains. (**A**) Δ9,Δ12-16:2; (**B**) Δ9,Δ12,Δ15-16:3; (**C**) Δ9,Δ12-18:2; (**D**) Δ9,Δ12,Δ15-18:3. Characteristic fragments are highlighted and fragmentation patterns of DMOX derivatives are shown.
doi:10.1371/journal.pone.0093322.g003

*Cp*FAD3 strain cultivated without PUFA supplementation (Fig. 2 and Table 1). Surprisingly, supplementing the *Cp*FAD3 cultivation medium with Δ9,Δ12-16:2 led to production of Δ9,Δ12,Δ15-16:3 (Fig. 4D). To rule out the possible interference of yeast Δ9-FAD in the metabolism of Δ9,Δ12-16:2, the Empty strain was also supplemented with Δ9,Δ12-16:2. GC/MS analysis confirmed that Δ9,Δ12-16:2 is not desaturated to hexadecatrienoic acid in the Empty strain (Fig. 4A).

To determine the distribution of novel PUFAs in individual lipid classes, the total lipidic extract was analyzed using liquid chromatography with mass spectrometric analysis. The preliminary data indicates that PUFAs are distributed in phospholipids, *i.e.*, phosphatidylserine, phosphatidylethanolamine, phosphatidylcholine, and triacylglycerols (data not shown). We have also investigated the effect of accumulation of PUFAs in the *Cp*FAD2 and *Cp*FAD3 strains on their growth rate and tolerance to alkali-

Table 1. Relative abundances of fatty acids in FAME extracts of total cellular lipids from yeast strains.

	Fatty acid composition (%)				
Fatty acid	**Empty**	**Empty+**	***Cp*FAD2**	***Cp*FAD3**	***Cp*FAD3+**
16:0	27.22 ± 0.98	24.64 ± 1.01	27.04 ± 0.12	29.32 ± 0.58	25.84 ± 0.56
Δ9-16:1	41.99 ± 1.15	5.07 ± 0.06	29.71 ± 0.10	36.56 ± 0.48	3.45 ± 0.74
Δ9, Δ12-16:2	n.d.	n.d.	5.25 ± 0.65	n.d.	n.d.
Δ9, Δ12, Δ15-16:3	n.d.	n.d.	0.77 ± 0.09	n.d.	n.d.
18:0	6.41 ± 0.51	6.21 ± 1.06	8.97 ± 0.30	8.72 ± 0.36	8.23 ± 0.61
Δ9-18:1	24.38 ± 1.07	2.72 ± 0.26	16.26 ± 1.41	25.41 ± 0.43	2.74 ± 0.41
Δ9, Δ12-18:2	n.d.	61.36 ± 1.99	11.88 ± 0.99	n.d.	52.79 ± 1.15
Δ11, Δ14-18:2	n.d.	n.d.	0.35 ± 0.01	n.d.	n.d.
Δ9, Δ12, Δ15-18:3	n.d.	n.d.	0.12 ± 0.11	n.d.	6.95 ± 0.99

The relative amount of fatty acids is expressed as a percentage of total fatty acid methyl esters. Strains supplemented with 0.5 mM linoleic acid and 1% tergitol are marked with "+". Values represent means of three cultivations ± standard deviation. n.d.: FAME not detected.
doi:10.1371/journal.pone.0093322.t001

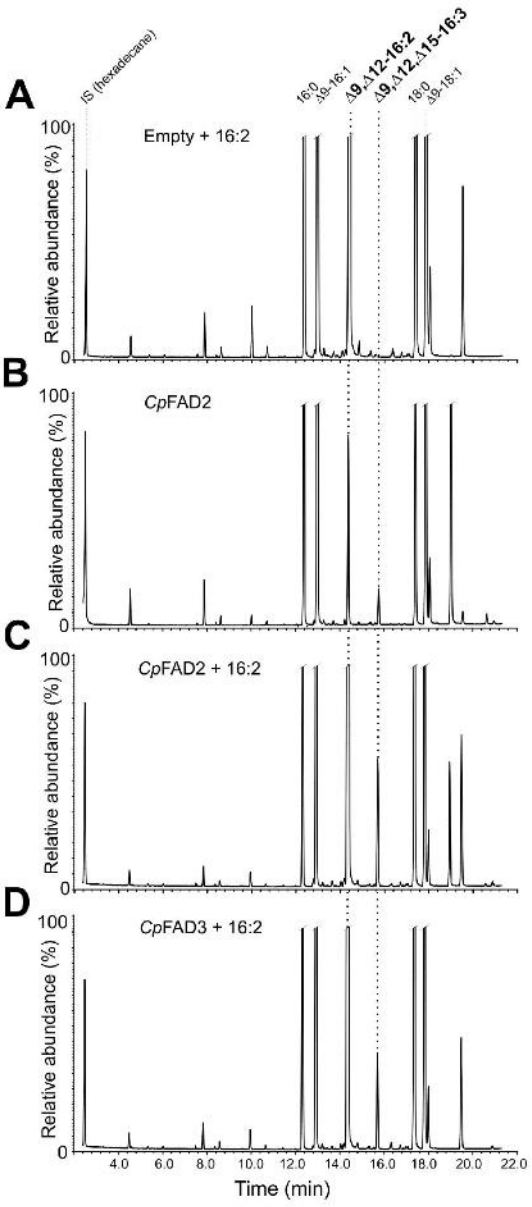

Figure 4. GC chromatograms of FAME extracts from yeasts supplemented with hexadecadienoic acid (Δ9,Δ12-16:2). GC/MS analysis of FAME extracts from (**A**) Empty strain supplemented with hexadecadienoic acid (Δ9,Δ12-16:2), (**B**) *Cp*FAD2 strain, (**C**) *Cp*FAD2 strain supplemented with Δ9,Δ12-16:2 and (**D**) *Cp*FAD3 strain supplemented with Δ9,Δ12-16:2. Hexane containing internal standard (hexadecane at concentration of 20 µg/ml) was used in preparation of all extracts.
doi:10.1371/journal.pone.0093322.g004

metal cations. When compared to the Empty strain, we observed a decreased growth rate for yeasts expressing *Cp*FAD2 on YNBgal-U agar plates (Fig. S4B). The decreased growth rate of the *Cp*FAD2 strain became even more prominent on YNBgal-U containing 0.65 M NaCl (Fig. S4C). The growth rate of the *Cp*FAD3 strain on

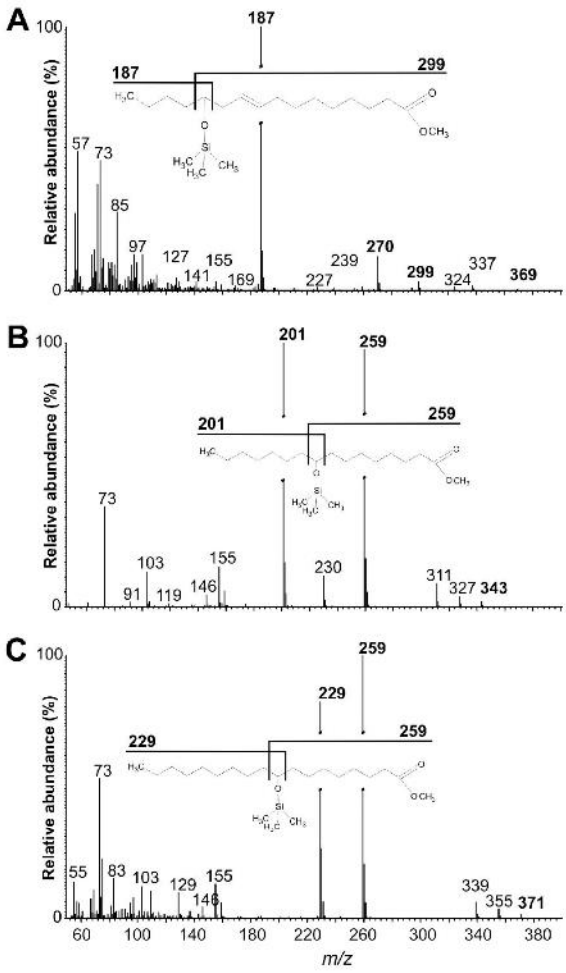

Figure 5. Mass spectra of TMS derivatives of hydroxy fatty acid methyl esters. (**A**) TMS-methyl ricinoleate detected in FAME extracts from *Cp*FAD2 yeast strain. (**B**) TMS- methyl hydroxypalmitate detected in all yeast strains. (**C**) TMS-methyl hydroxystearate detected in all yeast strains. Characteristic fragments are highlighted in bold, and fragmentation patterns of TMS derivatives are shown above the spectra.
doi:10.1371/journal.pone.0093322.g005

YNBgal-U or YNBgal-U supplemented with linoleic acid was unaltered compared to that of the Empty strain (Fig. S4B, D).

Hydroxylation activity of *Cp*Fad2 and *Cp*Fad3

To determine whether *Cp*Fad2 and *Cp*Fad3 are capable of FA hydroxylation, we treated the FAME extracts with *N,O*-bis(trimethylsilyl)acetamide to convert hydroxy FAMEs to their corresponding trimethylsilyl-FAMEs, which exhibit better chromatographic properties and provide MS fragment ions characteristic of particular TMS group locations [42]. Trace amounts of TMS derivatives of methyl 9-hydroxypalmitic acid (MS fragment ions at m/z 201 and 259) and methyl 9-hydroxystearic acid (MS fragment ions at m/z 229 and 259) were detected in all transformed yeast strains (Fig. 5, S5 and Table 2), providing evidence of the intrinsic Δ9-fatty acid hydroxylase activity of yeast Δ9-FAD Ole1p [22,24]. Notably, in the *Cp*FAD2 strain, an additional TMS derivative with low abundance (0.10% ± 0.02%) was detected (Table 2). This was

Table 2. Relative abundances of TMS derivatives of hydroxy FAs in FAME extracts from *Cp*FAD2, *Cp*FAD3 and Empty strains.

	TMS-derivative composition (%)				
TMS-derivative	**Empty**	**Empty+**	***Cp*FAD2**	***Cp*FAD3**	***Cp*FAD3+**
TMS-methy hydroxypalmitate	0.09 ± 0.01	0.05 ± 0.01	0.10 ± 0.03	0.09 ± 0.01	0.04 ± 0.01
TMS-methyl ricinoleate	n.d.	n.d.	0.10 ± 0.02	n.d.	n.d.
TMS-methyl hydroxystearate	0.06 ± 0.00	0.02 ± 0.00	0.09 ± 0.00	0.07 ± 0.01	0.02 ± 0.00

The relative amount of FAME-TMS derivatives is expressed as a percentage of total fatty acid methyl esters. Strains supplemented with 0.5 mM linoleic acid and 1% tergitol are marked with "+". Values represent means of three cultivations ± standard deviation. n.d.: TMS-derivative not detected.
doi:10.1371/journal.pone.0093322.t002

determined to be a TMS derivative of methyl ricinoleate (methyl 12-hydroxyoleate) based on its retention time, which was identical to that of TMS derivative of methyl ricinoleate standard, and on the presence of characteristic fragment ions, namely (M-15) ion at m/z 369 and ions at m/z 187, 270 and 299 (Fig. 5A). This observation indicates that *Cp*FAD2 exhibits 12-hydroxylation activity.

PUFA content in *C. parapsilosis*

Although the relative abundance of linoleic acid in *C. parapsilosis* (22.18%) was higher than that in the *Cp*FAD2 *S. cerevisiae* strain (11.88%), we detected only trace amounts of Δ9,Δ12-16:2 (0.04%) in *C. parapsilosis* in contrast to moderately abundant Δ9,Δ12-16:2 (5.25%) in the *Cp*FAD2 strain. Notably, Δ9,Δ12,Δ15-16:3 was completely absent in *C. parapsilosis* under the conditions tested (Table 3). No additional PUFAs were detected under low cultivation temperatures (25°C or 30°C) (data not shown).

Discussion

Fungal FAD research is largely motivated by the search for novel FADs that could be used in metabolic engineering of microorganisms to produce PUFAs and other valuable UFAs on an industrial scale [43,44]. Additionally, desaturation, as a part of fungal fatty acid metabolism, has been shown to play a crucial role in the growth and morphogenesis of pathogenic yeast species in plants and humans. Therefore, FADs have been suggested as potential targets for antifungal drugs [25–27,45,46].

Table 3. Relative abundance of fatty acids in FAME extracts from *C. parapsilosis*.

	Fatty acid composition (%)
Fatty acid	***C.parapsilosis***
16:0	12.54 ± 0.07
Δ9-16:1	3.38 ± 0.04
Δ9,Δ12-16:2	0.05 ± 0.01
Δ9,Δ12,Δ15-16:3	n.d.
18:0	4.31 ± 0.09
Δ9-18:1	54.96 ± 0.40
Δ9,Δ12-18:2	22.89 ± 0.15
Δ9,Δ12,Δ15-18:3	1.90 ± 0.24

The relative amount of fatty acids is expressed as a percentage of total fatty acid methyl esters. Values represent means of three cultivations ± standard deviation. n.d.: FAME not detected.
doi:10.1371/journal.pone.0093322.t003

Nguyen *et al.* [26] described the role of Δ9-FAD in the pathobiology of *C. parapsilosis*, a fungal pathogen that forms persistent biofilms on implanted medical devices such as catheters [29]. In addition to saturated and monounsaturated fatty acids, *C. parapsilosis* cellular lipids contain a major fraction of PUFAs, suggesting activity of Δ12- and Δ15-FADs [16]. In this study, we identified and characterized *Cp*Fad2 and *Cp*Fad3 desaturases responsible for production of PUFAs in *C. parapsilosis*.

Sequence analysis of *Cp*Fad2 and *Cp*Fad3 using TMHMM 2.0 and HMMTOP topology prediction algorithms indicated the presence of more than four transmembrane helices. The proposed topology, however, does not satisfy the requirement of arrangement of conserved histidine motifs on a common, cytosolic ER membrane face [47,48] (Fig. S1). Therefore, the third and fourth transmembrane helix likely represents a hydrophobic region peripherally associated with an ER membrane. This topology was previously proposed by Hoffmann *et al.* for Δ12-FAD and a bifunctional Δ12/Δ15-FAD from *Aspergillus nidulans* [10]. Alternatively, some of the additional TM helices might be correctly predicted and play a role in binding the acyl-lipid substrate, as hypothesized by Diaz *et al.* [49].

Several identified FADs can produce unusual terminally unsaturated Δ9,Δ12,Δ15-16:3 fatty acids, including FADs from the protozoon *Acanthamoeba castellanii* [18], the basidiomycete fungus *Coprinus cinereus* [5], the ascomycete filamentous fungus *Claviceps purpurea* [4], and the ascomycete budding yeast *Lipomyces kononenkoae* [17]. Δ9,Δ12,Δ15-16:3 also has been identified as an initially undiscerned product of Δ15-FAD from the zygomycete fungus *Mortierella alpina* [21] and Δ12-FAD from the nematode *Caenorhabditis elegans* [20].

Previously, Δ9,Δ12,Δ15-16:3 was not detected as a product of *Ca*Fad2 heterologously expressed in *S. cerevisiae* under control of the *GAL1* promoter. *Ca*Fad2 is a Δ12-FAD from *C. albicans*, which can produce Δ9,Δ12-16:2 and Δ9,Δ12-18:2 fatty acids [27]. However, the presence of Δ9,Δ12,Δ15-16:3 might be easily missed due to its overall low abundance or due to the low abundance of the molecular ion at m/z 264 and low abundance of fragments at m/z 74 and 87 characteristic of FAMEs (Fig. S3).

Production of α-linolenic, hexadecatrienoic (Δ9,Δ12,Δ15-16:3) and ricinoleic acid (12-hydroxyoleate) by *Cp*Fad2 suggests that *Cp*Fad2 is a bifunctional Δ12/Δ15-FAD. The Δ15-desaturase activity of Δ12-FAD from budding yeast (Saccharomycotina) has been reported only by Yan *et al.* [17], and the hydroxylase activity has not been investigated. Damude *et al.* suggested that Δ15-FADs independently evolved from ancestral Δ12-FADs multiple times [9]. The facile evolutionary shift between Δ12- and Δ15-FAD regioselectivities was further supported by the effect of site-directed mutagenesis of a single amino acid residue [4] and by domain-swapping experiments [4,10]. Analogously, one to four amino acid mutations were found to be sufficient to convert plant Δ12-FAD

into a bifunctional Δ12-FAD/hydroxylase [22,50]. Based on these observations and our current results, we hypothesize that minor Δ15-desaturase regioselectivity and hydroxylase activity might be present in numerous functionally characterized Δ12-FADs from budding yeasts, including *Ca*Fad2 from *C. albicans* [27]. The fact that minor PUFA and hydroxylated products were rarely detected in previously described Δ12-FADs from budding yeast might be caused by a low level of desaturase expression under the experimental conditions, by a low level of accumulation of PUFAs and hydroxylated fatty acids or by the low sensitivity of the FAME analysis procedure. The reason underlying the absence of specific Δ15-hydroxylated FAs in *Cp*FAD3 strain supplemented with linoleic acid might be the absence of *Cp*Fad3 Δ15-hydroxylase activity and/or the overall low enzymatic activity of *Cp*Fad3 compared to *Cp*Fad2 in our expression system.

Based on the range of observed desaturase specificities of *Cp*Fad2 [its capability of introducing a double bond at the Δ15 (ω1) position in Δ9,Δ12,Δ15-16:3 and Δ15(ω3) position in Δ9,Δ12,Δ15-18:3 and the lack of Δ9,Δ15-18:2 products], we propose that the primary regioselective mode of *Cp*Fad2 is v+3 and the secondary mode is Δ12. This would imply, in accordance with the FAD regioselectivity classification described by Meesapyodsuk *et al.* [4], that the preexisting double bond serves as a reference point for positioning of the introduced double bond and that the Δ12-position is preferred over the Δ15-position.

The *Cp*FAD3 strain produced Δ9,Δ12,Δ15-18:3 and Δ9,Δ12,Δ15-16:3 when supplemented with Δ9,Δ12-18:2 and Δ9,Δ12-16:2 PUFAs, respectively. The complete absence of novel PUFAs in the *Cp*FAD3 strain cultivated without addition of linoleic acid or hexadecadienoic acid (ω6 substrates) indicates that *Cp*FAD3 cannot desaturate the naturally present Δ9-FAs, in contrast to, for example, ω3-FADs from *Caenorhabditis elegans* [51] or *Saccharomyces kluyveri* [52]. Together, this data indicates that *Cp*Fad3 exhibits Δ15-regioselectivity requiring a preexisting Δ12-double bond and is capable of introducing a terminal double bond.

Overexpression of Δ12- and Δ15(ω3)-FADs in *S. cerevisiae* provides a tool to study the influence of PUFAs on yeast physiology [19,53–55]. The PUFAs were present in phospholipid fraction of the *Cp*FAD2 and *Cp*FAD3 strain supplemented with linoleic acid, suggesting that they might influence the membrane properties and the yeast phenotype. However, we did not observe any increase in tolerance to NaCl, which has been observed in yeast strains producing PUFAs [55]. A decreased growth rate of yeasts heterologously expressing Δ12-FADs was previously attributed to impairment of tryptophan uptake [54]. Although we employed the BY4741 yeast strain which is not auxotrophic for tryptophan, the modified structure and physical properties of yeast cell membranes containing PUFAs might affect the properties of numerous cell membrane proteins and result in a decreased growth rate.

In *C. parapsilosis*, the low amount or complete absence of C16 PUFAs and low amount of palmitoleic acid is in general agreement with the results of a previous study by Moss *et al.* [16] that describes the fatty acid composition of various *Candida* species. Together, these data suggests that in *Candida* species, C16 PUFAs do not accumulate. The low content of C16 PUFAs might be a consequence of a low amount of their precursor, palmitoleic acid. Alternatively, overexpression of *Cp*Fad2 under control of the *GAL1* promoter might result in higher expression and therefore higher desaturase activity of *Cp*Fad2 in *S. cerevisiae*, as compared to the activity of *Cp*Fad2 in *C. parapsilosis*.

Taken together, this study provides further evidence that, despite the growing database of functionally characterized FADs, detailed characterization of FADs by mass spectrometry analysis of fatty acid derivatives can reveal surprising desaturase specificities that cannot be inferred solely from sequence comparisons.

Supporting Information

Figure S1 Amino acid sequence alignment of *Cp*Fad2 and *Cp*Fad3. Three conserved histidine-rich regions (H1 H3) are marked by boxes. Predicted transmembrane domains for *Cp*Fad2 and *Cp*Fad3 are indicated by bars above or below the sequence, respectively. The consensus transmembrane region predicted by both HMMTOP and TMHMM 2.0 algorithms are indicated by solid bars; transmembrane regions predicted by only one algorithm are indicated by dashed bars. Identical residues are indicated by a black background, similar residues by a grey background.
(TIF)

Figure S2 Mass spectra of DMOX derivative of Δ11,Δ14-18:2-methylester detected in FAME extract from *Cp*FAD2 yeast strain. Characteristic fragments are highlighted, and the fragmentation pattern of the DMOX derivative is shown above the spectra.
(TIF)

Figure S3 Mass spectra of Δ9,Δ12,Δ15-16:3-methylester identified in FAME extract from *Cp*FAD2 yeast strain.
(TIF)

Figure S4 Comparison of growth rates of *Cp*FAD2, *Cp*FAD3 and Empty yeast strains. Yeast suspensions were spotted on (**A**) YNBglc-U agar plates, which repress heterologous protein expression, (**B**) YNBgal-U agar plates, (**C**) YNBgal-U agar plates containing 0.65 M NaCl and (**D**) YNBgal-U agar plates containing 1% tergitol and 0.5 mM linoleic acid. Prior to plating on solid media, yeast strains were grown on YNBglc-U agar plates and incubated overnight at 4°C. The cells then were resuspended in sterile water to an OD_{600} of 1.0. Serial 10-fold dilutions were spotted on the YNB agar plates using a replica plater. The agar plates were incubated at 30°C for 3 days and photographed. Representative images are shown.
(TIF)

Figure S5 Extracted ion chromatograms of TMS derivatives of hydroxy FAMEs. TMS derivatives of FAME extracts from the *Cp*FAD2 strain, *Cp*FAD3 strain supplemented with linoleic acid and Empty strain are displayed in ion chromatograms extracted at m/z values characteristic for individual TMS-hydroxy FAMEs. (**A**) Ion chromatograms extracted at m/z 201 and 259 characteristic for TMS-methyl hydroxypalmitate, (**B**) ion chromatograms extracted at m/z 229 and 259 characteristic for TMS-methyl hydroxystearate and (**C**) ion chromatograms extracted at m/z 187 and 299 characteristic for TMS-methyl ricinoleate.
(TIF)

Acknowledgments

We thank Dr. Petr Hamal (University Hospital in Olomouc, Czech Republic) for providing the clinical isolate of *C. parapsilosis* and H. Hoffman for proofreading of the manuscript.

Author Contributions

Conceived and designed the experiments: AB IP PM OHH HS. Performed the experiments: AB. Analyzed the data: AB. Contributed reagents/materials/analysis tools: IP HS. Wrote the paper: AB IP OHH.

References

1. Aguilar PS, de Mendoza D (2006) Control of fatty acid desaturation: a mechanism conserved from bacteria to humans. Mol Microbiol 62: 1507–1514.
2. Sperling P, Ternes P, Zank TK, Heinz E (2003) The evolution of desaturases. Prostaglandins Leukot Essent Fatty Acids 68: 73–95.
3. Shanklin J, Cahoon EB (1998) Desaturation and related modifications of fatty acids. Annu Rev Plant Physiol Plant Mol Biol 49: 611–641.
4. Meesapyodsuk D, Reed DW, Covello PS, Qiu X (2007) Primary structure, regioselectivity, and evolution of the membrane-bound fatty acid desaturases of Claviceps purpurea. J Biol Chem 282: 20191–20199.
5. Meesapyodsuk D, Reed DW, Covello PS, Qiu X (2007) Primary structure, regioselectivity, and evolution of the membrane-bound fatty acid desaturases of Claviceps purpurea. J Biol Chem 282: 20191–20199.
6. Sakuradani E, Kobayashi M, Ashikari T, Shimizu S (1999) Identification of Delta12-fatty acid desaturase from arachidonic acid-producing mortierella fungus by heterologous expression in the yeast Saccharomyces cerevisiae and the fungus Aspergillus oryzae. Eur J Biochem 261: 812–820.
7. Huang YS, Chaudhary S, Thurmond JM, Bobik EG, Yuan L, et al. (1999) Cloning of delta12- and delta6-desaturases from Mortierella alpina and recombinant production of gamma-linolenic acid in Saccharomyces cerevisiae. Lipids 34: 649–659.
8. Sakuradani E, Abe T, Iguchi K, Shimizu S (2005) A novel fungal omega3-desaturase with wide substrate specificity from arachidonic acid-producing Mortierella alpina 1S-4. Appl Microbiol Biotechnol 66: 648–654.
9. Damude HG, Zhang H, Farrall L, Ripp KG, Tomb J-F, et al. (2006) Identification of bifunctional delta12/omega3 fatty acid desaturases for improving the ratio of omega3 to omega6 fatty acids in microbes and plants. Proc Natl Acad Sci U S A 103: 9446–9451.
10. Hoffmann M, Hornung E, Busch S, Kassner N, Ternes P, et al. (2007) A small membrane-peripheral region close to the active center determines regioselectivity of membrane-bound fatty acid desaturases from Aspergillus nidulans. J Biol Chem 282: 26666–26674.
11. Wei DS, Li MC, Zhang XX, Zhou H, Xing LJ (2006) A novel Delta12-fatty acid desaturase gene from methylotrophic yeast Pichia pastoris GS115. Acta Biochim Pol 53: 753–759.
12. Zhang X, Li M, Wei D, Xing L (2008) Identification and characterization of a novel yeast omega3-fatty acid desaturase acting on long-chain n-6 fatty acid substrates from Pichia pastoris. Yeast 25: 21–27.
13. Kainou K, Kamisaka Y, Kimura K, Uemura H (2006) Isolation of Delta12 and omega3-fatty acid desaturase genes from the yeast Kluyveromyces lactis and their heterologous expression to produce linoleic and alpha-linolenic acids in Saccharomyces cerevisiae. Yeast 23: 605–612.
14. Oura T, Kajiwara S (2004) Saccharomyces kluyveri FAD3 encodes an omega3 fatty acid desaturase. Microbiology 150: 1983–1990.
15. Watanabe K, Oura T, Sakai H, Kajiwara S (2004) Yeast Delta 12 fatty acid desaturase: gene cloning, expression, and function. Biosci Biotechnol Biochem 68: 721–727.
16. Moss CW, Shinoda T, Samuels JW (1982) Determination of cellular fatty acid compositions of various yeasts by gas-liquid chromatography. J Clin Microbiol 16: 1073–1079.
17. Yan Z, Zhuo L, Mulan J, Xia W, Yangmin G, et al. (2013) Clone and identification of bifunctional Δ12/Δ15 fatty acid desaturase LKFAD15 from Lipomyces kononenkoae. Food Sci Biotechnol 22: 573–576.
18. Sayanova O, Haslam R, Guschina I, Lloyd D, Christie WW, et al. (2006) A bifunctional Delta12,Delta15-desaturase from Acanthamoeba castellanii directs the synthesis of highly unusual n-1 series unsaturated fatty acids. J Biol Chem 281: 36533–36541.
19. Peyou-Ndi MM, Watts JL, Browse J (2000) Identification and characterization of an animal delta(12) fatty acid desaturase gene by heterologous expression in Saccharomyces cerevisiae. Arch Biochem Biophys 376: 399–408.
20. Zhou X-R, Green AG, Singh SP (2011) Caenorhabditis elegans Delta12-desaturase FAT-2 is a bifunctional desaturase able to desaturate a diverse range of fatty acid substrates at the Delta12 and Delta15 positions. J Biol Chem 286: 43644–43650.
21. Kikukawa H, Sakuradani E, Kishino S, Park S-B, Ando A, et al. (2013) Characterization of a trifunctional fatty acid desaturase from oleaginous filamentous fungus Mortierella alpina 1S-4 using a yeast expression system. J Biosci Bioeng.
22. Broadwater JA, Whittle E, Shanklin J (2002) Desaturation and hydroxylation. Residues 148 and 324 of Arabidopsis FAD2, in addition to substrate chain length, exert a major influence in partitioning of catalytic specificity. J Biol Chem 277: 15613–15620.
23. Serra M, Gauthier LT, Fabrias G, Buist PH (2006) Delta11 desaturases of Trichoplusia ni and Spodoptera littoralis exhibit dual catalytic behaviour. Insect Biochem Mol Biol 36: 822–825.
24. Carvalho F, Gauthier LT, Hodgson DJ, Dawson B, Buist PH (2005) Quantitation of hydroxylated byproduct formation in a Saccharomyces cerevisiae Delta9 desaturating system. Org Biomol Chem 3: 3979–3983.
25. Krishnamurthy S, Plaine A, Albert J, Prasad T, Prasad R, et al. (2004) Dosage-dependent functions of fatty acid desaturase Ole1p in growth and morphogenesis of Candida albicans. Microbiology 150: 1991–2003.
26. Nguyen LN, Gacser A, Nosanchuk JD (2011) The stearoyl-coenzyme A desaturase 1 is essential for virulence and membrane stress in Candida parapsilosis through unsaturated fatty acid production. Infect Immun 79: 136–145.
27. Murayama SY, Negishi Y, Umeyama T, Kaneko A, Oura T, et al. (2006) Construction and functional analysis of fatty acid desaturase gene disruptants in Candida albicans. Microbiology 152: 1551–1558.
28. Ghannoum MA, Janini G, Khamis L, Radwan SS (1986) Dimorphism-associated variations in the lipid composition of Candida albicans. J Gen Microbiol 132: 2367–2375.
29. Trofa D, Gácser A, Nosanchuk JD (2008) Candida parapsilosis, an emerging fungal pathogen. Clin Microbiol Rev 21: 606–625.
30. Edgar RC (2004) MUSCLE: multiple sequence alignment with high accuracy and high throughput. Nucleic Acids Res 32: 1792–1797.
31. Tamura K, Peterson D, Peterson N, Stecher G, Nei M, et al. (2011) MEGA5: molecular evolutionary genetics analysis using maximum likelihood, evolutionary distance, and maximum parsimony methods. Mol Biol Evol 28: 2731–2739.
32. Krogh A, Larsson B, von Heijne G, Sonnhammer EL (2001) Predicting transmembrane protein topology with a hidden Markov model: application to complete genomes. J Mol Biol 305: 567–580.
33. Tusnády GE, Simon I (2001) The HMMTOP transmembrane topology prediction server. Bioinformatics 17: 849–850.
34. Buček A, Vogel H, Matoušková P, Prchalová D, Záček P, et al. (2013) The role of desaturases in the biosynthesis of marking pheromones in bumblebee males. Insect Biochem Mol Biol 43: 724–731.
35. Matoušková P, Luxová A, Matoušková J, Jiroš P, Svatoš A, et al. (2008) A delta9 desaturase from Bombus lucorum males: investigation of the biosynthetic pathway of marking pheromones. Chembiochem 9: 2534–2541.
36. Fay L, Richli U (1991) Location of double bonds in polyunsaturated fatty acids by gas chromatography-mass spectrometry after 4,4-dimethyloxazoline derivatization. J Chromatogr A 541: 89–98.
37. Spitzer V (1996) Structure analysis of fatty acids by gas chromatography-low resolution electron impact mass spectrometry of their 4,4-dimethyloxazoline derivatives-a review. Prog Lipid Res 35: 387–408.
38. Butler G, Rasmussen MD, Lin MF, Santos MAS, Sakthikumar S, et al. (2009) Evolution of pathogenicity and sexual reproduction in eight Candida genomes. Nature 459: 657–662.
39. Pereira SL, Huang Y-S, Bobik EG, Kinney AJ, Stecca KL, et al. (2004) A novel omega3-fatty acid desaturase involved in the biosynthesis of eicosapentaenoic acid. Biochem J 378: 665–671.
40. Christie WW, Robertson GW, Mcroberts WC, Hamilton JTG (2000) Mass spectrometry of the 4, 4-dimethyloxazoline derivatives of isomeric octadecenoates (monoenes). Eur J Lipid Sci Technol 102: 23–29.
41. Pan Z, Rimando AM, Baerson SR, Fishbein M, Duke SO (2007) Functional characterization of desaturases involved in the formation of the terminal double bond of an unusual 16:3Delta(9,12,15D) fatty acid isolated from Sorghum bicolor root hairs. J Biol Chem 282: 4326–4335.
42. Nicolaides N, Soukup VG, Ruth EC (1983) Mass spectrometric fragmentation patterns of the acetoxy and trimethylsilyl derivatives of all the positional isomers of the methyl hydroxypalmitates. Biol Mass Spectrom 10: 441–449.
43. Certik M, Shimizu S (1999) Biosynthesis and regulation of microbial polyunsaturated fatty acid production. J Biosci Bioeng 87: 1–14.
44. Uemura H (2012) Synthesis and production of unsaturated and polyunsaturated fatty acids in yeast: current state and perspectives. Appl Microbiol Biotechnol 95: 1–12.
45. Wilson RA, Calvo AM, Chang P-K, Keller NP (2004) Characterization of the Aspergillus parasiticus delta12-desaturase gene: a role for lipid metabolism in the Aspergillus-seed interaction. Microbiology 150: 2881–2888.
46. Calvo AM, Gardner HW, Keller NP (2001) Genetic connection between fatty acid metabolism and sporulation in Aspergillus nidulans. J Biol Chem 276: 25766–25774.
47. Prasad MR, Sreekrishna K, Joshi VC (1980) Topology of the delta 9 terminal desaturase in chicken liver microsomes and artificial micelles. Inhibition of the enzyme activity by the antibody and susceptibility of the enzyme to proteolysis. J Biol Chem 255: 2583–2589.
48. Stukey JE, McDonough VM, Martin CE (1990) The OLE1 gene of Saccharomyces cerevisiae encodes the delta 9 fatty acid desaturase and can be functionally replaced by the rat stearoyl-CoA desaturase gene. J Biol Chem 265: 20144–20149.
49. Diaz AR, Mansilla MC, Vila AJ, de Mendoza D (2002) Membrane topology of the acyl-lipid desaturase from Bacillus subtilis. J Biol Chem 277: 48099–48106.
50. Broun P, Shanklin J, Whittle E, Somerville C (1998) Catalytic plasticity of fatty acid modification enzymes underlying chemical diversity of plant lipids. Science 282: 1315–1317.
51. Meesapyodsuk D, Reed DW, Savile CK, Buist PH, Ambrose SJ, et al. (2000) Characterization of the regiochemistry and cryptoregiochemistry of a Caenorhabditis elegans fatty acid desaturase (FAT-1) expressed in Saccharomyces cerevisiae. Biochemistry 39: 11948–11954.
52. Oura T, Kajiwara S (2008) Substrate Specificity and Regioselectivity of Δ12 and ω3 Fatty Acid Desaturases from Saccharomyces kluyveri. Biosci Biotechnol Biochem 72: 3174–3179.

53. Kajiwara S, Shirai A, Fujii T, Toguri T, Nakamura K, et al. (1996) Polyunsaturated fatty acid biosynthesis in Saccharomyces cerevisiae: Expression of ethanol tolerance and the FAD2 gene from Arabidopsis thaliana. Appl Environ Microbiol 62: 4309–4313.
54. Rodríguez-Vargas S, Sánchez-García A, Martínez-Rivas JM, Prieto JA, Randez-Gil F (2007) Fluidization of membrane lipids enhances the tolerance of Saccharomyces cerevisiae to freezing and salt stress. Appl Environ Microbiol 73: 110–116.
55. Yazawa H, Iwahashi H, Kamisaka Y, Kimura K, Uemura H (2009) Production of polyunsaturated fatty acids in yeast Saccharomyces cerevisiae and its relation to alkaline pH tolerance. Yeast 26: 167–184.